Multifunctional passive-heart platforms for *in vitro* hemodynamic studies

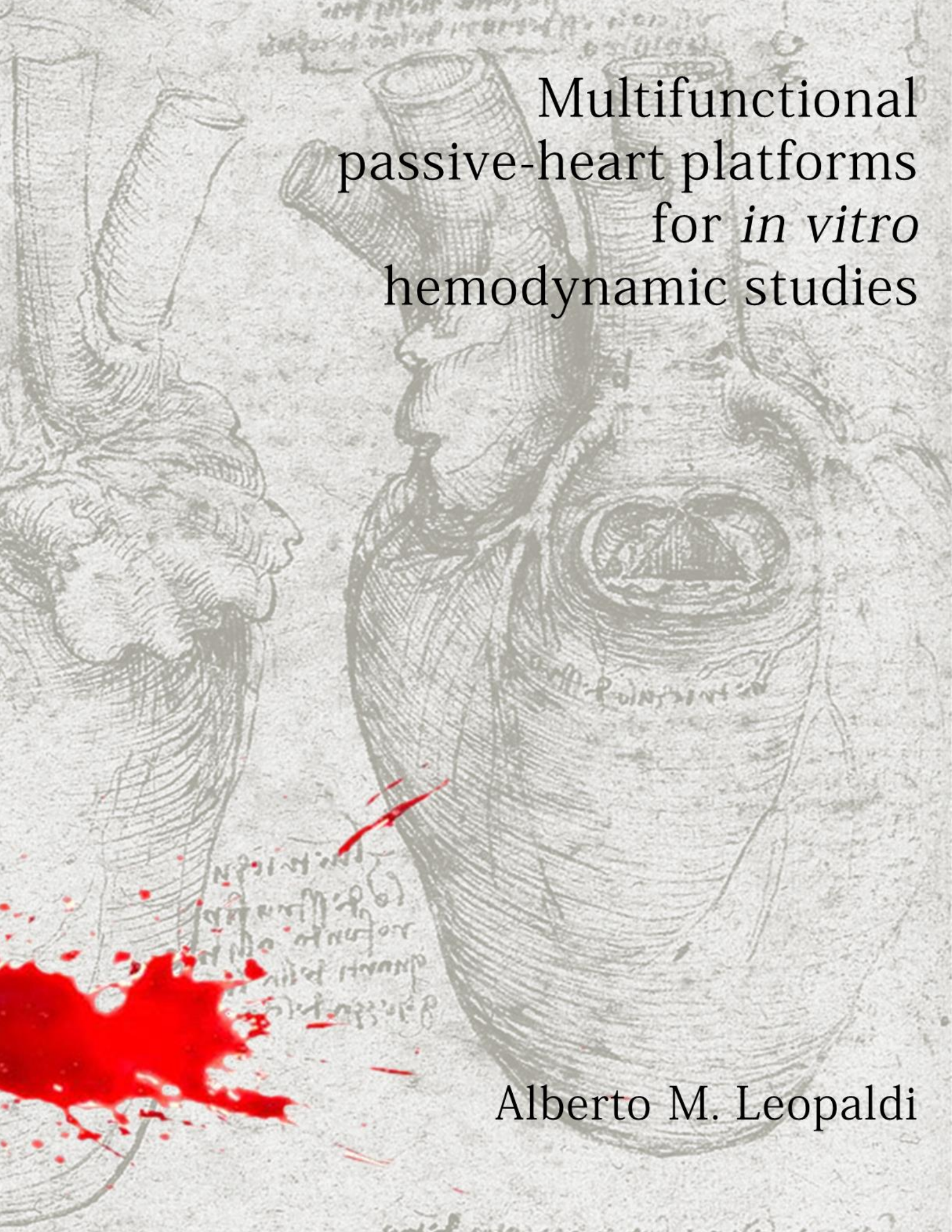

Alberto M. Leopaldi

POLITECNICO DI MILANO

SCUOLA INTERPOLITECNICA DI DOTTORATO

Doctoral Program in Bioengineering

Final Dissertation

Multifunctional passive-heart platforms for *in vitro* hemodynamic studies

Alberto Maria Leopaldi

Tutor
Prof. Alberto Redaelli

Advisor
Prof. Gianfranco B. Fiore

Co-ordinator of the Research Doctorate Course
Prof. Maria Gabriella Signorini

27/02/2014

Cover picture adapted from the anatomical drawings by Leonardo da Vinci.

The images from the title page of each Chapter are taken or adapted from the movie "Young Frankenstein" by Mel Brooks, as a tribute to the first developed passive-heart platform, among some known as *Frankenstin*.

Table of contents

Extended abstract

Background and aim of the work

The present work describes the design, development and application of innovative *in vitro* passive-heart platforms for the hemodynamic and biomechanical analysis of therapeutic approaches to cardiovascular pathologies. This work arises from two main collaborations: the first part of the work was carried out at FoRCardioLab, a laboratory co-founded by Politecnico di Milano, Universitá degli studi di Milano and the division of Cardiac Surgery in Luigi Sacco Hospital, in which surgeons and bioengineers cooperate to study new therapeutic approaches to cardiac pathologies. The work described in the second part of the thesis arises from the collaboration between Politecnico di Milano and the Cardiovascular Biomechanics Laboratory of the TU/e, Eindhoven (The Netherlands), where part of the research was performed under the supervision of Prof. van de Vosse and Prof. Rutten.

The use of *in vitro* mock circulation loops for the study of the cardiovascular system and the test of prosthetic devices dates back to the 70's [1,2] and finds its rationale in the possibility of performing tests in highly controllable experimental conditions and in a cost-effective fashion, thus reducing the need for animal models. In order to represent realistic models, *in vitro* platforms must be able to replicate the conditions to which the device will be subjected *in vivo*. Being historically associated with the development of mechanical heart valves, the classical approach to the design of mock circulatory systems was purely hydrodynamic-based.

In recent years, however, the need for realistic *in vitro* models has become more stringent due to the substantial changes of the clinical approaches towards reparative, minimally-invasive and transcatheter techniques [3–6]. For most of such applications, the interaction between implanted device or repaired structure and *in vivo* environment is not strictly limited to the hemodynamics, but involves anatomical and functional aspects that are crucial for the outcome of the procedure. Paravalvular leakage in transcatheter aortic valve implantation (TAVI) [7,8], complex aortic-mitral interactions following surgical or transcatheter procedures [9,10] and aortic valve insufficiency after continuous flow left

ventricular assist device (cf-LVAD) implantation [11,12] are only few examples of these important interplays.

Hence, being able to take into account these aspects is nowadays a challenging, yet fundamental, requirement for any modern *in vitro* mock circulatory loop. Recently, researchers addressed this issue and tried to fill the morphological and anatomical gap with both ex vivo and animal models by developing mock loops in which excised aortic [13–15] or mitral [16,17] valves could be tested. These systems permit both the imaging of valvular structures with high-speed cameras and/or echographic techniques and the execution of surgical procedures on the biological samples. In this way, surgeons can operate in a very familiar environment, where they can simulate surgical procedures and directly analyse their hemodynamic effects.

An interesting approach has been recently proposed by Richards et al. [18], who developed a dynamic passive-heart platform for the analysis of mitral valve repair techniques. The system was able to host an entire explanted heart and to provide the left ventricle with a cyclical flow rate thanks to a pulsatile pump connected to the apex. Given the very specific purpose for which the platform was designed, the hemodynamic conditions were far from being physiological. Nonetheless, the passive-heart approach represents a challenging and fascinating development of the excised valves platforms, towards a better replication of the *in vivo* anatomy and morphology. Indeed, the use of an entire heart allows a perfect preservation of the cardiac structures, still without involving all the complexities and ethical issues of the *ex vivo* and animal models. Furthermore, the use of entire hearts greatly widen the potential applications of an experimental apparatus by allowing, for example, the simulation of minimally invasive and multi-valvular surgical procedures.

The aim of this study is to develop novel *in vitro* passive-heart platforms that can represent effective tools for research, device testing and training purposes and reduce the need for ex vivo and animal models. The present work describes the development of two passive-heart platforms, which adopted different methodologies for the generation of the cardiac output, and their use for TAVI and LVAD applications. Also, the design of a 4-chamber mock loop, conceived in order to work with both passive or *ex vivo* beating hearts, is described. To this purpose, the present thesis is structured as follows:

- In the first part of the work, the development of an *in vitro* platform able to house an entire explanted porcine heart and subject it to pulsatile hemodynamic conditions, is

described. The system, similar to that proposed by Richards and colleagues [18], dynamically pressurizes the left ventricle by mean of a piston pump connected to the heart apex, and enables the hemodynamic analysis of simulated surgical procedures and the imaging of the valvular structures. The mock loop's hydrodynamic design was based on an ad-hoc defined lumped-parameter model.

- The evolution of the *in vitro* passive beating heart platform for TAVI applications was successively addressed. The development included both a feasibility study on a novel methodology to reproduce *in vitro* aortic valve stenosis, and the redesign of the setup layout and components in order to achieve an easy and cost-effective training platform. The proficiency of the system was assessed by performing transcatheter aortic valve and valve-in-valve implantations under multimodal imaging guidance in a catheterization lab.
- The research that was carried out at the Cardiovascular Biomechanics Laboratory of the TU/e led to the development of another *in vitro* passive-heart mock loop. This setup adopted a complementary functioning principle as compared to the first one that was designed. Indeed, this left heart platform mimics the pulsatile pumping function of the heart through the external pressurization of the ventricles, thus trying to reproduce the *in vivo* dynamic ventricular behavior. The system was also used for a pilot study aimed at analyzing the aortic valve (AV) opening dynamics during continuous-flow left ventricular assist device (cf-LVAD) support.
- The final part of the work describes the redesign of an existing model-controlled four-chamber mock loop, that could be used with both passive and beating heart models. An anatomical study was conducted in order to characterize the orientation of the main heart vessels, and to design a standard manifold for their connection to the hydraulic circuit. Preliminary assessments are being performed using passive hearts.

In the last Chapter, a general discussion of the PhD dissertation and the conclusive remarks are presented.

3. *In vitro* hemodynamics and valve imaging in passive beating hearts

In this Chapter, the development of a mock apparatus able to house an entire explanted porcine heart and subject it to pulsatile fluid-dynamic conditions is presented, in order to enable the hemodynamic analysis of simulated surgical procedures and the imaging of the valvular structures. The mock loop's hydrodynamic design was based on an ad-hoc defined lumped-parameter model.

The left ventricle of an entire swine heart was dynamically pressurized by an external computer-controlled pulse duplicator. The ascending aorta was connected to a hydraulic circuit, which simulated the input impedance of the systemic circulation; a reservoir passively filled the left atrium. Accesses for endoscopic imaging were located in the apex of the left ventricle and in the aortic root. The experimental pressure and flow tracings (Figure 1) were comparable with the typical *in vivo* curves; a mean flow of 3.5±0.1 lpm and a mean arterial pressure of 101±2 mmHg was obtained. High-quality echographic and endoscopic video recordings demonstrated the excellent potential of the developed system in the observation of the cardiac structures dynamics.

The proposed mock loop represents a suitable *in vitro* system for the testing of minimally invasive cardiovascular devices and surgical procedures for heart valve repair.

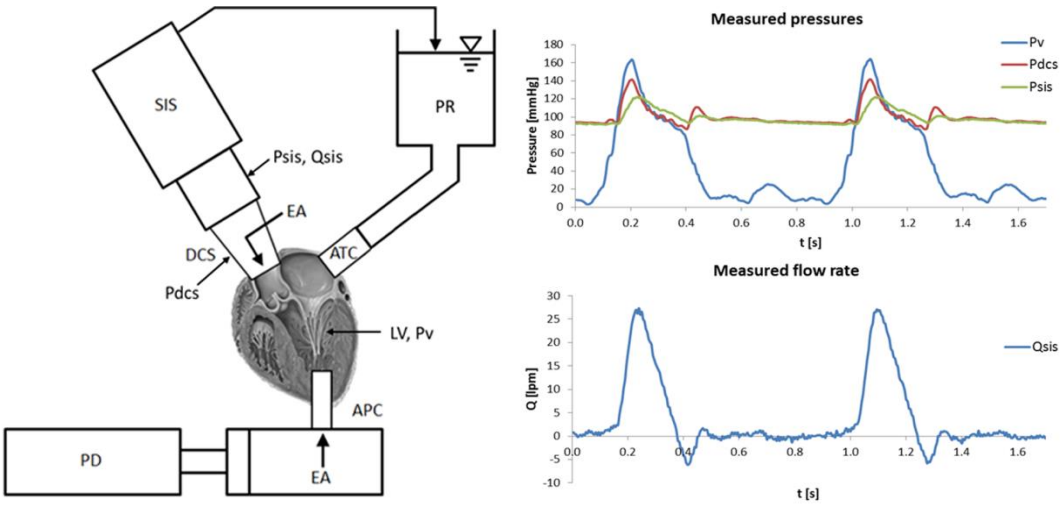

FIGURE 1. Left: schematic of the mock loop. Pulse duplicator (PD), systemic impedance simulator (SIS), preload reservoir (PR), apical connector (APC), atrial connector (ATC), double cone system (DCS), endoscopic accesses (EA). Right: Measured pressure (top) and flow rate (bottom) in the mock loop.

4. Evolution of the passive beating heart platform for TAVI applications

In this Chapter, the evolution towards TAVI applications of the passive beating heart platform is presented. Our goal was to develop a platform capable of simulating the typical environment physicians are working with when performing TAVI, in order to provide them with a multi-functional tool that could be used for training, research and educational purposes. The key requirements for our design were the possibility of performing multimodal imaging, the simulation of the anatomo-morphological environment and the achievement of physiologic hemodynamic conditions in a simple, reliable and cost-effective system.

In order to achieve these goals, the passive beating heart setup was optimized with improved TAVI-specific design solutions. Moreover, a methodology to simulate *in vitro* aortic valve stenosis by glueing human aortic calcified leaflets to the healthy porcine aortic cusps, was developed. The experimental assessments proved the reliability of the proposed methodology, which allowed clear visualization of the stenotic valve during fluoroscopy and induced mild to severe degrees of aortic stenosis. The passive beating heart platform, with the model of aortic stenosis, was profitably used to perform several TAVI procedures under fluoroscopic guidance and simultaneous intracardiac visualization in a catheterization lab (Figure 2).

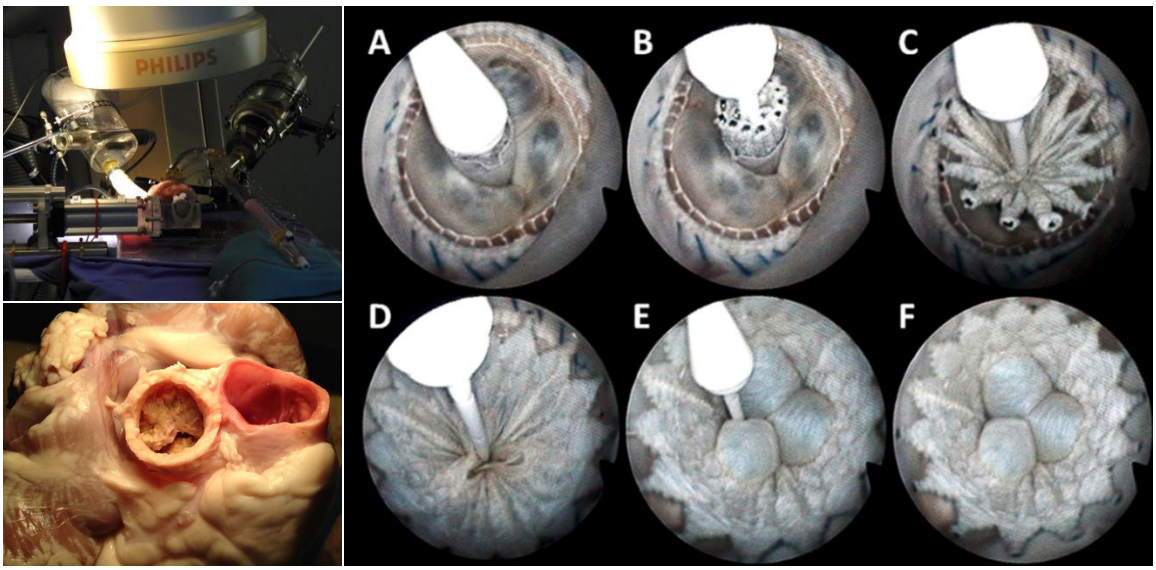

FIGURE 2. Left: Pictures of the platform in the cath lab (top) and the in vitro model of aortic valve stenosis (bottom). Right: Snapshots of the valve-in-valve procedure that was performed, obtained with intracardiac endoscopy [19].

5. A novel passive left heart platform for device testing and research

In this Chapter, the development of a novel *in vitro* left heart platform capable of simulating the pulsatile pumping function of the heart through the external cyclic pressurization of the ventricular walls is described. The system (Figure 3, left) is composed by a fluid-filled chamber, in which the ventricles of the heart are housed and sealed by means of a rapid-prototyped vacuum seal, which excludes the atria from any external load. The fluid-filled chamber is connected to a piston pump, whose cyclic action drives the motion of the ventricular walls. The aorta is connected to a mock circulatory system simulating the human systemic impedance, and the left atrium is fed by an adjustable preload.

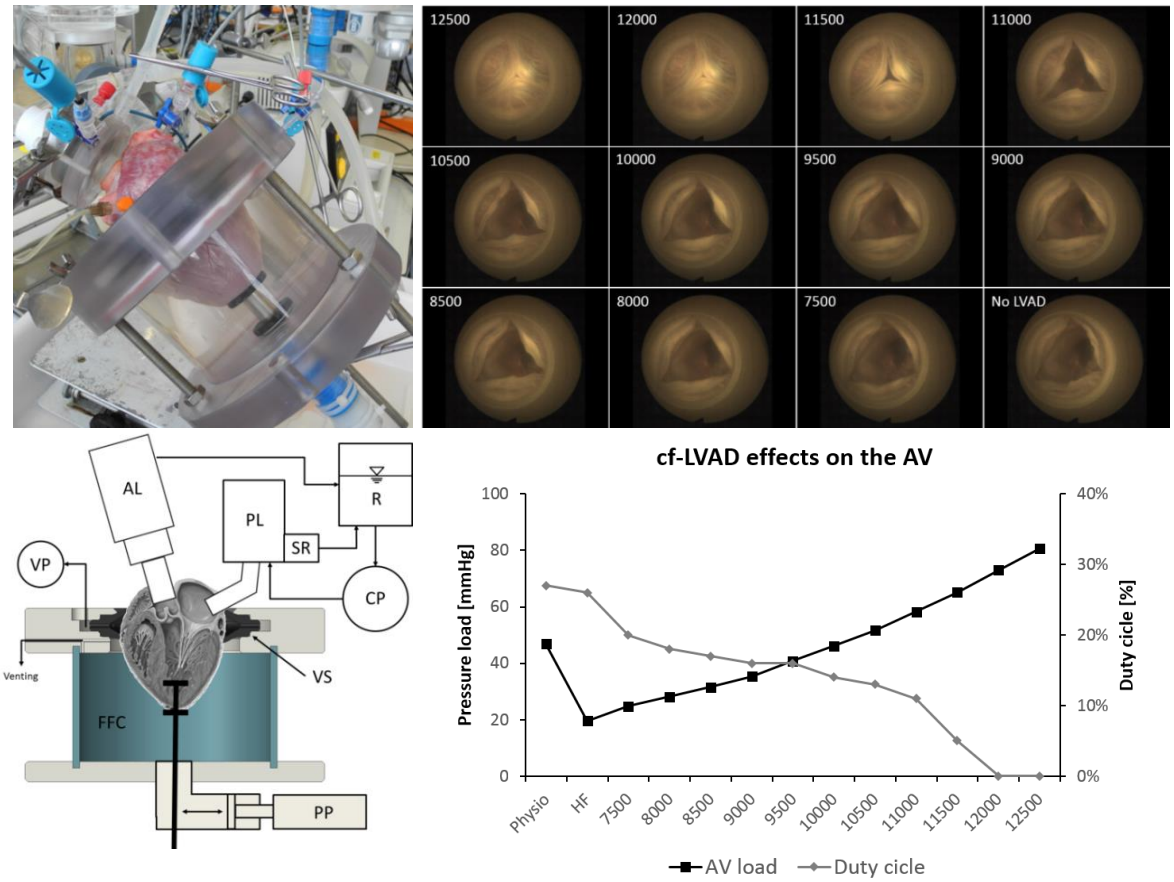

FIGURE 3. Left: mock loop photograph (top) and schematic (bottom). Piston pump (PP), fluid-filled chamber (FFC), vacuum seal (VS), vacuum pump (VP), afterload module (AL), reservoir (R), centrifugal pump (CP), preload module (PL), starling resistor (SR). Right: snapshots of the aortic valve at maximum opening recorded with the high speed camera for all the tested conditions (top). Mean aortic valve pressure load (mmHg) and duty cycle (%) for all the tested condition: physiologic systemic conditions (Physio), heart failure (HF), and different pump speeds (bottom).

The platform was capable of reproducing physiologic hemodynamic conditions, i.e. aortic pressures of 120/80 mmHg with 4.5 lpm of cardiac output, and allowed for endoscopic imaging of the cardiac structures. The potential of the system for device-testing and visualization studies was also assessed, with a continuous flow LVAD connected to the heart, so to investigate the effects induced on the aortic valve function by different levels of support. Results were in line with clinical observations and previous studies, showing an increased load on the valve for increasing pump speeds, as well as a reduced valve duty cycle (Figure 3, right). High-speed video recordings of the aortic valve also allowed the visualization of the transition between a fully opening valve and a permanently closed configuration, which only happened within a very narrow pump speed range. In conclusion, the system showed to be an effective tool for the hemodynamic assessment of devices, the simulation of surgical or transcatheter procedures and for visualization studies.

6. Towards the development of four-chamber passive and beating heart platforms

This Chapter describes the redesign of an existing 4-chamber purely hydraulic model-controlled mock circulatory loop, that was developed at the Cardiovascular Biomechanics Laboratory of the TU/e and features a complete 4-chamber circulation, whose actuation is controlled by a heart contraction model and a heart rate control model. Our challenging goal was to redesign the system in order to make it capable of working in a 4-chamber mode with entire heart structures, being either passive hearts actuated by model-controlled pumps, or isolated beating hearts.

The first design step consisted in the characterization of the spatial orientation of the main afferent and efferent heart vessels, so to design a standard connection with the afterload circuit. These measures were used as inputs to redesign the afterload circuit accordingly to the heart layout, taking into account also the requirements related to the performance of isolated beating heart experiments, e.g. different working modes, blood oxygenation, venting. The setup was then manufactured and assembled. The first experimental assessments are currently being performed with passive hearts (Figure 4), investigating the feasibility of the

approach in which external cyclic pressurization is applied to the ventricular walls in a 4-chamber working mode. With this respect, the main issue that is being addressed is represented by the different compliance of the right and left ventricles, which leads to relevant abnormalities in the generation of the stroke volumes. In order to reduce this gap, we are currently investigating several ways to stiffen the right ventricle using both classical chemical fixation methodologies and external mechanical stiffening of the walls.

FIGURE 4. Pictures of the 4 chamber mock loop during one of the first experimental assessments that were carried out with passive hearts.

7. Main findings and future developments

The present work explored the potentiality of *in vitro* passive-heart mock circulatory systems as multi-functional *in vitro* platforms for research, device-testing, visualization studies, training and educational purposes in the cardiovascular field. Our findings demonstrated the feasibility of this innovative approach, as the developed passive-heart systems were capable of i) closely reproducing the physiologic hemodynamics, ii) allowing intracardiac endoscopy and multimodal imaging, iii) performing surgical and/or transcatheter procedures, iv) assessing cardiovascular devices and v) being used as training platforms.

Two platforms were designed, developed and tested in order to assess two alternative approaches for the generation of the stroke volume. The first system, whose design principle was inspired by the worked of Richards et al. [18], pressurized the left ventricle internally by

means of a piston pump connected to the heart apex. This actuation methodology ensured the achievement of physiological hemodynamic conditions, excellent imaging capabilities, and no abnormalities in valve function, though it caused a paradoxical motion of the ventricular walls during the cardiac cycle and an altered fluid dynamic field inside the left ventricle. The platform was optimized for TAVI applications, and used in a catheterization lab to perform implantations under fluoroscopic guidance and simultaneous intracardiac visualization on an *in vitro* model of aortic valve stenosis, that was developed to mimic the real pathological scenario.

The second passive-heart mock loop was designed to mimic the pulsatile pumping function of the left heart through the external dynamic pressurization of the ventricular walls, and ensured a better simulation of the dynamic behaviour of the ventricular walls. Physiological hemodynamics were achieved, although mitral valve prolapse was observed in some samples at high stroke volumes, due to the absence of papillary muscle contraction. The potential of the developed system as a platform for device testing was assessed with a pilot study, in which the acute post-operative scenario after the implantation of a cf-LVAD was simulated, and the AV function for different levels of mechanical support was analysed.

Future developments, whose initial steps were described in the last Chapter of this dissertation, will face two relevant, yet unavoidable, challenges. On one side, the development of four chamber mock loops, so to broaden the potential applications of these systems and to allow the study of the interactions between left and right circulation, which are often fundamental. On the other side, achieving a model-controlled actuation of passive-heart platforms may definitely close the existing gap between this approach and the state-of-the-art *in vitro* hybrid loops. With respect to both these directions, the internal pressurization approach may represent a more sensible choice both to develop a full circulatory loop and to implement a model-controlled actuation.

References

1. Westerhof N, Elzinga G, Sipkema P. An artificial arterial system for pumping hearts. J Appl Physiol. 1971; 31:776–81.
2. Swanson WM, Clark RE. A simple cardiovascular system simulator: design and performance. J. Bioeng. 1977; 1:135–45.
3. Schmitto JD, Mokashi SA, Cohn LH. Minimally-invasive valve surgery. J. Am. Coll. Cardiol. 2010; 56:455–62.
4. Aicher D, Fries R, Rodionycheva S, Schmidt K, Langer F, Schafers HJ. Aortic valve repair leads to a low incidence of valve-related complications. Eur. J. Cardio-Thoracic Surg. 2010; 37:127–32.
5. Tang GHL, Lansman SL, Cohen M, Spielvogel D, Cuomo L, Ahmad H, et al. Transcatheter aortic valve replacement: current developments, ongoing issues, future outlook. Cardiol. Rev. 2013; 21:55–76.
6. Karimov J. Overview of current sutureless and transcatheter mitral valve replacement technology. Expert Rev. Med. 2013; 10:73–83.
7. Généreux P, Head SJ, Hahn R, Daneault B, Kodali S, Williams MR, et al. Paravalvular leak after transcatheter aortic valve replacement: the new Achilles' heel? A comprehensive review of the literature. J. Am. Coll. Cardiol. 2013; 61:1125–36.
8. Vallabhajosyula P, Bavaria JE. Transcatheter aortic valve implantation: complications and management. J Hear. Valve Dis. 2011; 20:499–509.
9. Vergnat M, Levack MM, Jackson BM, Bavaria JE, Herrmann HC, Cheung AT, et al. The effect of surgical and transcatheter aortic valve replacement on mitral annular anatomy. Ann. Thorac. Surg. 2013; 95:614–9.
10. De Chiara B, Moreo A, De Marco F, Musca F, Oreglia J, Lobiati E, et al. Influence of corevalve revalving system implantation on mitral valve function. Catheter. Cardiovasc. Interv. 2011; 78:638–44.
11. Aggarwal A, Raghuvir R, Eryazici P, Macaluso G, Sharma P, Blair C, et al. The development of aortic insufficiency in continuous-flow left ventricular assist device-supported patients. Ann. Thorac. Surg. 2013; 95:493–8.
12. Soleimani B, Haouzi A, Manoskey A, Stephenson ER, El-Banayosy A, Pae WE. Development of aortic insufficiency in patients supported with continuous flow left ventricular assist devices. ASAIO J. 2012; 58:326–9.
13. Erasmi A, Sievers H, Scharfschwerdt M, Eckel T, Misfeld M. *In vitro* hydrodynamics, cusp-bending deformation, and root distensibility for different types of aortic valve–sparing operations: Remodeling, sinus prosthesis, and reimplantation. J. Thorac. Cardiovasc. Surg. 2005; 130:1044–9.
14. Notzold A, Scharfschwerdt M, Thiede L, Huppe M, Sievers H. In-vitro study on the relationship between progressive sinotubular junction dilatation and aortic regurgitation for several stentless aortic valve substitutes. Eur. J. Cardio-Thoracic Surg. 2005; 27:90–3.

15. Vismara R, Fiore GB, Mangini A, Contino M, Lemma M, Redaelli A, et al. A novel approach to the *in vitro* hydrodynamic study of the aortic valve: mock loop development and test. ASAIO J. 2010; 56:279–84.
16. Arita M, Tono S, Kasegawa H, Umezu M. Multiple purpose simulator using a natural porcine mitral valve. Asian Cardiovasc. Thorac. Ann. 2004; 12:350–6.
17. Vismara R, Pavesi A, Votta E, Taramasso M, Maisano F, Fiore GB. A pulsatile simulator for the *in vitro* analysis of the mitral valve with tri-axial papillary muscle displacement. Int. J. Artif. Organs. 2011; 34:383–91.
18. Richards AL, Cook RC, Bolotin G, Buckner GD. A Dynamic Heart System to Facilitate the Development of Mitral Valve Repair Techniques. Ann. Biomed. Eng. 2009; 37:651–60.

1

Introduction

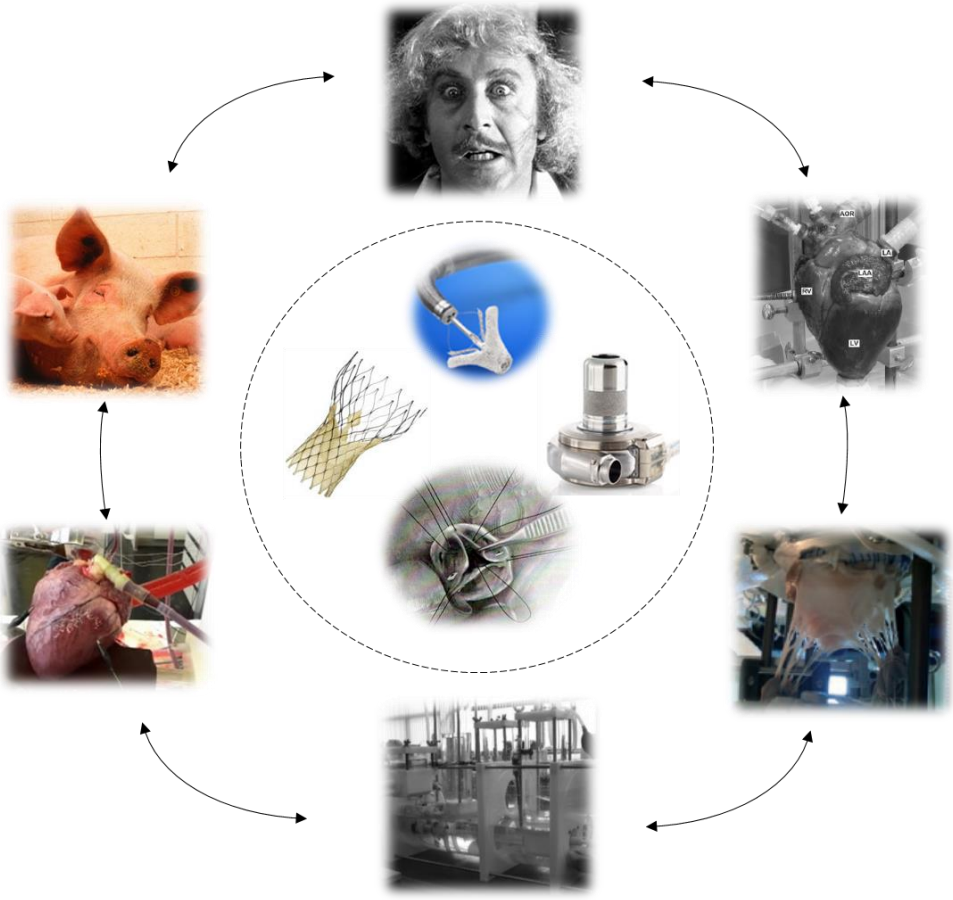

1.1 Background

Cardiovascular disease (CVD) is the leading cause of death in the world, and its incidence is expected to grow in the next years [1–3]. Heart failure (HF) accounts for 35% of CVD deaths [4] and may result from several disorders, among which impaired left ventricular (LV) myocardial function and heart valve abnormalities are the most relevant. The clinical management of HF depends on the specific patient condition and etiology, but in many cases requires the performance of surgical procedures, such as coronary artery bypass or valve repair and/or the implantation of devices, such as ventricular assist devices (VAD) or valvular prosthesis, [5].

All these devices and procedures must undergo extensive testing before and after the introduction in the clinical practice, so to prove their effectiveness and safety for the patients, improve their clinical use, optimize their design, better characterize their functioning etc. The experimental models that are currently available to perform these investigations range from *in vivo* animal models to *ex vivo* and *in vitro* platforms. Each of these approaches represents a different compromise between fundamental, yet contrasting, requirements: control and repeatability of the experimental conditions, complexity of the model, accurate simulation of the physiological and pathological *in vivo* environment, and cost-effectiveness. The choice of the best model depends on several factors, such as the aim of the analysis or the development stage of the device, but most of the times different models are used and the resulting experimental evidences combined.

The use of animal models is, generally, a mandatory step, since is the only methodology that is able to fully mimic the complexity of the *in vivo* environment. Nevertheless, the control that is achievable on the test conditions is limited, and analysing the role played by a specific parameter is often unfeasible. Furthermore, the economical and ethical issues make animal models inefficient choices in most cases.

The *ex vivo* approach for cardiovascular applications was firstly proposed in 1895 by Langendorff [6], who showed the feasibility of restoring physiologic cardiac function on isolated hearts through appropriate myocardial perfusion. In the last decades, many research groups pursued this methodology and successfully developed *ex vivo* beating heart platforms [7–10] that were used for numerous applications [10–22].

Indeed, these systems have a tremendous potential, since they are able to accurately reproduce the *in vivo* cardiac physiology and hemodynamic, still without involving all the complex milieu of the intact animal. However, most of the published *ex vivo* models still make use of laboratory animal excised hearts, thus involving ethical issues similar to those of the *in vivo* experiments. Only a few groups were able to overcome these drawbacks by using slaughterhouse hearts [8,23,24], and among these only de Hart and colleagues [8] were able to achieve physiologic hemodynamics. Anyhow, the complex experimental protocol and the costs that are associated with the *ex vivo* methodology often limit its use.

Differently from both the *in vivo* and *ex vivo* approaches, *in vitro* models, i.e. laboratory models based on an artificial-only approach, can provide a controlled and reproducible environment to perform accurate studies in a very efficient and cost-effective way. Moreover, the *in vitro* approach allows the selective modelling of the features of the *in vivo* system that are relevant for a specific analysis. For example, as far as the hemodynamic performance of an aortic valvular prosthesis is concerned, the replication of the systemic pressure and flow waveforms in a hydraulic circuit will represent a simplified, yet effective, controllable and cost-effective model. For these reasons, *in vitro* models are generally the choice of election for any experimental analysis, provided that they can adequately mimic the *in vivo* features that are relevant for the study.

After the first pioneering research of Otto Frank [25], many *in vitro* mock circulatory loops have been developed and extensively used to study the cardiovascular system and to test a multitude of implantable devices and procedures [26–32]. Driven by the evolving needs of both researchers and industry, and by the development of mathematical models of the *in vivo* physiology [33–37], mock loops evolved significantly in the last decades, so to provide solutions to different needs. Most of these developments were aimed at replicating the hemodynamics of the human circulation [31,38,39], and some of the main dynamic *in vivo* responses, such as the Frank-Starling mechanism or the baroreflex response [40–45].

Nonetheless, the main limit of the *in vitro* approach still relies in the unavoidable simplification of the *in vivo* scenario, which is nowadays mainly related to the limited possibility of replicating cardiac morphology and physiology. With this respect, the development of more realistic mock loops is mandatory for the next generation of cardiovascular devices and therapies.

1.2 Motivation and aim

In the last years, the therapeutic approaches to CVD have been significantly evolving towards reparative [46–48], minimally invasive [49] and transcatheter procedures [50–52], which ensure less trauma for the patient and lower costs for the health care system thanks to shorter hospitalization [53,54]. All these clinical methodologies are characterized by the attempt of preserving the natural structures as much as possible, minimizing the invasiveness of the intervention and restoring their physiological function when possible.

As a consequence, the interaction between implanted device or repaired structure and *in vivo* environment involves anatomical and functional aspects that are crucial for the outcome of the procedure. Paravalvular leakage in transcatheter aortic valve implantation (TAVI) [55,56], complex aortic-mitral interactions following surgical or transcatheter procedures [57,58] and aortic valve insufficiency after continuous flow left ventricular assist device (cf-LVAD) implantation [59,60] are only few examples of these important interplays. Hence, being able to take into account these aspects is nowadays a challenging, yet fundamental, requirement for any *in vitro* mock circulatory loop.

Recently, researchers addressed this issue and tried to fill the morphological and anatomical gap with both *ex vivo* and animal models by developing ways to host passive cardiac sub-structures in *in vitro* apparatuses. Literature examples of this approach are recent mock loops in which excised aortic [61–64], mitral [65–67] or tricuspid [68,69] valves can be tested. These systems permit both the imaging of valvular structures with high-speed cameras and/or echographic techniques and the execution of surgical procedures on the biological samples. In this way, surgeons can operate in a very familiar environment, where they can simulate surgical procedures and directly analyse their hemodynamic effects.

An interesting further evolution of this approach has been recently proposed by Richards et al. [70], who developed a dynamic *in vitro* passive-heart platform for the analysis of mitral valve repair techniques. The system was able to host an entire explanted heart and to provide the left ventricle with a cyclical flow rate thanks to a pulsatile pump connected to the apex. Given the very specific purpose for which the platform was designed, the hemodynamic conditions were far from being physiological. Nonetheless, the *in vitro* passive-heart approach represents a challenging and fascinating development of the excised valves platforms, towards a better replication of the *in vivo* anatomy and morphology. Indeed, the

use of an entire heart allows a perfect preservation of the cardiac structures, still without involving all the complexities and ethical issues of the *ex vivo* and animal models. Furthermore, the use of entire hearts greatly widen the potential applications of an experimental apparatus by allowing, for example, the simulation of minimally-invasive and multi-valvular surgical procedures.

The aim of this study is to develop novel *in vitro* passive-heart platforms that can represent effective tools for research, device testing and training purposes and reduce the need for *ex vivo* and animal models. The present work describes the development of two passive-heart mock loops, which adopted different methodologies for the generation of the cardiac output, and their use for TAVI and LVAD applications.

1.3 Outline of the thesis

The thesis is structured into the following Chapters:

2. In the first part of the thesis, the state of the art of the *in vitro* and *ex vivo* platforms for the study of the cardiovascular system is reported. Coherently with the motivation of the study, the historical evolution of these platforms towards a better representation of the physiological environment will be discussed.
3. In Chapter 3, the development of an *in vitro* platform able to house an entire explanted porcine heart and subject it to pulsatile hemodynamic conditions, is described. The system, similarly to what proposed by Richards and colleagues [70], dynamically pressurizes the left ventricle by mean of a piston pump connected to the heart apex, and enables the hemodynamic analysis of simulated surgical procedures and the imaging of the valvular structures. The mock loop's hydrodynamic design was based on an *ad-hoc* defined lumped-parameter model.
4. Chapter 4 describes the evolution of the *in vitro* platform described in Chapter 3 towards the investigation of minimally invasive applications. In particular, new design solutions were introduced in order to allow the performance of transcatheter aortic valve implantation (TAVI) under direct endoscopic visualization. An *in vitro*

pathological model of aortic stenosis was also developed, with human calcified leaflets that were glued to the native porcine cusps. The developed setup was tested in a catheterization lab, where simulated TAVI procedures were carried out under multimodal imaging guidance.

5. In Chapter 5, the development of another *in vitro* passive-heart mock loop is described. This setup adopted a different and complementary functioning principle as compared to the one described in Chapter 3. Indeed, this left heart platform mimics the pulsatile pumping function of the heart through the external pressurization of the ventricles, thus trying to mimic the *in vivo* dynamic ventricular behavior. The system was also used for a pilot study aimed at analyzing the aortic valve (AV) function during continuous-flow left ventricular assist device (cf-LVAD) support.
6. Chapter 6 reports the first development steps of a platform designed to work in a 4-chamber closed-loop configuration with both passive and beating hearts. An anatomical study was conducted in order to characterize the orientation of the main heart vessels, and to design a standard connection between the heart and the circulatory loop. The system was designed, assembled and some preliminary tests were conducted to proof the feasibility of a four-chamber passive-heart approach.
7. In the last Chapter, a general discussion of the PhD dissertation and the conclusive remarks are presented.

The work described in the dissertation arises from different collaborations: the activities described in Chapter 3 and 4 were carried out at the FoRCardioLab, a laboratory co-founded by Politecnico di Milano, Universitá degli Studi di Milano (Milan, Italy), and the Division of Cardio-thoracic surgery of the "L. Sacco" Hospital (Milan, Italy). The research presented in Chapter 5 and 6 was conducted at the Cardiovascular Mechanics Laboratory of the Technische Universiteit Eindhoven (Eindhoven, The Netherlands).

2

In vitro and *ex vivo* platforms for the study of the cardiovascular system: state of the art

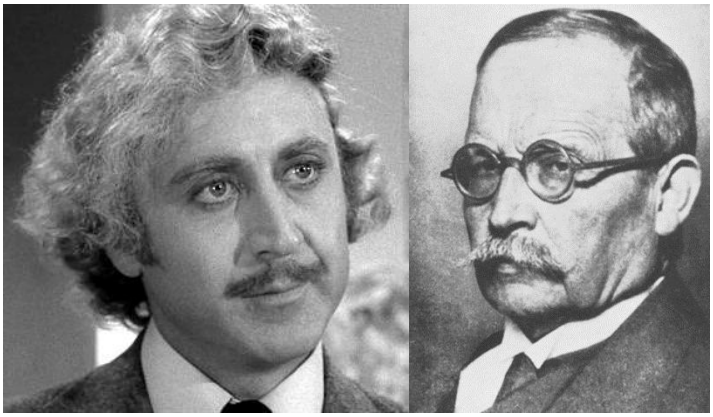

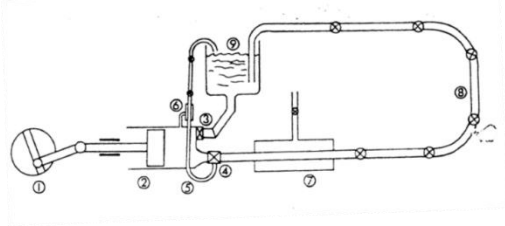

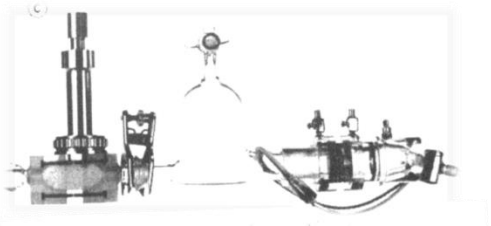

2.1 Preliminary considerations

As discussed in Chapter 1, the *in vitro* approach for the study of the cardiovascular system dates back to the 19th century and, in the last decades, have undergone substantial changes. Providing an extensive review of these developments is beyond the purpose of this dissertation. Therefore, consistently with the motivations of the study, this Chapter will offer a brief overview of the main approaches that are described in the literature with respect to both *in vitro* and *ex vivo* models. Given the aim of the present research, i.e. the development of innovative passive beating heart platforms, the state of the art platforms will be grouped in four main categories, according to the different level of integration of biological structures in the setups: classic hydraulic mock loops, simulators for excised valvular samples, passive-heart platforms and *ex vivo* beating heart models.

2.2 Hydraulic mock circulatory loops

The history of *in vitro* mock circulatory loops is intimately linked to the evolution of the clinical approaches to cardiovascular disease and, consequently, to the development of novel devices. Not surprisingly, the first significant works in this field were boosted, in the early 1960s, by the first successful surgical replacements of diseased human heart valves [71,72], that revealed new challenging perspectives for both surgeons and engineers. Indeed, the development and test of novel heart valve prosthesis was of primary interest, and required the design of *in vitro* mock ups capable of reproducing the *in vivo* hemodynamics. Similarly to many other engineering fields, research was carried out on two parallel and complementary paths: the study and the mathematical modelling of the human circulatory system, and the design of physical models.

Regarding the mathematical modeling of the circulation, the measure and characterization of the human vascular impedance, coupled with the development of mathematical models of the circulation, represented the first fundamental step. In particular, lumped parameter analogs of the arterial tree played a primary role, as their results can be directly applied to the design of experimental mock ups, thus obtaining hydraulic circuits able

to recreate a physiologic load on the heart. In this field, essential contributions were given by the research group of Noordergraaf and Westerhof [33,34,73–78], who extensively measured the input impedance of both systemic and pulmonary circulation, developed various analytical models and compared their ability to mimic the *in vivo* physiopathology. As an example, Figure 2.1 reports some of the results obtained by Toy et al. [34], who compared several lumped parameter models of the arterial tree demonstrating that more complex models are able to better mimic the human systemic input impedance, with particular respect to the high frequency wave reflection.

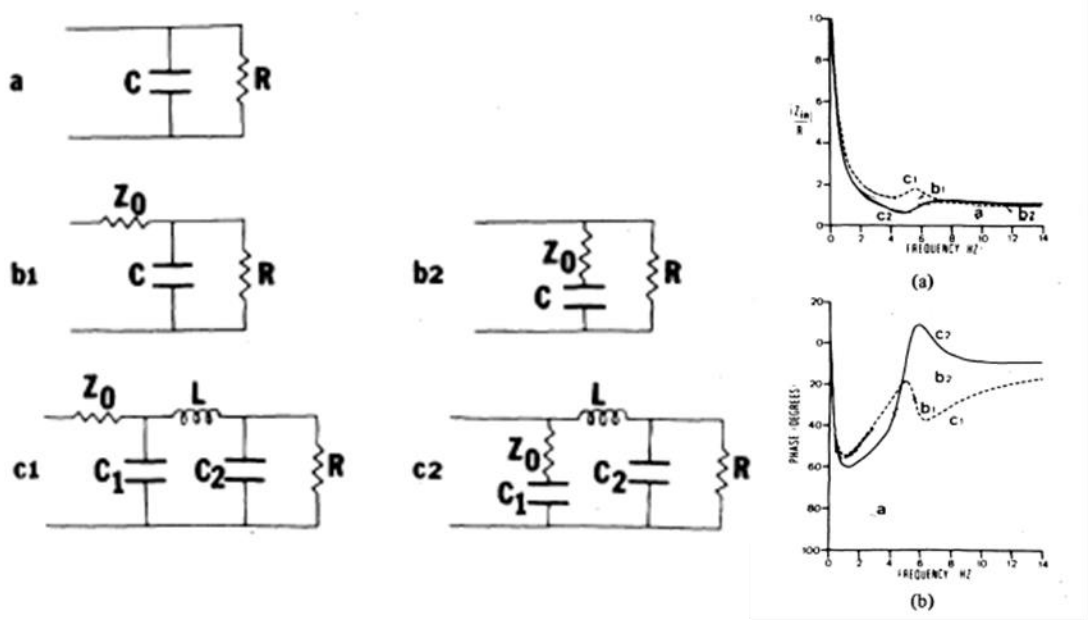

FIGURE 2.1. Left: lumped parameter models analyzed by Toy et al. [34]*. Right: magnitude (a) and phase (b) of the input impedance of the different models for the systemic arterial system.*

These and other works created a solid theoretical background that was applied to the design of the experimental models in order to achieve physiologic hemodynamic conditions. In this respect, first pioneering setups were proposed by Bjork [79] and Duran [80], followed by the more structured works of Westerhof [45] Cornhill [81], Swanson [39], Störmer [82], Verdonck [31] and Sharp [38].

All these platforms were designed to perform the mechanical and hemodynamic characterization of prosthetic devices, with particular focus to valve substitutes. They typically consisted in hydraulic loops with adjustable preload and afterload modules, actuated

by either pneumatic or volumetric systems, and capable of testing devices under controllable and reproducible conditions. Figure 2.2 shows the platform developed by Swanson, and a picture of a ball valve during its hemodynamic evaluation in the mock loop.

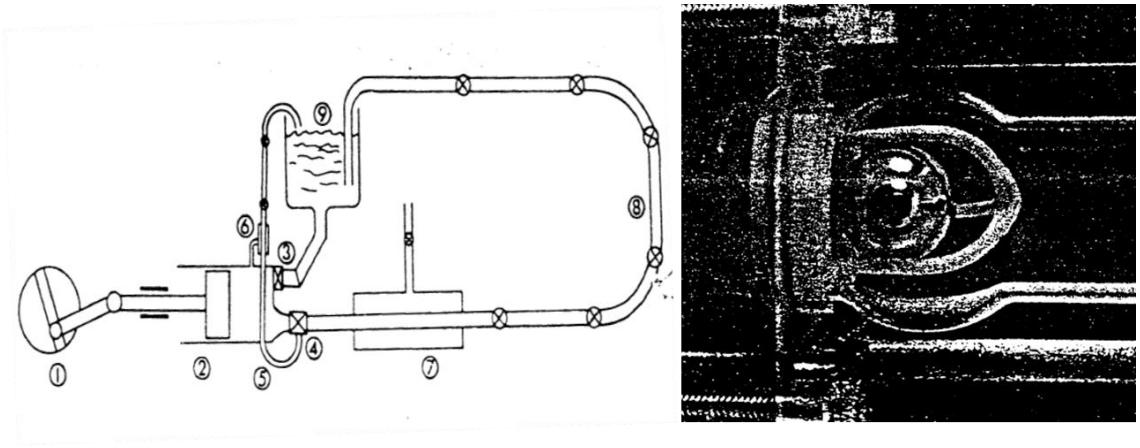

FIGURE 2.2. The mock loop developed by Swanson and Clark [39]. *Left: schematic of the circulatory system simulator. (1) Variable stroke and speed drive, (2) piston pump, (3) mitral valve, (4) aortic valve, (5), coronary artery, (6) coronary occluder, (7) simulated chest cavity, (8) distributed inertance, compliance, resistance elastic vessel, (9) venous reservoir and left atrium. Right: picture of a ball valve installed in the mock loop.*

Through the last decades, mock loops have undergone substantial evolutions trying to better reproduce the human physiology and to adapt to both technological innovations and novel cardiovascular devices. New experimental techniques, such as particle image velocimetry, echo-Doppler, magnetic resonance imaging and high-speed video, were introduced providing new insights into aspects that were largely unexplored. Novel devices, characterized by more complex interactions with the cardiovascular system (ventricular assist devices, artificial hearts, intra-aortic balloon pumps), were introduced in the clinical practice. As a consequence, researchers addressed these aspects designing *in vitro* platforms compatible with these emerging technologies and mimicking several dynamic aspects of the human physiology: the interactions between right and left circulation, the dynamic properties of the heart, the nervous regulation.

Similarly to what happened for the hemodynamic aspects, the evolution of mock loops and the development of mathematical models run in parallel. As for the latter, the time-varying elastance theory of Suga and Sagawa [35] has been widely used to describe ventricular function in terms of pressure-volume loops. Arts et al. [83] developed a one-fiber

model relating single sarcomere fiber stress and strain to ventricular pressure and volume. Heart rate variations due to cardiovascular dynamic regulations were investigated, among many, by Hyndman [84], de Boer [36], Saul [85] and van Roon [86]. All these studies contributed to develop a solid theoretical modeling of the human physiology, that has been applied by researchers to the investigation of clinically relevant issues. A representative example is given by the paper of Cox et al. [37], who used a complex model, featuring a mathematical model of the ventricular function, a lumped parameter model of the human circulation and a baroreflex model to compare different control strategies for mechanical circulatory support (Figure 2.3).

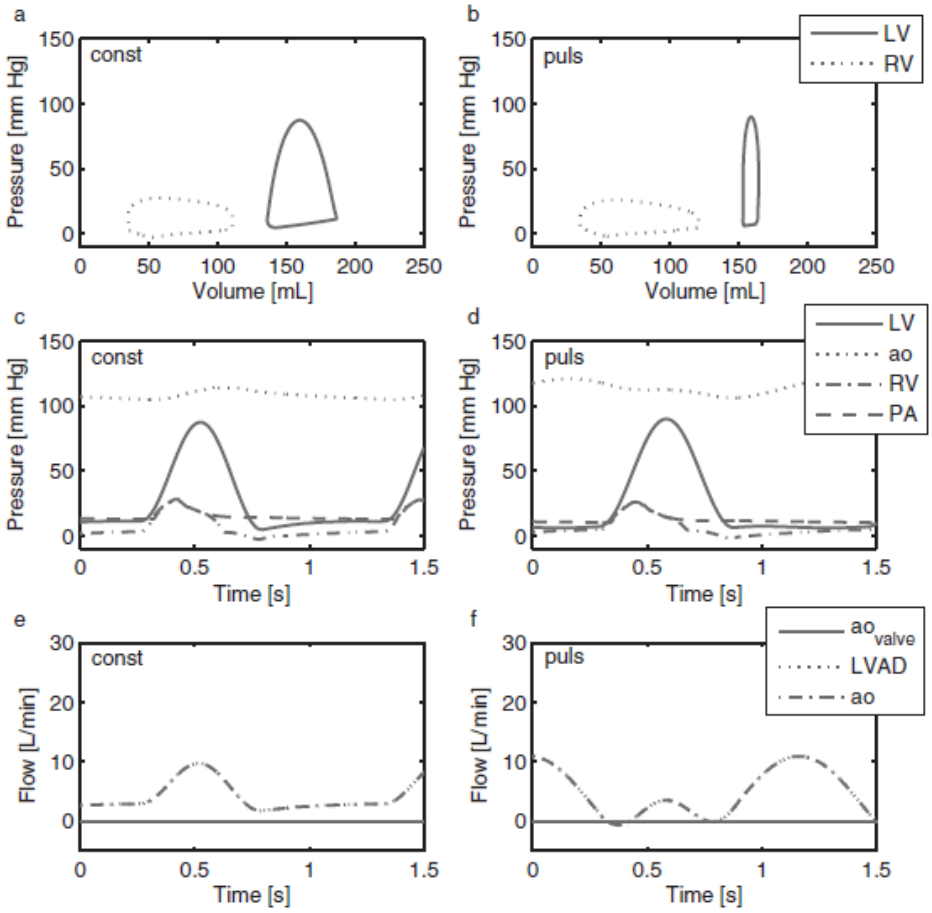

FIGURE 2.3. Results obtained by Cox et al. [37]. *Left ventricular (LV) and right ventricular (RV) pressure-volume loops for (a) constant speed and (b) pulsatile speed support. Left ventricular, right ventricular, aortic (ao), and pulmonary artery (PA) pressures for (c) constant and (d) pulsatile speed support. Flow through the aortic valve (aovalve), left ventricular assist device flow, and total aortic flow (ao) for (e) constant and (f) pulsatile speed support.*

The design of experimental *in vitro* mock loops took advantage from the just mentioned developments, as these mathematical models were increasingly implemented in order to dynamically control the actuation of the setups. Moreover, given the clinical relevance of the interactions between left and right circulation for mechanical circulatory support, *in vitro* simulators were often designed as 4-chamber closed loop systems. With respect to this evolution, relevant contributions were given by the research group of Ferrari et al. [40,87–90], that developed hybrid mock loops for the study of several support devices. Complete circulatory loops with model-controlled actuations were also developed by Baloa et al. [41], Pantalos et al. [42], Timms [43,91] (Figure 2.4), Colacino [44,92], Rutten [26,93] and others.

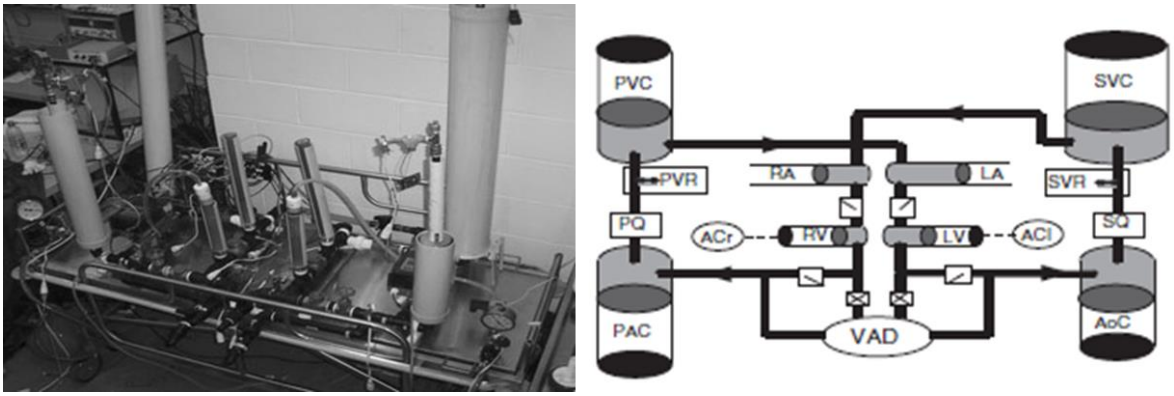

FIGURE 2.4. The mock circulatory loop designed by Timms and colleagues [43]*. Left: picture of the setup. Right: schematic of the loop. ACl, left air compressor; ACr, right air compressor; AoC, aortic compliance; LA, left atrium; LV, left ventricle; PAC, pulmonary arterial compliance; PQ, pulmonary flow rate; PVC, pulmonary venous compliance; PVR, pulmonary vascular resistance; RA, right atrium; RV, right ventricle; SVC, systemic venous compliance; SVR, systemic vascular resistance; SQ, systematic flow rate; VAD, ventricular assist device.*

Nowadays, these systems represent the gold standard for hydraulic mock loops, as they are able not only to mimic the hemodynamics of the full circulation, but also to reproduce the main dynamic responses of the cardiovascular system. Therefore, they are extensively used for device-testing and for the investigation of clinically relevant issues. Still, their main limitation relies in the complete absence of anatomical structures. As already discussed in Chapter 1, this feature does not allow the use of such platforms for the study of reparative surgeries and the analysis of minimally invasive procedures, which are becoming progressively more adopted by physicians.

2.3 Mock loops for excised valves

In order to extend the possible applications of the classical hydraulic *in vitro* approach, innovative setups capable of hosting excised valvular samples were developed in the last years. The main advantage of this methodology, in terms of possible applications, mainly relies in the possibility of studying surgical reparative procedures and performing studies on the physiopathology of the valvular structures.

This novel approach was mainly pursued, in the last years, by *i)* the group of Yoganathan, who developed and extensively used mock loops for the aortic [64,94], mitral [67,95–105] and tricuspid [68,69] valve, *ii)* the research group of Fiore and Redaelli, who designed simulators for both the aortic [63,106,107] and the mitral [66] valve, *iii)* the team of Sievers and Scharfschwerdt in Lubeck, that comprehensively studied *in vitro* the aortic valve [61,62,108–113], and *iv)* the research group of Umezu and Yamane, that focused on both the aortic [114] and mitral [65,115] valves. In the next paragraphs, two representative platforms for the aortic and mitral valve will be described more in detail, so to provide the reader with a more detailed overview of the design solutions that can be adopted and the potential applications of such simulators.

2.3.1 The mock loop for aortic valves of the Politecnico di Milano

Vismara and colleagues [63] proposed a novel approach to the *in vitro* study of the aortic valve hemodynamics, based on the preservation of the whole aortic root functional unit (ARFU). In order to achieve this goal, the authors developed a mock loop capable of housing excised aortic roots by mean of an adjustable valve holder, that allows the direct execution of surgical procedures on the valve.

The setup is reported in Figure 2.5. The mock loop is equipped with a computer-controlled piston pump, which is capable of generating both systolic and diastolic waveforms, and with an adjustable three-element windkessel module, designed to mimic the human input impedance. The platform also allows the acquisition of high-speed movies (Figure 2.6) and echo of the valve. The authors were able to obtain satisfying hemodynamic conditions, and the setup was validated analysing a state-of-the-art bioprosthesis.

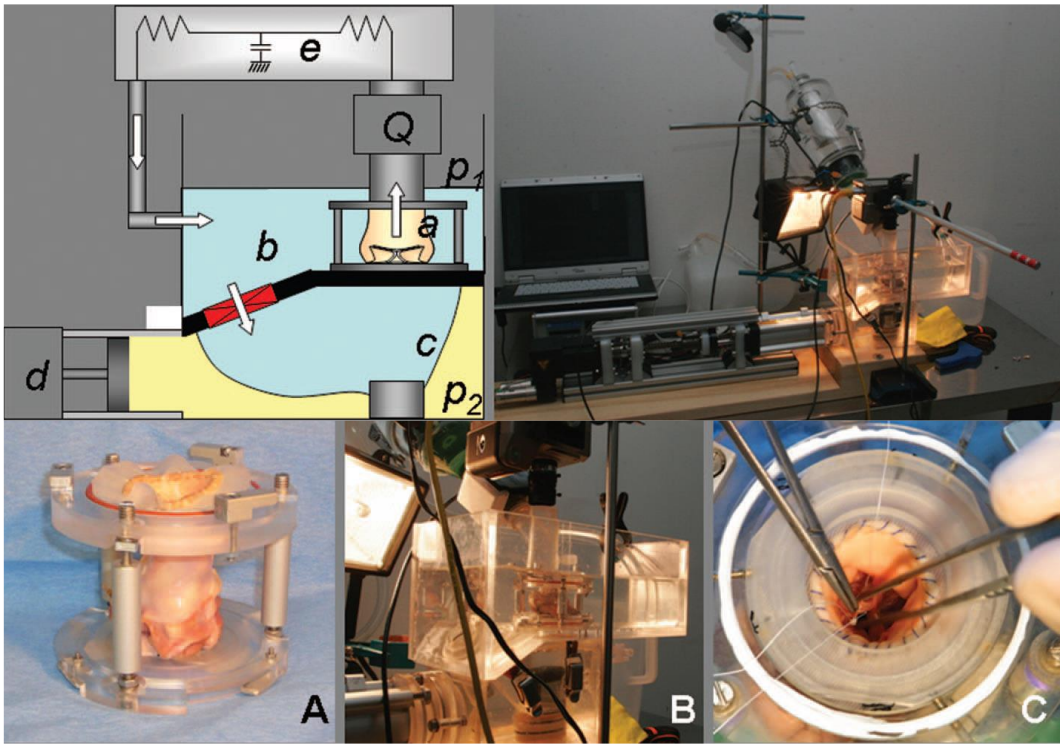

FIGURE 2.5. The mock loop for aortic root functional unit developed by Vismara et al. [63]. *Top: schematic of the simulator (left) and photograph of the complete setup with pulsatile pump and afterload (right). Bottom: detail of the holder with porcine aortic root functional unit (ARFU) sample (A); the sample holder housed in the simulator's main reservoir (B); surgery simulation on a porcine ARFU (C).*

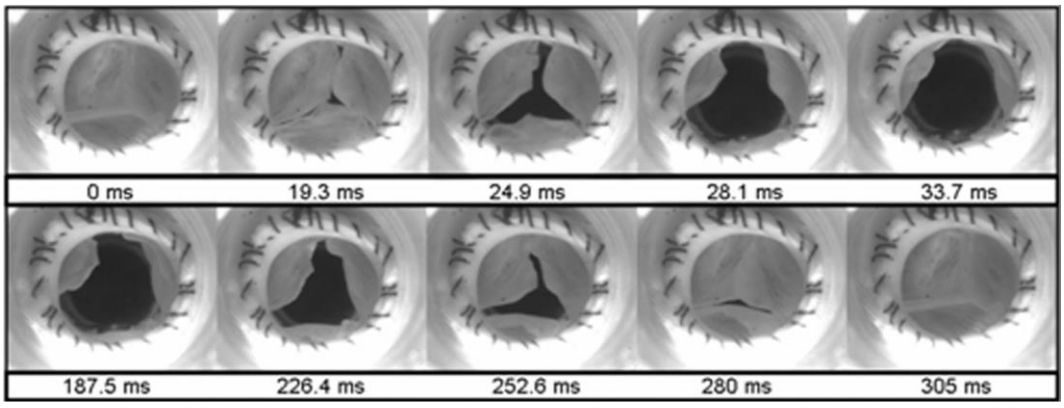

FIGURE 2.6. Sequence of snapshots recorded at 1200 fps of the opening/closing of a 21-mm porcine aortic root functional unit sample [63].

The peculiar feature of this work, which is also its most relevant innovation, is the possibility of using the whole explanted aortic root, thus ensuring a better modelling of the valve function. Indeed, the important role played by all the elements of the aortic complex (the ventricle-aortic junction, the leaflets, the sinus of Valsalva, and the sinotubular junction) in order to achieve a proper functioning of the ARFU has been clearly shown in the literature [116,117]. This uniqueness allowed the authors to investigate, in a later study, a very particular reparative surgery for aortic valve incontinence, which involves the implantation of a neo-chordae graft between the cusp and the aortic wall [106].

2.3.2 The Georgia Tech mitral valve simulator

In the past years, the research group of Yoganathan carried out extensive investigations on the mitral valve, that were mainly performed using a left heart simulator capable of housing excised mitral valve samples. The setup is shown in Figure 2.7.

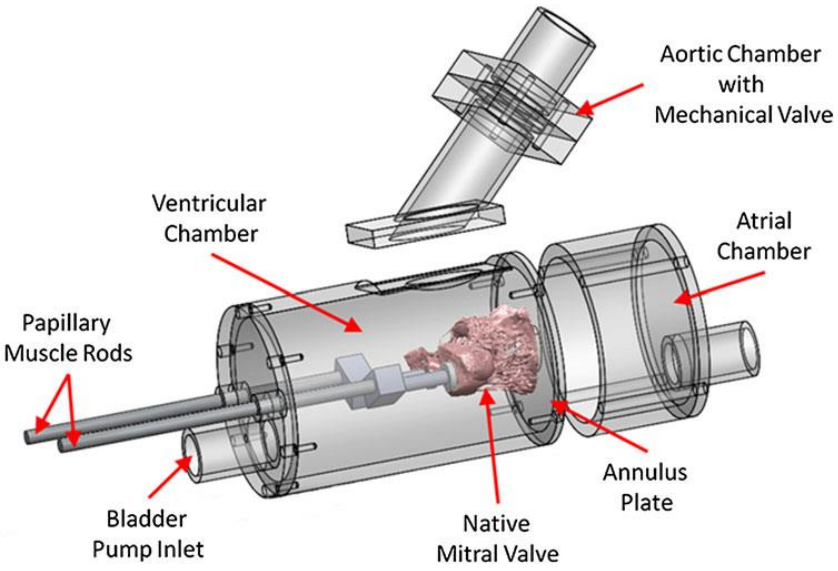

FIGURE 2.7. The left heart model developed by the research group of Yoganathan [96]*. The chamber was designed to allow for micro-CT imaging and stereoscopic PIV of native mitral valves.*

Differently from the platform of Vismara et al. [63], it consists of a computer-controlled, pressure-driven, compressible bladder system that is designed to replicate the physiologic

pulsatile flow of the left heart. The preload is obtain with a simple reservoir, that fills the left ventricle, and the afterload circuit is constituted by an RCR module with adjustable elements.

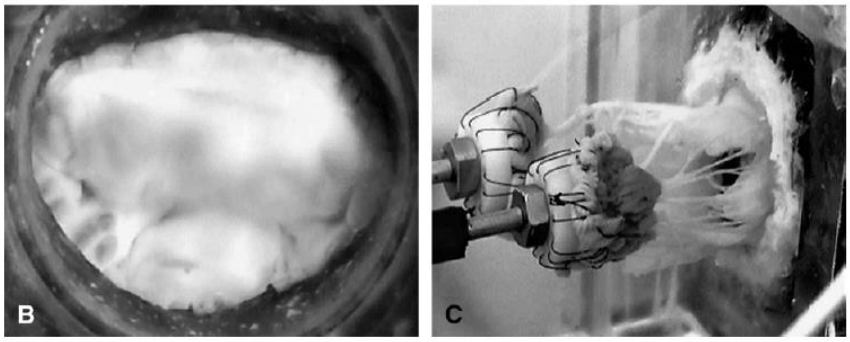

FIGURE 2.8. Pictures of mitral valves samples in the modified Georgia Tech mock loop [118]*. Left: atrial view of the mitral valve showing the anterior and the posterior leaflets. Right: ventricular view of the valve showing the chordae tendineae and the papillary muscles.*

The mitral valve housing system (Figure 2.8) is undoubtedly the most interesting feature of this setup, as it allows a fine control of each anatomo-structural element of the valvular complex. The valve annulus is sutured to a flexible silicon ring, whose shape and configuration can be varied so to simulate different pathologies. Similarly, the papillary muscles are mounted on two adjustable arms, whose 3-dimensional position can be finely tuned in order to reproduce various *in vivo* configurations. The holders are also equipped with force rods that enable the simulator to measure the total force applied on each papillary muscle. The performance of echo, high-speed movies, micro-CT, dual-camera stereo photogrammetry and stereoscopic digital particle image velocimetry (Figure 2.9) is also possible on the setup.

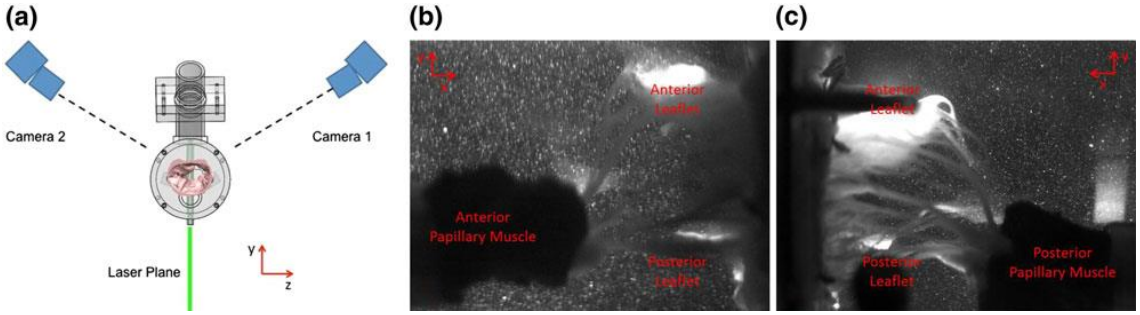

FIGURE 2.9. Characterization of native mitral valve geometry and fluid mechanics with PIV measurements carried out by Rabbah et al. [96]*. Stereoscopic configuration of the CCD cameras and orientation of the laser plane used for PIV measurements (a). Representative images of the resultant PIV field of view from the two cameras (b-c).*

2.4 The passive-heart approach

The passive heart approach represents the natural evolution of the excised valve mock loops, as it extends the same design principle, i.e. the integration of biological samples into classical *in vitro* setups, to a whole heart. The rationale for this methodology consists in the improved modelling of the *in vivo* environment from the anatomical and morphological point of view, so to broaden the spectra of possible applications of such platforms. In particular, an entire heart allows the performance of transcatheter interventions, intracardiac endoscopy, transapical procedures, multi-valvular surgeries, and may represent a more valuable model for the validation of new imaging protocols or techniques as well as for training purposes.

Nonetheless, given both its recent introduction and the experimental challenges that implies, the literature concerning passive-heart platforms is scarce. The group of Iaizzo [119] and the group of Sahn [120] developed two simple entire heart setups for imaging purposes. The first study used entire hearts as anatomical models to compare the accuracy of different imaging techniques in the measure of aortic annulus. The latter research developed a passive-heart *in vitro* model aimed at assessing interventricular dyssynchrony with 3D echography. The use of entire hearts was a mandatory requirement for both studies, as these investigations would not have been possible without a complete modelling of the heart anatomy and morphology. However, the sole use of a full heart does not represent an effective approach if the physiological functioning of the cardiac structures, in terms of hemodynamics and kinematics, is not modelled.

The first significant attempt in this direction has been made by Richards and colleagues [70], who developed a dynamic heart platform to study mitral valve repair techniques. The system was specifically designed to be an effective and affordable precursor to animal and clinical trials and to represent a platform for the evaluation of newly emerging heart repair techniques and devices.

The functioning principle of the setup (Figure 2.10) consists in the dynamic pressurization of the left ventricle of an entire swine heart by mean of a computer-controlled positive displacement pump, which is connected to the heart apex. The left atrium is passively filled by a reservoir and the systemic afterload is simply obtained with an adjustable column of fluid and a resistance. During diastole, the retrograde motion of the piston draws fluid from the left atrium through the mitral valve and into the left ventricle and piston cylinder. During

systole, forward piston motion expels fluid from the left ventricle through the aortic valve. The mock loop can also be operated in static pressure mode, with a centrifugal pump pressurizing to the left ventricle, allows the performance of both echo and endoscopic imaging.

As for the hemodynamics, Richards' goal was mainly the achievement of a physiological mitral valve load, so to compare the effects of different techniques for mitral valve repair. With respect to this, he reported satisfying results in terms of trans-mitral pressure waveforms and a good correlation between atrial pressure, cardiac output and mitral valve regurgitation. However, the overall hemodynamic behaviour of the platform was far from physiologic, in particular with respect to the aortic valve and to the extremely simplified afterload that was adopted.

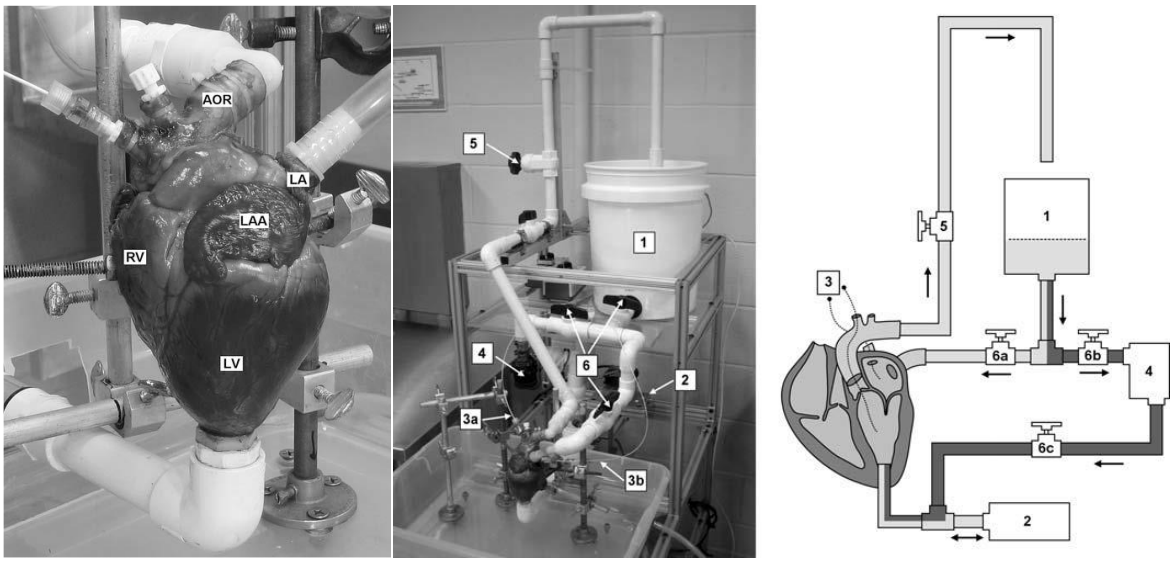

FIGURE 2.10. The passive-heart platform developed by Richards eet al. [70]*. Left: photograph of the system in operation. Right: schematic of system components: atrial filling reservoir (1), PD pump (2), pressure catheters (3), centrifugal pump (4), aortic outflow resistance valve (5), and static pressure mode valves (6). Dynamic and static pressure mode pathways are shaded light and dark, respectively.*

2.5 *Ex vivo* isolated heart models

The *ex vivo* approach consists in restoring the physiological contractility of isolated hearts through an appropriate perfusion of the myocardium. This approach was firstly described by Langendorff [6], and in the last decades isolated heart platforms were extensively applied to a wide range of fields, ranging from physiology and biochemistry to pharmacology and genetics [121]. Most of the published literature describes *ex vivo* models that were not specifically developed for the assessment of devices and/or therapies. Therefore, small animal were used as donors and the setups were mostly used in Langendorff conditions, i.e. with retrograde perfusion of the coronary bed through the cannulation of the aorta [122–126]. Obviously, none of these models is of interest for the present dissertation, since both the human anatomy and hemodynamics are not modelled.

Only few groups were able to develop ex vivo working heart models using swine hearts. Huysmans and colleagues successfully developed a two-chamber left heart model to studied the anatomy and function of the mitral and aortic valve [127,128]. Two-chamber working-heart platforms were also recently developed by other research groups [10,129,130]. Iaizzo and colleagues successfully developed a 4-chamber swine model [7,11,22], that was also extended to human hearts [9] and used for the simulation of minimally invasive procedures [20,131–133]. Nonetheless, none of these groups managed to use slaughtered hearts for their experiments, thus adopting a complex experimental procedure that is similar to organ transplantation and does not solve the ethical concerns related to the animal sacrifice.

These issues were firstly overcome by some research groups [23,24], that showed the feasibility of developing isolated heart models using hearts from slaughtered pigs. This approach has been improved by de Hart and colleagues [8,19], who developed the PhysioHeart platform (Figure 2.11), i.e. a modular *ex vivo* model, capable of working in both Langendorff perfusion and two- and four-chamber working mode.

This platform represents nowadays the gold standard of *ex vivo* models, being the only one using slaughtered hearts and coupling the heart with a carefully designed mock circulatory loop. Indeed, differently from the previously published literature, the PhysioHeart setup is equipped with specifically designed afterload and preload modules, therefore allowing the achievement of physiologic pressure and flow tracings.

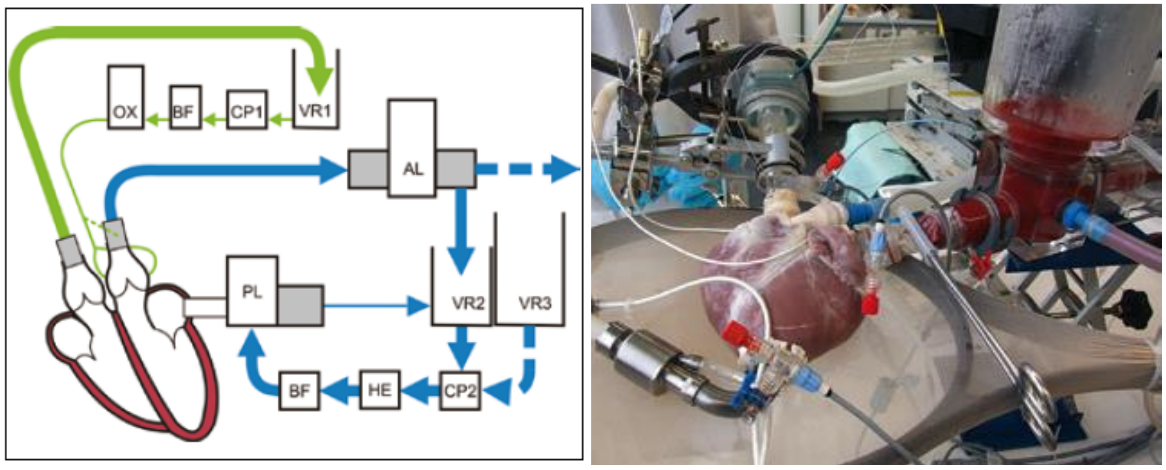

FIGURE 2.11. The PhysioHeart platform [8]. *Left: schematic representation of perfusion (green) and systematic (blue) fluid loops of the two-chamber working left heart mode. Venous Reservoirs (VR1, 2, 3), centrifugal pumps (CP1, 2), two blood filters (BF), a combined oxygenator–heat exchanger (OX) and a heat exchanger (HE) are incorporated in the fluid loops. The heart is loaded physiologically by using dedicated PreLoad (PL) and AfterLoad (AL) modules. Right: a Micromed LVAD attached to the Physioheart Platform.*

The platform, differently from other published works in which crystalloid perfusates are used [7,130], uses oxygenated whole blood as reperfusion medium, and is designed to work either with natural or selective perfusion of the coronary arteries with oxygenated blood. The latter modality permits an independent control of the myocardial perfusion, thus allowing the execution of unrestricted interventions on the beating heart and the use of a transparent buffer for the circulatory loop, which is mandatory to perform intracardiac endoscopy.

As regards the circulatory loop, the afterload consists in a compliant polyurethane tube, designed to match the *in-vivo* pressure wave speed of the aorta, and an adjustable RCR module. The preload module was constantly filled with oxygenated blood by a centrifugal pump, and was designed so to control the atrial filling pressure with an overflow through a Starling resistance. Thanks to the careful hydraulic design of the loop, the PhysioHeart achieved physiological hemodynamics, and the *ex vivo* beating heart was capable of maintaining a relevant performance for more than 4 hours.

The potential applications of the PhysioHeart, and of the *ex vivo* platforms generally, is extremely broad and include device-testing applications [10–14], imaging and visualization studies [15–20], and the study of the cardiac physiology [21,22].

2.6 Conclusive remarks

The summary of the state of the art presented in this Chapter aimed at providing the reader with an overview of the historical evolution of the different approaches that have been proposed as *in vitro* and *ex vivo* models.

Ex vivo models are able to reproduce the cardiac physiology and hemodynamics in a more controllable and repeatable setting as compared to animal models. Anyhow, the high complexity and costs often limit the use of this methodologies. Furthermore, to the best of our knowledge, no studies describing 4-chamber closed-loop models were published.

The classical *in vitro* hydraulic approach dates back to the 1960's, and thanks to the important improvements that were made in the last decades still represents a valuable and interesting platform for many studies. The main strength of this methodology is the accurate modelling of both the *in vivo* hemodynamics and the dynamic interactions between tested device and cardiovascular system. However, these platform do not model any anatomical or morphological feature, while these aspects are essential in order to study the physiopathology of the cardiac valves and to analyse both reparative surgeries and transcatheter procedures.

Therefore, *in vitro* mock loops able to house biological samples have been recently proposed and extensively used with valuable results for a wide range of applications. The existing gap between these two approaches, with particular respect to the real-time feedback of the setups and to the design of 4-chamber closed loops, is mainly imputable to the recent development of the excised samples platforms. Indeed, there is no technical contra-indication in the design of mock loops capable of housing excised samples and, at the same time, maintaining all the complex real-time controls of the state of the art hydraulic platforms.

Among the systems for excised biological samples, passive-heart platforms represent a very challenging and interesting approach, which is substantially unexplored and may represent a breakthrough with respect to the state of the art. Indeed, the use of an entire heart allows a perfect preservation of the cardiac anatomy, and may represent an ideal model for many purposes. Moreover, the development of passive-heart systems capable of recreating physiologic hemodynamic conditions would help bridging the gap with *ex vivo* and animal models, whose use is unavoidable but should be minimized for both ethical and economic reasons.

3

In vitro hemodynamics and valve imaging in passive beating hearts

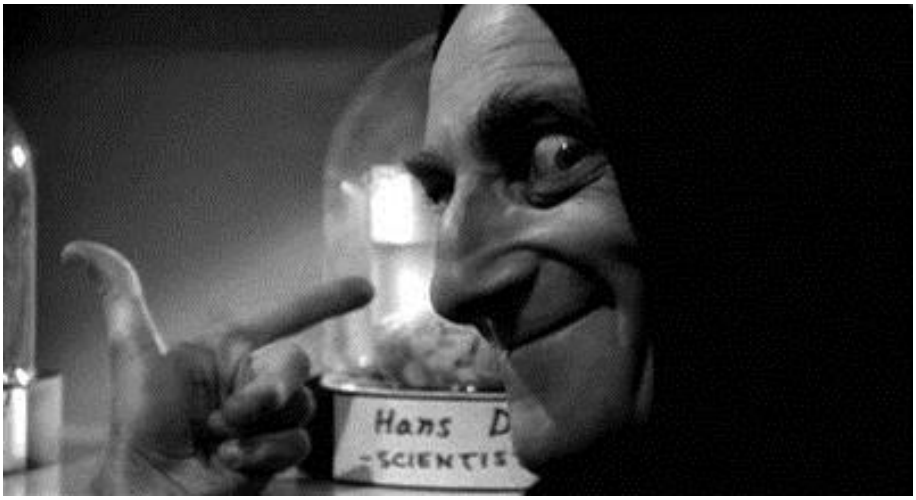

This Chapter is based on: Leopaldi A.M., Vismara R., Lemma M., Valerio L., Mangini A., Contino M., Redaelli A., Antona C. and Fiore G.B., "*In vitro hemodynamics and valve imaging in passive beating hearts*". Journal of Biomechanics, 2012, 45(7):1133-39.

3.1 Introduction

In recent years, there has been increasing evidence that both the aortic and the mitral valves should be considered as complex structures wherein different anatomic elements play strictly related roles, leading, physiologically, to the proper valve function [117,134]. In this vision, any alteration of such anatomo-functional interactions may affect both the valvular functional integrity and the ventricular function. Hence, when feasible, reparative surgical techniques have become the elective choice to restore valvular competence since they preserve the biological structures and aim at restoring the physiological biomechanical behaviour [46,48,135]. These approaches may lead to an excellent recovery of the cardiac function and to a lower incidence of valve-related complications [136]. New minimally-invasive surgical approaches to valve repair are emerging [49], whose associated mortality is comparable to that of standard surgery [137], but with less pain for the patient and lower costs thanks to a lower trauma [53,54].

In this context, as shown in the previous Chapters, the use of *in vitro* fluid-dynamic mock loops can provide reliable and quantitative information about the effectiveness of the investigated solutions [67,102,138]. Indeed, *in vitro* tests are potentially characterized by high controllability and repeatability of the simulated hemodynamic conditions.

In order to attain more realistic simulators, in the recent years mock systems able to host *ex vivo* aortic root functional units [61–63] or entire mitral valve complexes [65,66] were successfully developed. A step forward in the integration of biological samples into *in vitro* setups has been proposed by some authors, who used entire explanted hearts. Indeed, the use of an entire heart allows a better preservation of the anatomical structures, still without involving all the physiological complexities of animal models. Moreover, the use of entire hearts greatly widen the potential applications of an experimental apparatus by allowing, for example, the simulation of minimally-invasive and multi-valvular surgical procedures.

As discussed in Chapter 2, most of such entire-heart mock loop designs tried to maintain cardiac contractility *ex vivo* through myocardium perfusion [7,9,130]; these working-heart models were capable of reproducing the physiological ventricle pressure-volume relationship, although the complexity and costs of the related experimental protocols represented serious drawbacks. Alternatively, Richards et al. [70] suggested to use the heart as a passive structure, dynamically pressurized by an external pulsatile pumping system, thus

significantly reducing both complexity and cost. Although this solution showed to be effective and reliable, the hemodynamic conditions obtained by Richards and co-workers with their mock loop were not optimal. In particular, the mean flow rates and the pressure waveforms were not comparable with the typical *in vivo* ones.

In the present Chapter, we present a mock apparatus able to house an entire explanted porcine heart, whose left ventricle is pressurized by an external pumping system. In order to obtain hemodynamics conditions representative of the *in vivo* environment, and consistent with the ISO guidelines [139] in terms of numerical values and waveforms, a methodological approach, based on a lumped parameter model, was adopted for the design. The system allows for the acquisition of video recordings of the valves with endoscopic and echographic techniques and for the evaluation of the hemodynamic effects of surgical procedures in pulsatile conditions.

3.2 Design of the passive-heart platform

3.2.1 Mock loop architecture

The general layout of the mock loop is shown in Figure 3.1. The system comprises three main components, hydraulically connected to the heart sample: a computer-controlled pulse duplicator (PD), a simulator of the hydraulic input impedance of the systemic circulation (SIS) and a preload reservoir (PR).

Both the PD and the SIS were developed in a previous study at Politecnico di Milano and their detailed description can be found in the paper by Lanzarone et al. [140]. The PD is a volumetric piston pump, which can accurately replicate both systolic and diastolic flow waveforms [39,141], connected to the left ventricle apex. The SIS consists of a hydraulic circuit, based on a classical three lumped parameter model (RCR): a characteristic resistance, a capacitance and a peripheral resistance. The characteristic resistance is a polymeric net with a square mesh, the peripheral resistance is a bundle of PP hollow fibers and the capacitance is obtained with an air chamber. Both the peripheral resistance and the compliance can be adjusted in order to obtain the desired pressure waveforms. The SIS outflow drains into the

PR, which passively fills the left atrium. Atrial preload can be changed by adjusting the height of the fluid in the reservoir.

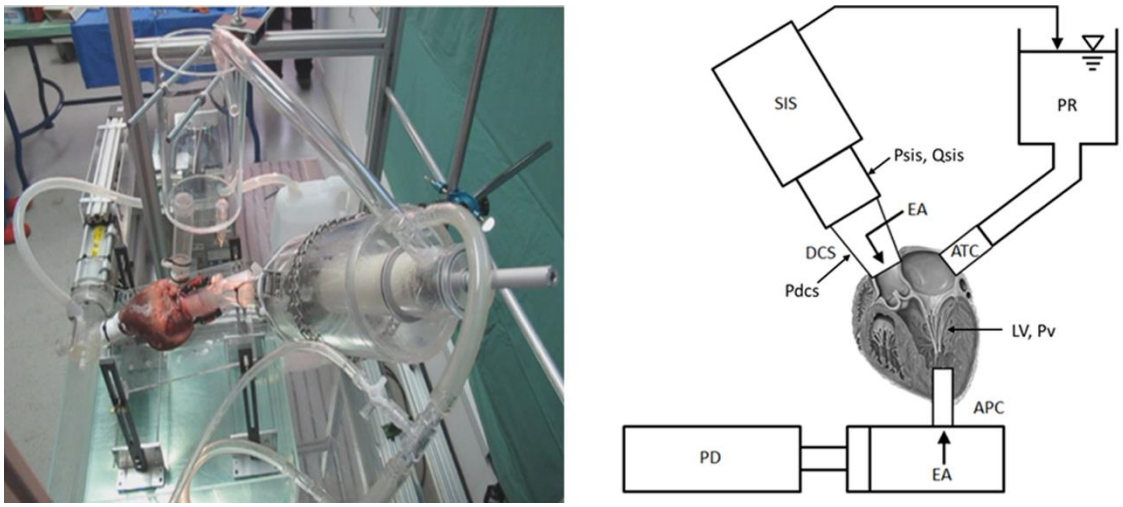

FIGURE 3.1. Mock Loop. Left: photography of the system. Right: schematic of mock loop: pulse duplicator (PD), systemic impedance simulator (SIS), preload reservoir (PR), apical connector (APC), atrial connector (ATC), double cone system (DCS), endoscopic accesses (EA).

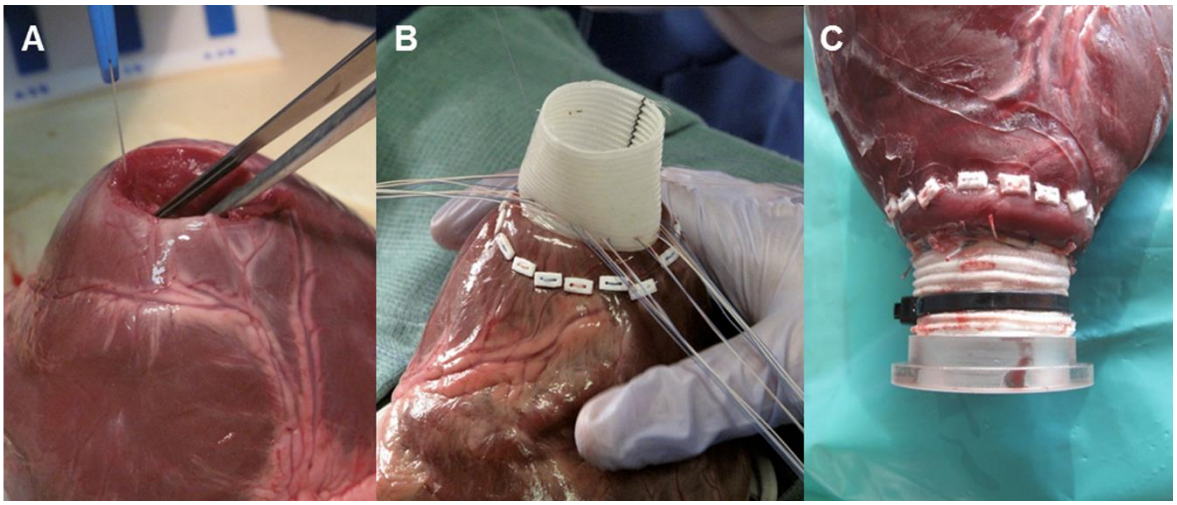

FIGURE 3.2. Sequence of the apical connection procedure. A: a 25 mm hole was surgically made in the left ventricle apex. B: the Dacron vascular prosthesis was sutured to the myocardium around the hole. C: the connector was inserted in the hole and the Dacron Prosthesis is banded to it.

The left ventricle (LV) connection with the PD is ensured through an apical connector (APC), consisting in a hollow PMMA cylinder (25 mm inner diameter), inserted in the LV through a hole punched in the myocardium (Figure 3.2A). To ensure water tightness, a Dacron vascular

prosthesis (30 mm diameter) is sutured to the myocardium (Figure 3.2B), and bound to the APC through a band (Figure 3.2C). For the atrial connection a similar solution was adopted, with an atrial connector (ATC) inserted into the atrial wall. The connection between the aorta and the SIS is obtained by using a double-cone system (DCS), i.e., the aortic wall is fixed between two coaxial hollow cones having the same taper angle. This solution allows for an easy and sutureless connection, ensuring both mechanical securing and water tightness. The mock loop is also provided with two endoscopic accesses (EA), located in the apical region and in the aorta.

3.2.2 **Design methodology**

In order to achieve satisfying hemodynamic conditions in the mock loop, a lumped parameter model (LPM) was used preliminarily to and during the design phase as a predictive tool; its electrical analog is shown in Figure 3.3. By providing the flow waveforms imposed by the pumping system (Q_{pd}) as an input, the solution of the ordinary differential equations governing the LPM gave an estimation of the mock loop pressure and flow patterns (P_v, P_{dcs}, P_{sis}, P_{at}, Q_{sis}) as outputs [140].

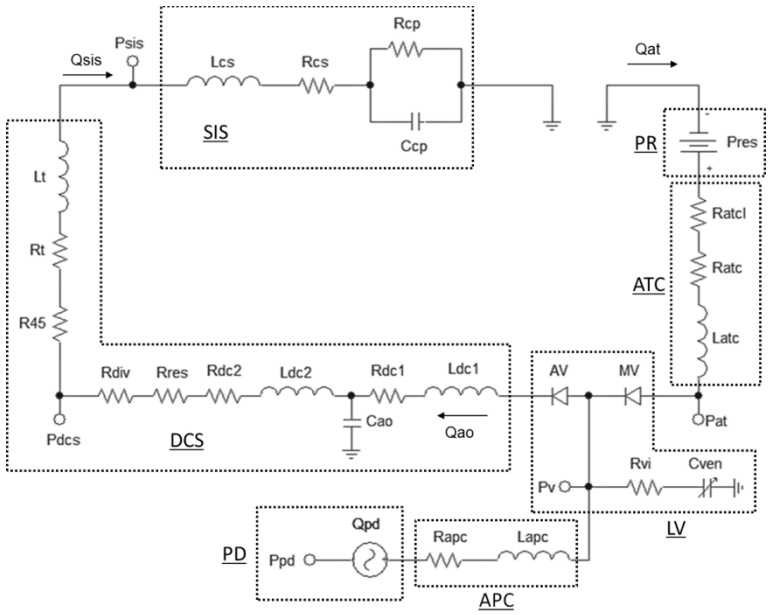

FIGURE 3.3. Lumped parameter model electrical analog. The blocks are referred to the mock loop components reported and labelled in Fig. 3.1.

The design started from the identification of the general requirements and constraints, i.e. connections to existing components (PD, SIS), imaging, instrumentation, manageability. Firstly, the effects of either different sizings of the hydraulic components (APC, DCS, AOC) or different mock loop working conditions (Q_{pd}, P_{res}) were investigated with the LPM. The results of the numerical simulations were compared to the *in-vivo* curves, and the best sizing in order to achieve good hemodynamic conditions in the mock loop was identified. Then, the effects of different hydraulic properties of the heart sample on the system were analyzed, thus allowing for the investigation of the effects of the biological sample variability.

The definition of model variables and parameters, referred to the mock loop general layout of Figure 3.1, is reported in Table 3.1. The numerical values reported are those that were finally identified after the model-aided design process. The resistances and the inertances were determined according to classical hydraulic laws [142,143]. In particular, the distributed resistances (R_{apc}, R_{dc1}, R_{dc2}, R_t, R_{atc}) were determined according to the Blasius formula [143]:

$$\Delta P = 0.3164 * Re^{-0.25} * \rho \frac{v^2}{2} \frac{l}{D} \qquad \text{(eq 3.1)}$$

where *Re* is the Reynolds number, *v* is the velocity of the fluid, *ρ* is the density of the fluid, *l* is the length of the duct and *D* is its diameter. The localized resistances (R_{res}, R_{div}, R_{45}, R_{atcl}) were estimated according to the classical hydraulic laws [143]:

$$\Delta P = \beta \rho \frac{v^2}{2} \qquad \text{(eq 3.2)}$$

where *β* is a coefficient depending on the geometrical discontinuity. All these resistances were multiplied by a safety coefficient of 1.5. The inertances of the cylindrical ducts (L_{apc}, L_{dc1}, L_{dc2}, L_t, L_{atc}) were determined according to the following expression, valid for a flat velocity distribution [142]:

$$L = \rho \frac{l}{A} \qquad \text{(eq 3.3)}$$

where *l* and *A* are the length and the section of the duct. The values of both the aortic root compliance (C_{ao}) and the systemic impedance simulator components (R_{cs}, R_{cp}, C_{cp}, L_{cs}) were taken from the literature [140,144].

The ventricular chamber was modelled with the series of a non-linear compliance and a linear resistance, respectively accounting for the exponential pressure-volume relation of

the passive LV [145,146] and the viscoelastic behaviour of the myocardial tissue [147,148]. The non-linear compliance was modelled according to the data by Diamond [145], who measured the value of the parameters *a* and *b* in *rigor mortis* canine left ventricles, thus yielding an estimation of the LV compliance:

$$C_{ven} = \frac{dV}{dP} = k\,\frac{1}{aP + b} \qquad \text{(eq 3.4)}$$

The factor k in Eq. 3.4 was set to 2.5, since the average LV volume of the porcine hearts used in the present study was 2.5 times as large as the ones measured by Diamond with canine hearts. The value for the ventricular viscous resistance was derived from the work of Schmitt [149], who measured τ, a parameter of early diastolic relaxation time, in an *in vivo* pig model. Coherently with the RC model adopted for the description of the left ventricle, the viscous resistance was determined as:

$$R_{vi} = \frac{\tau}{C_{ven}} \qquad \text{(eq 3.5)}$$

where C_{ven} was calculated according to Eq. 3.4 with a reference working pressure of 100 mmHg. Numerical simulations were performed (Simnon 3.0, SSPA, Göteborg, Sweden) using a fixed time step of 5 ms. In order to compare the predictions of the model with the experimental measurements, the root mean square error (RMSE) was computed for the measured variables (P_v, P_{DCS}, P_{sis}, Q_{sis}) according to equation 3.6:

$$RMSE = \sqrt{\frac{1}{N}\sum_{i=1}^{N}(X_{mod} - X_{mea})^2} \qquad \text{(eq 3.6)}$$

where X_{mod} is the value of the variable as predicted by the model and X_{mea} is the measured value. N is the number of samples constituting one cycle, as the time step in the simulations was set to be the consistent with the acquisition frequency of the experimental data (200 Hz).

TABLE 3.1. Description of the variables and of the parameter of the model. The numerical values that are reported for the LPM parameters are the ones that were identified, after the design process, as the best ones for the achievement of satisfying hemodynamic conditions, given the other system requirements.

Component	Parameter/Variable	Value	Description

PD	*Qpd*	-	Flow rate pattern imposed by the PD
	Ppd	-	Pressure in the PD
APC	*Lapc [kg m-4]*	$2\ 10^{5}$	Inertance of the APC
	Rapc [kg m-4 s-1]	$1.2\ 10^{4}$	Resistance of the APC (minor losses neglected)
LV	*Pv*	-	Ventricular pressure
	a [ml^{-1}]	0.124	Parameters used to calculate the LV compliance (Eq. 4)
	b [mmHg ml^{-1}]	0.57	
	τ [s]	$3.18\ 10^{-2}$	Early diastolic relaxation time (Eq. 5)
	Rvi [kg m^{-4} s^{-1}]	$2.2\ 10^{7}$	Viscous resistance (Eq. 5)
	MV, AV	-	Ideal diodes describing the mitral and aortic valve
DCS	*Qao*	-	Flow rate in the aortic root
	Rdc1 [kg m^{-4} s^{-1}]	$5.7\ 10^{7}$	Distributed resistances of the DCS
	Rdc2 [kg m^{-4} s^{-1}]	$5.7\ 10^{7}$	
	Ldc1 [kg m^{-4}]	$5.1\ 10^{4}$	Inertances of the DCS
	Ldc2 [kg m^{-4}]	$5.1\ 10^{4}$	
	Cao [m^{3} Pa^{-1}]	$7.5\ 10^{-10}$	Aortic root compliance
	Rres [kg m^{-7}]	$2.9\ 10^{5}$	Minor resistances due to the geometry of the aortic connection
	Rdiv [kg m^{-7}]	$3.7\ 10^{5}$	
DCS	*Pdcs*	-	Pressure in the DCS
	R45 [kg m^{-7}]	$3.9\ 10^{5}$	Minor resistance due to the bended DCS outflow
	Rt [kg m^{-4} s^{-1}]	$4.3\ 10^{7}$	Resistance of the duct between DCS and SIS
	Lt [kg m^{-4}]	$2.9\ 10^{5}$	Inertance of the duct between DCS and SIS
SIS	*Qsis*	-	Flow rate in the SIS
	Psis	-	Working pressure of the SIS
	Rcs [kg m^{-4} s^{-1}]	$1.1\ 10^{7}$	Characteristic resistance of the SIS
	Rcp [kg m^{-4} s^{-1}]	$2.4\ 10^{8}$	Peripheral resistance of the SIS
	Lcs [kg m^{-4}]	$5\ 10^{5}$	Inertance of the SIS
	Ccp [m^{3} Pa^{-1}]	$2.7\ 10^{-8}$	Compliance of the SIS
PR	*Qat*	-	Flow rate in the preload circuit
	Pres [Pa]	$3.3\ 10^{3}$	Geodetic pressure due to the fluid in the PR

ATC	*Latc [kg m^{-4}]*	1.9 10^5	Inertance of the ATC
	Ratc [kg m^{-4} s^{-1}]	2.9 10^7	Resistance of the ATC
	Ratcl [kg m^{-7}]	9.8 10^5	Minor resistance due to atrial geometry
	Pat	-	Atrial pressure

3.2.3 **Functional assessment**

In order to verify the mock loop hemodynamics, three experimental trials were carried out. Fresh entire explanted hearts from 150-170 kg pigs were obtained from a local abattoir. Surgeons examined the biological samples and ensured for the absence of valvular pathologies. The heart was housed in the mock loop and connected respectively with the APC, ATC and DCS. The system was filled with physiologic saline solution (0.9% NaCl) by using a peristaltic pump (model 10-10-00; Stöckert Shiley Instruments, München, Germany). The PD was then gradually activated until a heart rate of 70 bpm was reached. Finally, the compliance and the resistance of the SIS were adjusted in order to reach a SIS working pressure included in the range 80-120 mmHg. The time needed for each whole experimental procedure was around 2 hours.

The mock loop was equipped with piezoresistive transducers (PC140 series, Honeywell Inc., Morristown, NJ) and with an ultrasound flowmeter (HT110R, Transonic Systems Inc., Ithaca, NY) for hemodynamic measurements (Figure 1 - P_v, P_{dcs}, P_{sis}, Q_{sis}). All data were acquired with an A/D converter (USB-6210, National Instruments, Austin, TX) at a sampling frequency of 200 Hz. Endoscopic video recordings of the valvular complexes were obtained with a rigid 10 mm endoscope lens (Olympus Europe, Hamburg, Germany), coupled with a lighting column (Olympus Visera CLV-S40) and a video acquisition column (Olympus Visera OTV-S7 Digital Processor). Echocardiographic images and videos were obtained with an ultrasound system (HDI 5000, Philips, Eindhoven, NL) with a 12 to 3 MHz probe (Philips L12-3).

3.2.4 Error analysis

The absolute accuracy for each component of the data acquisition system is defined as:

$$\mathrm{AA} = \pm (V_i * \%R_m + O + N + T_D) \qquad \text{(eq 3.7)}$$

where V_i is the input voltage, $\%R_m$ is the percentage of the reading, O is the offset value, N is the system noise, and T_D is the temperature drift. The uncertainty in the analog to digital conversion for the USB-6210 data acquisition card is negligible as the 16 bit unit yield an error of less than 0.01%.

Regarding pressure measurements, the 143PC05 transducers that were used for the present work are differential sensors which are compensated for temperature drifts in a wide range (-18° to 63°C), that included our working temperatures. As reported by the manufacturer, sensors' hysteresis and non-linearity were ±0.15% and ±0.75% respectively. Before every experiment, a two-point calibration was performed on the whole measurement setup. Null pressure was calibrated by exposing both pressure ports in atmosphere, while a manometer with an accuracy of ±2 mmHg was used to apply a pressure of 200 mmHg, which was used as second point for the calibration. This calibration protocol provided for the removal of any offset and, given the accuracy of the manometer, resulted in a percentage error of ±1% on the pressure readings. The errors deriving from the sensor's hysteresis, non-linearity and from the calibration can be combined to estimate the percentage of the reading accuracy of the sensor ($\%R_m$) using the root of the sum squared approach:

$$\%R_m = \sqrt{\left(\varepsilon_{hys}\right)^2 + (\varepsilon_{lin})^2 + (\varepsilon_{cal})^2} \qquad \text{(eq 3.8)}$$

This results in an accuracy of ±1.26%. The input-referred noise level due to the whole measurement chain was estimated from the standard deviation of the measured signal with a constant input pressure, and was ±0.3 mmHg. Anyhow, all acquired data were averaged over 5 consecutive cycles, thus improving the signal to noise ratio of a factor $\sqrt{5}$ and resulting in a noise level of ±0.13 mmHg. Therefore, according to equation 3.7, and assuming a working pressure of 100 mmHg, the absolute accuracy on the pressure measurements was ±1.39 mmHg.

Regarding flow measurements, the absolute accuracy of the flow probe, as given by the manufacturer, was ± 4% after on-site sensor calibration with the system Flow Module for

the tubing and liquid in use. The uncertainty ω_R of a quantity R, which is derived from n independent variables, e.g. $R=R(X_1, X_2, \ldots X_n)$, is defined as:

$$\omega_R = \pm \sqrt{\sum_{i=1}^{n} \left(\frac{\partial R}{\partial X_i}\omega_i\right)^2} \qquad \text{(eq 3.9)}$$

In our study, the only derived quantities are the pressure differences, for which equation 3.9 gives an absolute accuracy of ± 1.97 mmHg.

3.3 Performance assessment of the platform

3.3.1 Hemodynamic evaluation

The simulated pressure and flow tracings obtained with the LPM are reported in Figure 3.4.

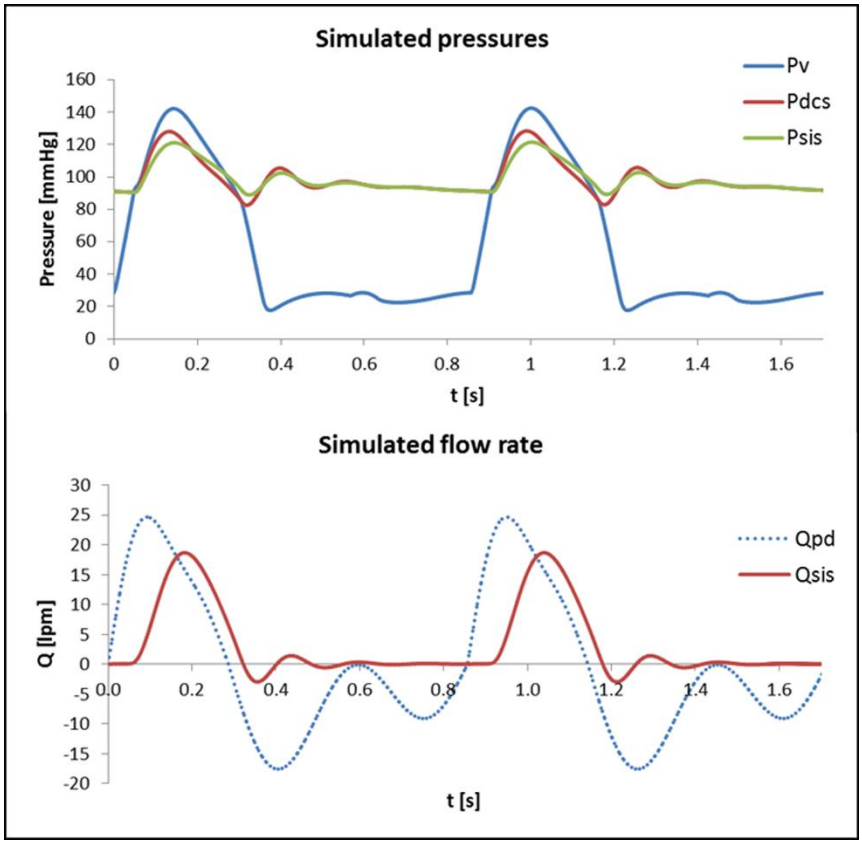

FIGURE 3.4. Pressure (top) and flow (bottom) tracings obtained from the simulations carried out on the LPM. The legend refers to the electrical scheme reported in Fig. 3.3.

Tracings are affected by two main constraints, which sensibly affect the overall behaviour: the presence of a non-contracting distensible heart and the presence of rigid connectors between the heart and the SIS, which introduces local resistances and inertial effects. Despite such constraints, results are satisfying both in terms of wave morphology and numerical values. Ventricular, DCS and SIS pressures are respectively included in the 20-140, 80-130 and 90-120 mmHg range, thus in good agreement with the expected values. The systolic pressure

drop between the ventricular and the DCS tracings is mainly caused by the DCS, whose geometry causes an appreciable hydraulic hindrance downstream of the aortic valve. The early diastolic oscillations that can be observed in the DCS pressure tracing were unavoidable and due to inertial effect. The mean flow rate in the afterload circuit is 3.2 lpm, lower than the 5 lpm imposed by the PD because of the capacitive effect of the LV. This difference is due to a net volume sequestration of 25.7 ml/cycle, which would correspond, under the hypothesis of cylindrical geometry for the LV (length 70 mm, diameter 40 mm), to a radial dilatation of 2.7 mm. The LV compliance, moreover, causes a phase displacement between the two flow rate tracings.

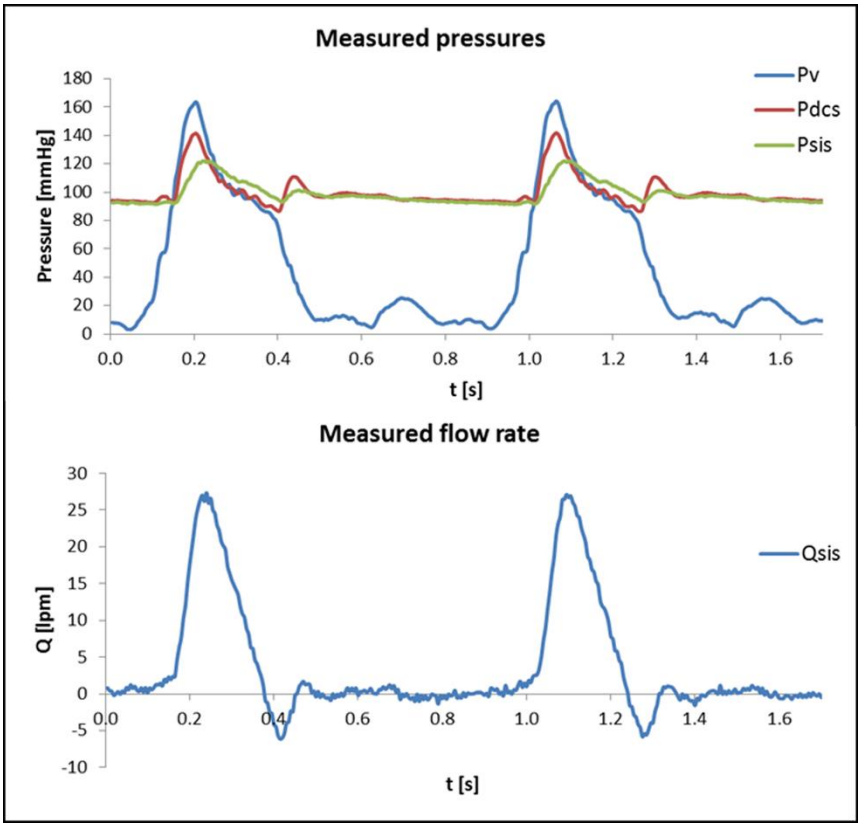

FIGURE 3.5. Measured pressure (top) and flow rate (bottom), with reference to the functional assessment Nr.2. The legend refers to the mock loop layout reported in Fig. 3.1.

Figure 3.5 shows, with reference to experiment Nr.2, the measured pressure and flow tracings. All the experimental tracings showed a good correspondence with the physiological wave shapes and a good reproducibility was observed among the three different experimental

campaigns (Table 3.2). The pressure tracings are comparable with the typical *in vivo* curves; maximum ventricular, DCS and SIS pressure are respectively 160, 140 and 120 mmHg. The diastolic ventricular pressure is higher than the typical physiological one because of the geodetic pressure of the atrial reservoir that was aimed at ensuring a correct diastolic filling. The flow measured at the SIS inlet resembles the physiological waves and the maximum peak flow is up to 26 lpm.

TABLE 3.2. Average pressure and flows for the experiments and the simulations, and the respective root mean square error (RMSE). Data is reported as mean ± SD. The notation refers to the variables reported in Figure 3.3.

	Qsis	**Pv**	**Pdcs**	**Psis**
Measured	3.5±0.1 lpm	50±2 mmHg	101±2 mmHg	97±1 mmHg
Simulated	3.2 lpm	40 mmHg	95 mmHg	96 mmHg
RMSE	2.3±1.1 lpm	20.2±1.9 mmHg	8.3±1.2 mmHg	3.8±1.4 mmHg

Table 3.2 shows the average values of both the experimental and simulated variables, together with the root mean square error calculated between the measured and the simulated tracings. Figure 3.6 shows a direct comparison between the modelled and the measured tracings, with reference to experiment Nr.2.

The small standard deviation in the experimental average values (Table 3.2) confirms the high hemodynamic reproducibility between different experimental sessions. Moreover, on the average the LPM prediction is fairly good, although some experimental peaks are underestimated by the model (Figures 3.6). In particular, at the systolic peak, the maximum percentage differences for the ventricular pressure and flow rate tracings are 15% and 46%, respectively. This observation is in good agreement with the RMSE, which is significantly higher for the flow rate (2.3±1.1 lpm, i.e. about 66% of the mean) and the ventricular pressure (20.2±1.9 mmHg, i.e. 40% of the mean) as compared to the one computed for the DCS and SIS pressures (8.3±1.2 and 3.8±1.4 mmHg, respectively).

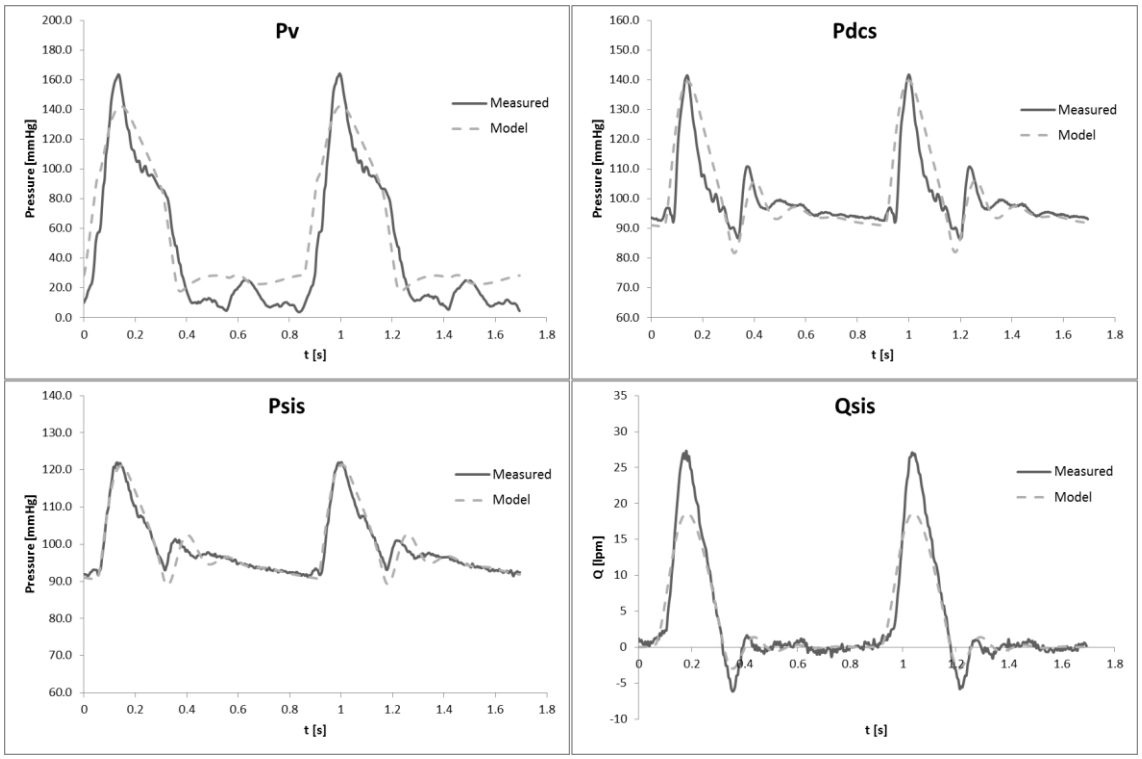

FIGURE 3.6. Comparison between measured and simulated pressure and flow rate tracings. Measured data are taken from experiment Nr.2. The notation of the variables refers to the lumped parameter model reported in Fig. 3.3.

3.3.2 Imaging of valvular structures

During the mock loop functional assessments, both endoscopic and echocardiographic video images of the valvular structures were obtained; some representative frames are reported in Figure 3.6, while movies are available online.

The co-axiality between the endoscopic lens and the aortic root provided very good images of the aortic valve, and the apical access showed to be extremely effective in the simultaneous imaging of the mitral and aortic valves. In particular, the dynamics of both the chordae tendineae and the papillary muscles could be observed.

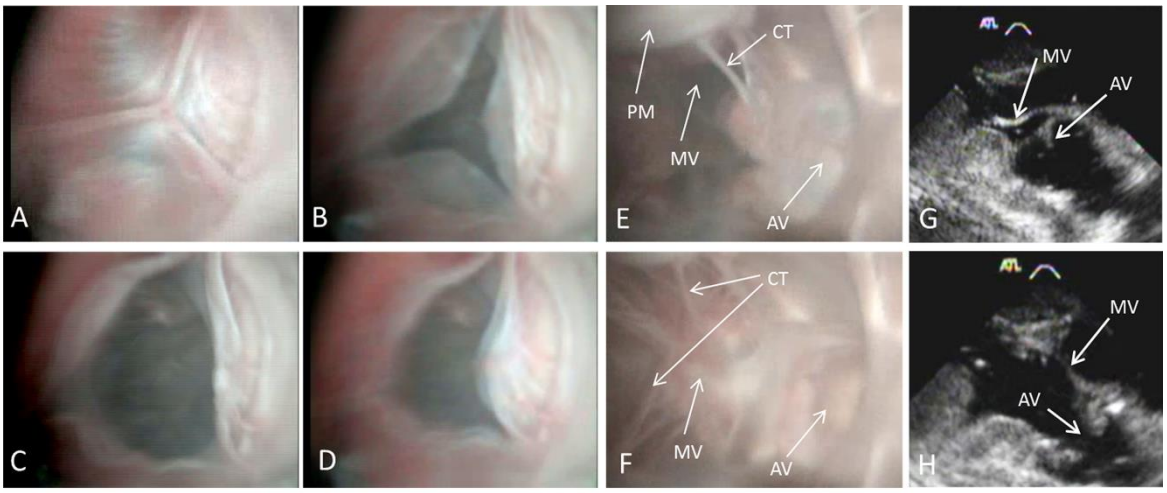

FIGURE 3.6. Left: sequence of endoscopic images showing the opening and closure of the aortic valve (A, B, C, D). Centre: endoscopic images (E, F) obtained from the apical access, showing the opening and closure of the mitral and aortic valve (MV, AV). The apical access enable the visualization of both the chordae tendineae (CT) and the papillary muscles (PM). Right: echocardiographic images of the diastole (G) and of the systole (H) showing the mitral and aortic valves (MV, AV).

3.3.3 Analysis of the mitral valve functionality

An analysis of the mitral valve was carried out in order to verify that the passive actuation of the left ventricle did not cause any oddity in the valve function. Figure 3.7 compares the tracings of the pressure differential across the mitral valve measured in the proposed mock loop (left), with the results obtained by Ritchie et al. [67] with an *in vitro* mock loop specifically designed for mitral valve samples (right).

Mean diastolic mitral pressure drop was 0.2 mmHg, thus showing a very good hemodynamic behavior of the mitral valve during diastole. As concerns the systole, the peak trans-mitral pressure was 144 mmHg, comparable with the 106 mmHg measured by Ritchie and colleagues.

Moreover, the trans-mitral pressure difference tracings obtained with our mock loop show a good correspondence, in terms of wave morphology, with both the typical *in vivo* curves and the results obtained by Ritchie and colleagues. The bumps that are present in our curves during the systole are mainly due to the oscillations in the atrial pressure caused by

the dilatation of the left ventricle, which does not apply for Ritchie's mock, wherein valve samples are housed within rigid conduits.

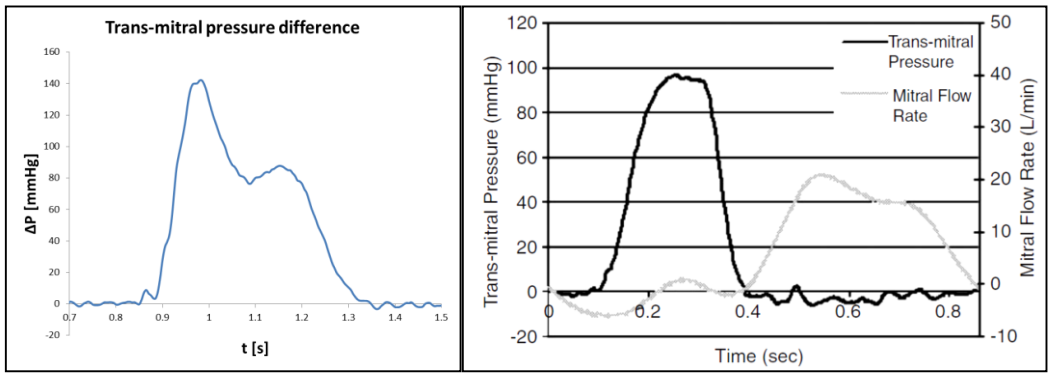

Figure 3.7. Trans-mitral pressure difference across the mitral valve in the presented mock loop (Left) and in the system developed by Ritchie et al. [67] *(Right).*

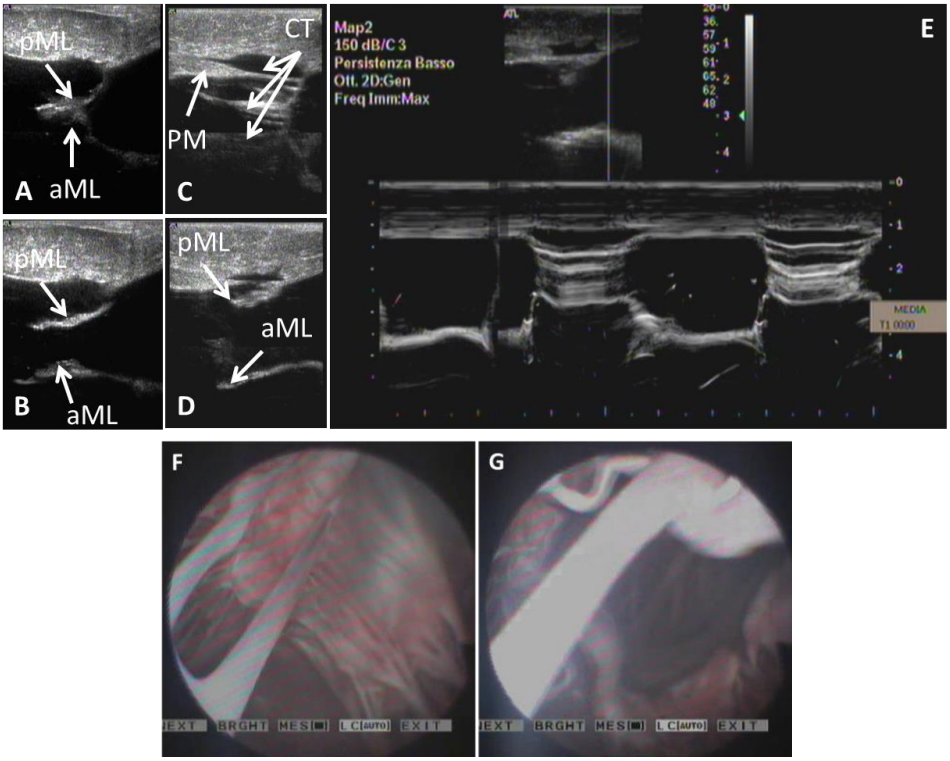

Figure 3.8. A-D: 2D echographic images showing the closed (A, C) and opened (B, D) mitral valve. Both the anterior and the posterior mitral leaflet (aML, pML) are clearly visible, as well as the papillary muscles (PM) and the chordae tendineae (CT). E: M-mode echo of the mitral valve during the opening and closing phase. F-G: Endoscopic images showing the closed (F) and opened (G) mitral valve.

One expert cardiologist and one expert surgeon also performed a detailed echo and endoscopic analysis of the mitral valve function (Figure 3.8). Despite being qualitative, this analysis aimed at evaluating the proper functioning of the mitral valve in the mock loop.

As these images demonstrate, the mitral valve appears to be perfectly competent and there is no evidence of leaflet prolapse. Indeed, the M-mode echo (Figure 3.8, E) shows a very good leaflet coaptation depth during systole, as well as a proper leaflet opening during diastole. This observation is confirmed by the analysis of both the long-axis echo images (Figure 3.8, A-D) and the endoscopic images (Figure 3.8, F-G). In particular, the reported frames show that, during the systole, the chordae tendineae are tensioned.

3.4 Discussion

In principle, the use of integral heart structures in *in vitro* tests of heart valve hydrodynamics is intrinsically superior with respect to the use of excised valvular structures mounted in artificial structures. Indeed, maintaining the whole structural continuity of the natural heart tissues offers the possibility to replicate the physiological and/or surgical scenarios in a way that is hardly attainable otherwise. In practice, however, obtaining satisfying performances by a whole-heart *in vitro* apparatus is a demanding task of biomechanical design, which involves finding a suitable trade-off among highly heterogeneous specifications concerning hemodynamic likelihood, sample handling, surgical and imaging access, standardization, reproducibility, etc.

In this Chapter we presented a novel reliable and cost-effective mock loop, suitable for hosting an entire explanted swine heart activated as a passive structure by an external mechanical pump. Thanks to a model-aided design process, the system was capable of replicating flow and pressure waveforms that resembled the typical *in vivo* ones, while allowing the acquisition of high-quality echo and endoscopic images of the cardiac valves. Regarding the performance of surgical procedures on the hosted heart, both the optimized system layout and the heart-circuit connections made the access to the valvular structures comparable with the operating room one.

A LPM was purposely developed as a simulation tool for the mock loop's hydrodynamic design. With the optimized circuit layout, simulations predicted a satisfying hemodynamic behaviour, which was then confirmed during the experimental functional assessments. Indeed, most outputs of the LPM were highly resembling the respective experimental tracings, as qualitatively shown in Figure 3.6 and confirmed by the values of the RMSE coefficients. Major discrepancies were found only in the flow rate and in the ventricular pressure tracings, for which average values were coherent but the oscillation range was underestimated by the model, suggesting that the value of the ventricular compliance used in the model overestimated the real one. Anyhow, this was deemed acceptable in light of the efforts spent to adapt exponential pressure-volume relations and time constant values taken from the literature to model the real viscoelastic behavior of the passive LV myocardium.

The morphology of all the experimental pressure tracings was coherent with the known physiological curves and the ventricular, DCS and SIS pressure peaks were respectively equal to 160, 140 and 120 mmHg. Some non-physiologic oscillations were present in the early diastole in the DCS pressure tracing; the LPM showed that the amplitude of these oscillations is dependent on the fluid inertia in the DCS. Indeed, the interaction between the inertance of the rigid hydraulic conduits downstream of the aortic valve (L_{dcs} and L_t, Figure 3.3) and the natural compliance of the aortic root (C_{ao}) results in a non-physiological mass oscillation just after the closure of the valve. The DCS geometry was improved during the design by maximizing the inner cross section area and minimizing duct lengths; nonetheless, the imaging and instrumentation requirements did not allow for a complete removal of the related hydraulic inertance.

The measured flow waveform had a fair physiologic resemblance, although the cycle-averaged flow rate was 30% smaller than that imposed by the pumping system. Indeed, the LV distensibility caused a fluid volume sequestration at each pump cycle, which resulted in a reduction of the net flow delivered to the afterload circuit, still without any major distortion of the systolic flow waveform. The behavior of the mock loop to this respect represents a remarkable step forward compared to the previous works in the field [70], even if some room for improvement still exists to reach physiological levels of flow rate [150].

For what concerns the imaging, endoscopic accesses allowed for an excellent visualization of both the aortic and the mitral valve. The placement of the echographic probe directly on the myocardium enabled clinicians to easily acquire high-quality images of the

cardiac structures. Moreover, clinicians highlighted the increase of awareness attainable by the simultaneous acquisition of both endoscopic and echocardiographic images; indeed, this allowed a direct comparison between the two images, thus ensuring a more complete understanding of cardiac valves dynamics. It is worthy of note that the choice of physiologic saline solution in these trials was due to its transparency that permitted the endoscopic visualization. Nevertheless, the described system is capable of working with different fluids, including heparinized blood or solutions that emulate blood viscosity. Alternatively, suitable changes might be applied to pump frequency to compensate for viscosity mismatch, in obedience to the Reynolds and Womersley similitude.

One of the limitations of this work relies in the fact that the assessment of the hemodynamic performance of the mock loop was only based on the analysis of the flow and pressure tracings. As reported in literature, this approach may not be adequate in order to correctly model the *in vivo* response, since the details of dynamic response should also be considered.

The choice of dynamically pressurizing the ventricle chamber by means of an external pumping system ensured both low costs and simple experimental protocols, as compared to the use of *in vitro* beating heart models. The developed mock loop showed an excellent manageability during all the functional assessment and allowed for a high controllability and repeatability of the experimental conditions. On the other hand, this pumping modality implies a non-physiological motion of the cardiac walls during the whole cycle, which could directly influence the kinematics and dynamics of the heart's sub-structures. For instance, papillary muscle motion might be expected to occur in a highly non-physiological way, thus leading to mitral valve regurgitation. Nevertheless, our results demonstrated the proper functioning of the mitral valve as an effective one-way valve in our mock loop, with a hemodynamic behavior comparable to the *in vivo* conditions. This result might be explained considering that, during the artificially generated systole, LV dilatation moves the papillary muscles away from the valvular plane, thus stretching the chordae tendineae just as in a natural systole. Anyway, this does not mean that the biomechanical, dynamic and kinematic behavior of the mitral valvular and sub-valvular structures strictly mimics the physiological one.

Future investigations of the 3D motion of the papillary muscles with respect to the mitral valvular plane during the cardiac cycle might provide further insight into mitral valve dynamics in the passive beating heart.

4

Evolution of the passive beating heart platform for TAVI applications

Part of this Chapter is based on: Leopaldi A.M., Vismara R., Gelpi G., Romagnoni C., Fiore G.B., Redaelli A., Lemma M. and Antona C., "*Intracardiac visualization of transcatheter aortic valve and valve-in-valve implantation in an in vitro passive beating heart*". JACC: Cardiovascular Interventions, 2013, 6(1):92-3.

4.1 Introduction

Transcatheter aortic valve implantation (TAVI) is nowadays the treatment of choice for non-operable and high-risk surgical candidates with severe aortic stenosis. Given its potentially life-threatening complications, e.g. paravalvular leak, valve malposition, coronary obstruction, stroke and vascular injuries, a TAVI requires the expertise of a multidisciplinary team composed by cardiovascular surgeons, interventional cardiologists, perfusionists and anaesthesiologists [151].

The impact of the learning curve on the outcome of the implant procedure is well recognised in literature [152–155]. Alli and colleagues [152] reported a significant decrease in intraprocedural time, contrast and radiation dose with increasing number of procedures performed by physicians. Hayashida et al. [153] proved that team experience reduced major vascular complications in a percutaneous approach for transfemoral-TAVI. The impact of the learning curve on the outcome of TAVI was also analysed by Kempfert and colleagues [154], who reported improving mortality rates with increasing clinical experience. These studies pointed out how TAVI requires specific knowledge and expertise with respect to several aspects of the procedure, such as proper preoperative and perioperative sizing of the annulus, optimal positioning by use of fluoroscopic and transesophageal echocardiographic guidance, stepwise valve implantation with the capability for minor position adjustments.

In this context, a training platform that allows the operators to practice in the delivery and deployment manoeuvre of the prosthesis could help to speed up the learning process and to develop a deeper awareness of TAVI-related issues. An ideal training platform should be simple, easily manageable and cost-effective, thus boosting its widespread use in laboratories as well as in hospitals. At the same time, it should mimic the *in vivo* operating environment physicians are used to, possibly providing additional features and tools aimed at enhancing the learning experience. With respect to this, the achievement of relevant hemodynamic conditions in the system, the preservation of the heart anatomy and the replication of the aortic valve dynamics are mandatory requirements. Moreover, with respect to imaging, a training platform should allow the operator to perform the implantation under standard guidance, i.e. angiography and/or echocardiography, and with the additional aid of intracardiac endoscopy, so to provide a straightforward cognition of the procedure.

A first step in this direction was made by de Weger and colleagues [19], who implanted an Edwards Sapien 26 transcatheter prosthesis (Edwards Lifesciences Inc, Irvine, California) into an isolated swine working-heart model under direct endoscopic visualization. Similarly, Quill et al. [131] implanted a CoreValve (Medtronic Inc, Minneapolis, USA) within an isolated human heart, comparing different imaging modalities and underlining the tremendous educational value for patients, clinicians, and design engineers that these experiments can provide. Nonetheless, both these studies were performed on *ex vivo* platforms, whose complex management and high running costs limit their applicability for training purposes, and did not try to replicate the pathological scenario of aortic valve stenosis.

The latter aspect is critical when dealing with TAVI applications, as the presence of a calcified structure is a fundamental reference for the implantation under fluoroscopic guidance. Indeed, although the aortic valve position can be identified by the only use of contrast agent injections, the presence of a calcified structure makes the valve easily visible during the whole procedure. Furthermore, a calcified valvular structure with a realistic morphology could help reproducing the feeling that the physician experience during a real deployment, thus increasing the training potential of the platform. Therefore, the development of an *in vitro* model of aortic stenosis is a challenging, yet necessary, step in order to replicate a scenario that is realistic and familiar for the physician. With regard to this, to the best of our knowledge, the only work was published by Azadani and colleagues [156,157], who developed a technique to simulate the stenotic degeneration of bioprosthesis. The proposed methodology consisted in applying BioGlue to stiffen the valve leaflets and simulate stenosis. Although their degenerated model showed to be quite reproducible and able to simulate the hemodynamic behaviour of a stenotic bioprosthesis, it did not include any calcific structure or radio-opaque material, and, therefore, it does not represent a valid option for the simulation of TAVI procedures under fluoroscopy.

In this Chapter, the evolution of the passive beating heart platform, described in Chapter 3, for TAVI applications will be discussed. Indeed, the passive-heart approach represents a promising methodology to achieve the above mentioned requirements: realistic hemodynamic conditions, good anatomical representation, simulation of the pathological scenario, remarkable imaging capabilities, low experimental costs and manageability. The passive-heart platform development included both a feasibility study on a novel methodology

to reproduce *in vitro* aortic valve stenosis, and the redesign of the setup layout and components in order to achieve an easy and cost-effective training platform. The proficiency of the system was assessed by performing transcatheter aortic valve and valve-in-valve implantations of CoreValve valves under multimodal imaging guidance in a catheterization lab.

4.2 Optimization of the passive-heart platform for TAVI

4.2.1 *In vitro* model of aortic stenosis: proof of concept

The technique we developed to simulate aortic valve stenosis (Figure 4.1) consisted in gluing human aortic calcified leaflets, excised from patients undergoing surgical valve replacement, to the healthy porcine aortic cusps. Given the use of human material, the experiments involving the pathological model were always performed in a hospital environment.

The experimental protocol was as follows. Briefly, the calcified leaflets were explanted from patients undergoing aortic valve replacement and fixed in glutaraldehyde solution. On the porcine heart, aortotomy was performed 2 mm above the sinotubular junction, so to expose the aortic valve that was cleaned and dried with tissues. In order to stretch the leaflets during the gluing, stitches were applied to the Arantium nodules of each cusp. Then, the acrylic glue was deposited on both the aortic surface of the healthy leaflet and on the human calcified cusp. The calcified leaflet was then applied on the porcine cusp with tweezers, and pressure was applied for about 30 seconds. If necessary, more glue was deposited in regions that were not properly attached. Then, the glue was left drying for about 5 minutes and the procedure was repeated for the remaining leaflets. Finally, the valve functionality was checked to avoid complete gluing between adjacent leaflets or severe insufficiency due to the partial leaflet retraction following the gluing. In the latter case, three 6-0 stitches were applied at the aortic commissures in order to help the coaptation of the valve during the diastolic phase. Finally, the stitches on the Arantium nodules were removed and the aorta sutured.

The reliability, efficacy and hemodynamic performance of the pathological model was assessed with an experimental campaign on five valves. The experiments were performed at 70 bpm in typical systemic conditions, i.e. with aortic pressures of about 120/80 mmHg and a cardiac output of 4 lpm. For each sample, the hemodynamic data were acquired, averaged over five consecutive cycles, and processed in order to evaluate the classical indexes of aortic valve performance: mean and maximum pressure drop and regurgitant fraction. The pathological model was also used to perform TAVI procedures under both endoscopic and fluoroscopic guidance.

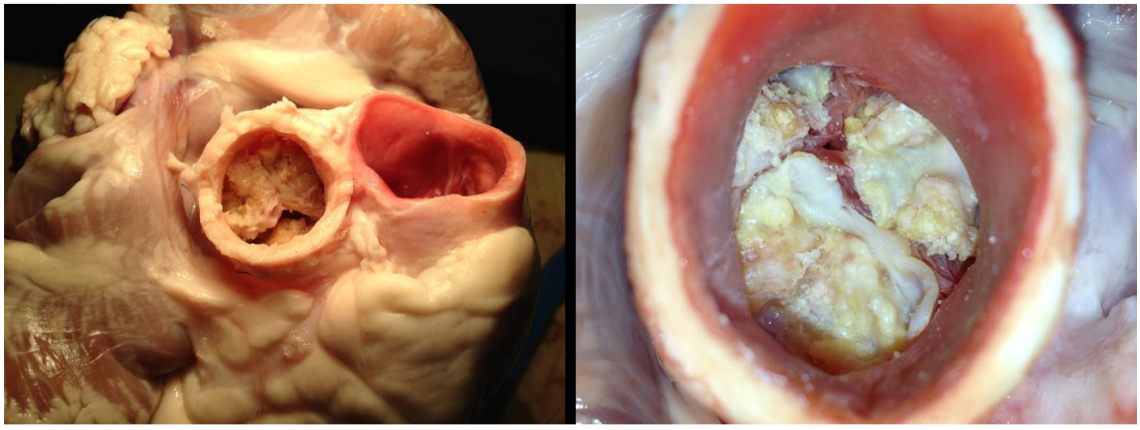

FIGURE 4.1: images of the developed in vitro model of aortic stenosis.

4.2.2 **Redesign of the system**

The passive beating heart setup described in Chapter 3 was optimized with improved design solutions in order to obtaining an easy to use and cost-effective platform suitable for TAVI applications. Figure 4.2 shows two pictures of the system both in a laboratory environment and in a cath lab.

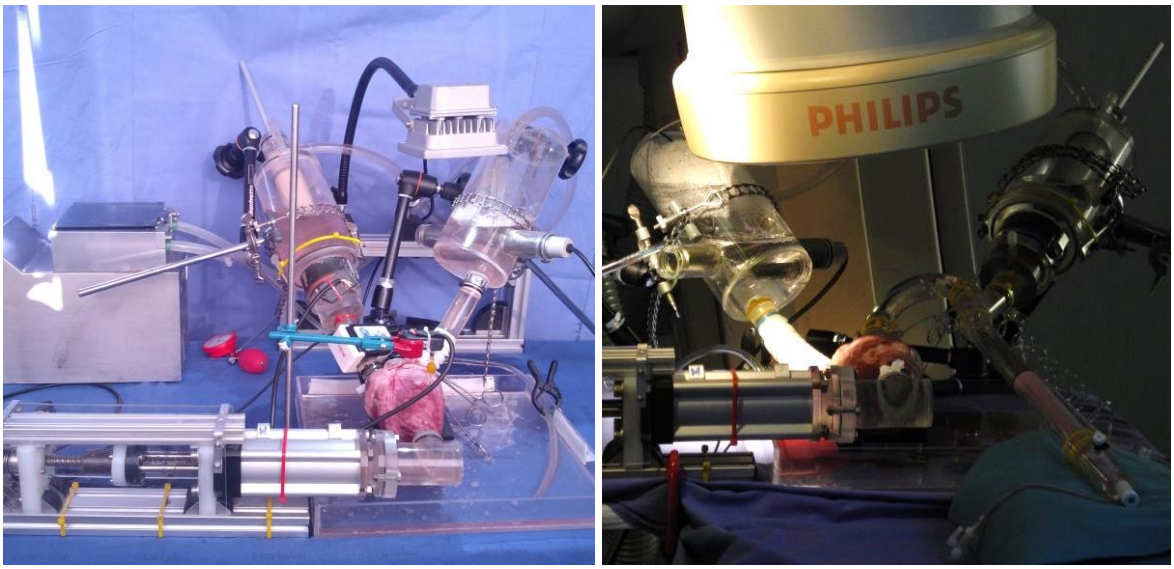

FIGURE 4.2: pictures of the passive beating heart platform in the laboratory (left) and in the cath lab (right).

All the hydraulic connectors between the heart and the setup were redesigned. The new atrial connector consisted in a simple corrugated and extensible plastic tube, which allows for an easy and adjustable connection between the left atrium and the preload reservoir. Given the low atrial pressure, sealing of the tube is simply obtained by tying the atrial wall around the tube with a silicone vessel loop. As for the connection of the aorta with the afterload circuit, the double-cone system was replaced by a simpler and smaller connector, consisting in a hollowed PMMA tube to which the aorta was fixed with a tie-wrap. In both cases, the length of the hydraulic connections was reduced with respect to the previous design, so to minimize hydraulic inertances.

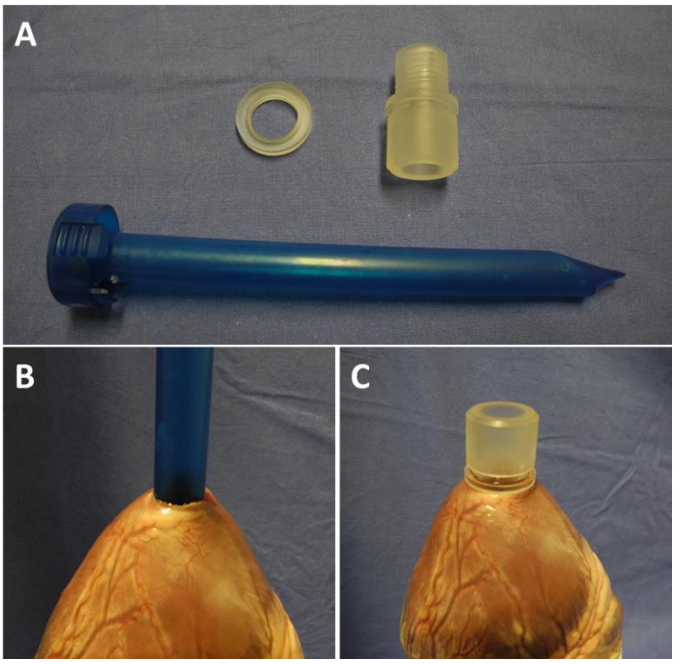

FIGURE 4.3: Sequence of the apical connection procedure. Panel A shows the threaded connector, the nut and the dilatator. Panel B shows the dilatation of the apical hole, and panel C shows the apical connector after its insertion in the left ventricle.

The novel apical connector consists in a 20 mm PMMA hollowed and threaded cylinder, which is forced into the ventricle through a small hole punched in the myocardium, that is progressively dilated (Figure 4.3). The diametric interference between the connector and the punched hole is conceived in order to increase the stability of the connection, thanks to the passive elastic response of the cardiac tissue. A PMMA nut, inserted into the left ventricle through the mitral valve and screwed to the apical connector, compresses the apical

myocardium, ensuring both mechanical stability and sealing. In some hearts, cyanoacrylate glue was also applied in order to seal small leaks.

In order to allow for the execution of TAVI procedures with self-expanding valves, the setup was also equipped with a compact heat exchanger (Heater 300, Schego, Germany). To minimize the size of the overall setup, without including extra components, the heat exchanger was integrated within the atrial reservoir (Figure 4.2) and connected to a temperature-controlled switcher (430el, Eden, Italy).

As concerns the accesses for TAVI, specific components were designed to allow the use of the standard 18 Fr CoreValve delivery system. Figure 4.4 shows the schematic of the two mock loop configurations that were developed in order to provide convenient solutions for different experimental needs. The first layout provided an access for the delivery system directly downstream the aorta, coaxially with the valve, thus allowing for a rapid and straightforward implantation of the valve under direct intracardiac visualization and/or echo guidance. On the contrary, the second configuration was designed to perform TAVI procedures in a catheterization lab, under fluoroscopic guidance. The access for the delivery system was intended to simulate a standard femoral artery access, and was therefore provided at the end of a 25 mm PMMA tube of about 50 cm, reproducing the gross anatomical features of the aortic arch and the descending aorta (curvatures, diameters, length of sections). Moreover, this layout enabled the physician to operate far from the high density radiation region. In both configurations, compact multi positioning arms (244N, Manfrotto, Italy) were used to support the mock loop components and allow for their easy, accurate and adjustable positioning.

Regarding imaging, in order to improve the potential benefits of intracardiac endoscopy the platform was equipped with a 3.6 mm fiberscope (ENF-P4, Olympus Europe, Hamburg, Germany), coupled with a light source (CLV-S40, Olympus Europe, Hamburg, Germany) and an acquisition system (OTV-S7 Digital Processor, Olympus Europe, Hamburg, Germany). The broadly steerable lens (±130°) and the wide field of view (85°) of this fiberscope allowed for very effective navigation inside the ventricle. The access for the fiberscope was provided just downstream the aortic valve; as for intra-ventricular and atrial imaging, the small diameter of the fiberscope allowed its easy insertion in the ventricular wall with a simple tobacco-pouch suture.

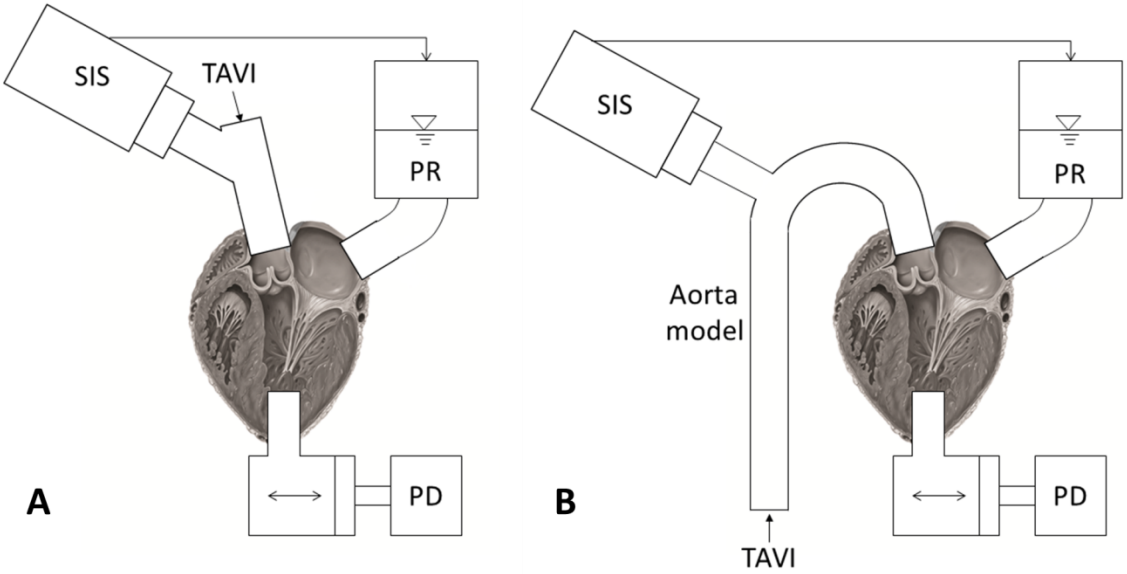

FIGURE 4.4: Schematic representation of the two different layouts. Left: layout for the direct implantation of the TAVI in the aortic root. Access is provided downstream the aortic root, coaxially with the valve. Right: system layout for the simulation of trans-femoral TAVI in the catheterization lab. Access for the delivery system is provided at the end of a simple plastic model of the descending aorta. SIS: systemic impedance simulator. PR: preload reservoir. PD: pulse duplicator.

4.3 Results

4.3.1 Assessment of the pathological model

Figure 4.5 shows some representative frames of the pathological valve model that were acquired in the experimental assessments with both endoscopy and fluoroscopy. The methodology that was developed to simulate *in vitro* aortic valve stenosis showed to be reliable, as none of the tested samples showed detachment of the glued calcific leaflets from the cusps or other oddities. Moreover, the leaflets were clearly visible under fluoroscopy, thus representing a constant reference for the physician during TAVI.

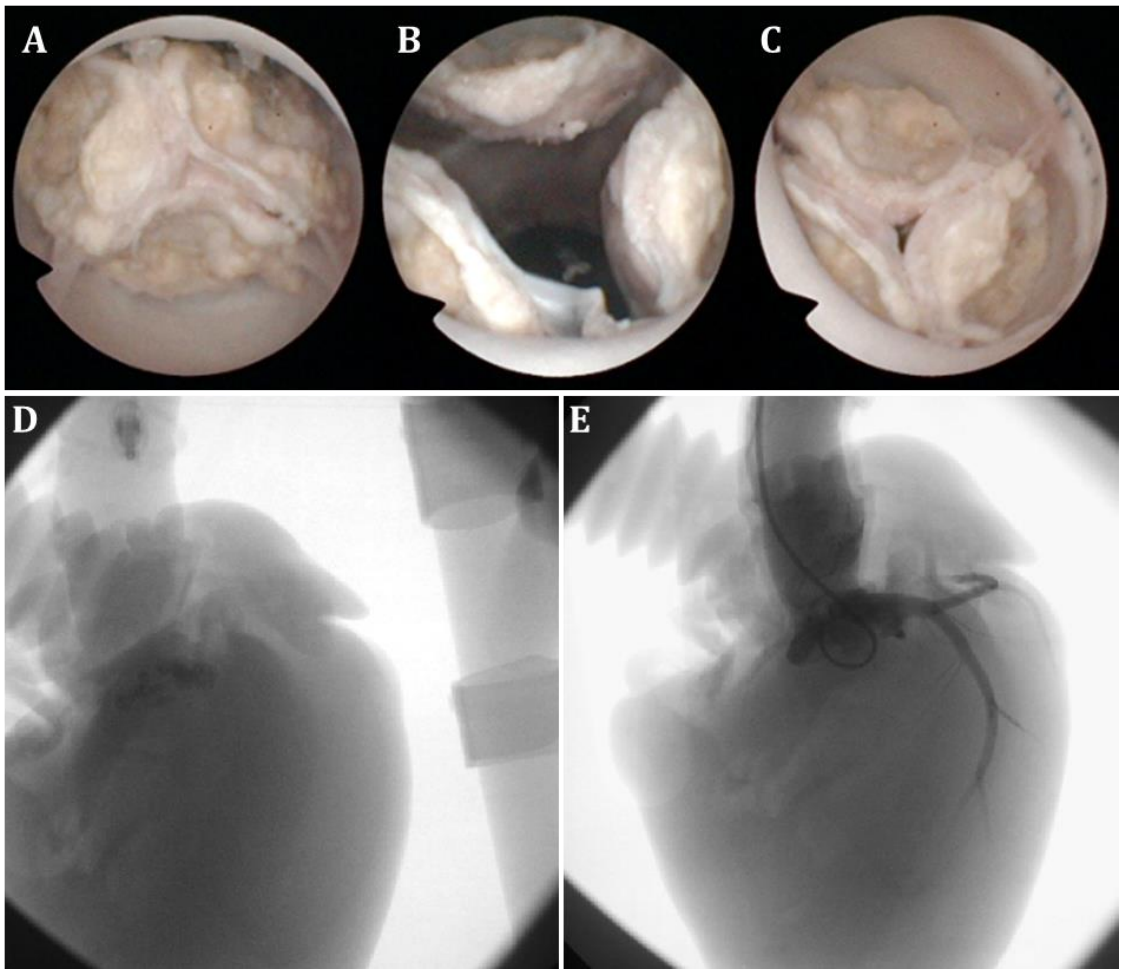

FIGURE 4.5: representative snapshots of the developed pathological model tested in the mock loop. Images acquired with endoscopy (A-C) and with fluoroscopy (D-E).

The single-sample results of the hemodynamic evaluation of the pathological model, which was carried out in dynamic working conditions, are reported in Figure 4.6. Average values of the hemodynamic parameters, averaged over the five samples and expressed as median (interquartile range) were: 18 mmHg (14-39) for the mean pressure drop, 43 mmHg (32-78) for the maximum pressure drop and 11% (4-11) for the regurgitant fraction. As it is clearly visible from both the standard deviations and the trend in Figure 4.6, the variability of the pathological model in terms of hemodynamic performance was relevant.

When looking at the single-sample results (Figure 4.6), the proposed methodology was able to induce mild aortic stenosis in the first three valves, while in the last two severe aortic stenosis was successfully achieved [158]. For these two samples, as specified in paragraph 4.2.2, three stitches were applied at the commissures of the valve to reduce its annulus and avoid severe insufficiency, since the gluing protocol induced leaflet retraction. As for aortic regurgitation, mild levels of aortic valve insufficiency were induced in all the valves by the procedure [159].

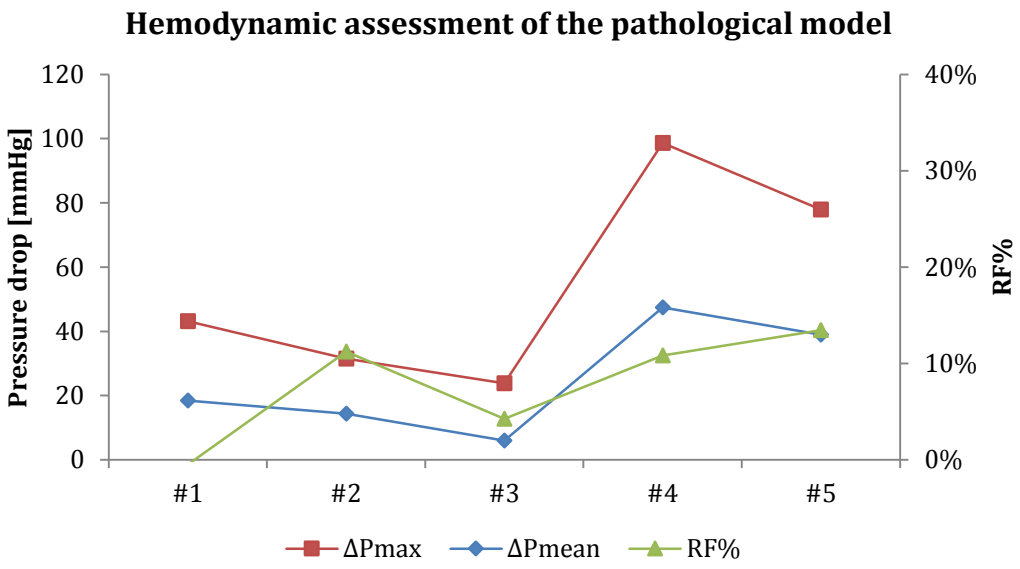

FIGURE 4.6: Single-sample (#i) results of the hemodynamic assessment of the developed in vitro pathological model. ΔPmax: maximum systolic pressure drop. ΔPmean: mean systolic pressure drop. RF%: regurgitant fraction.

4.3.2 Intracardiac visualization of transcatheter aortic valve and valve-in-valve implantation

The passive beating heart platform in the A configuration with reference to Figure 4.4, i.e. without a model of the descending aorta, was used to record *i)* a standard TAVI of a 29mm CoreValve and *ii)* a valve-in-valve procedure of a 26mm CoreValve implanted within a 23mm Hancock II® (Medtronic Inc, Minneapolis, USA). For these experiments, the pathological model was not adopted and the procedure was carried out under endoscopic guidance.

Freshly explanted porcine hearts were obtained from a local abattoir and housed in the mock loop. The system was filled with saline solution at 37°C and physiological hemodynamic conditions, i.e. 70 bpm heart rate, 120/80 mmHg arterial pressure and ≈4 Lpm mean flow, were set. The implant protocol adopted for both the standard TAVI and the valve-in-valve procedure was as follows. Firstly, a guide-wire was inserted into the left ventricle through the ascending aorta to facilitate the positioning of the delivery catheter across the aortic valve. Then, the outer sheath was partially withdrawn until a proper positioning was achieved and the CoreValve was completely released. Since in these experiments the calcific pathological model was not used, balloon valvuloplasty was not performed; nevertheless, there is no technical contraindication with respect to the performance of this procedure.

The movies are available in the online-only Data Supplement of the published paper [160] and show the TAVI and the valve-in-valve procedures in detail, with views from both the left ventricle and the aorta (in Figure 4.7 and 4.8, representative snapshots from the valve in valve procedure are reported).

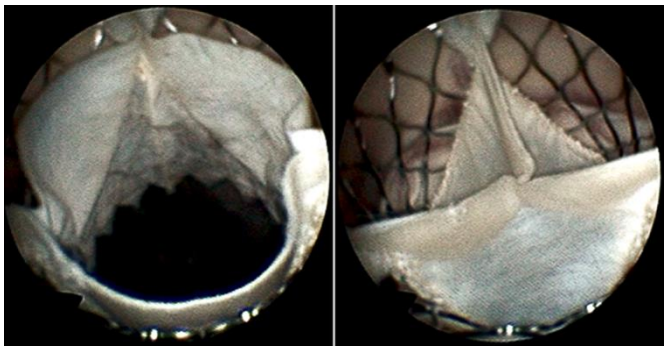

FIGURE 4.7: Snapshots of the transcatheter aortic valve (Aortic View). Open (left) and closed (right) valve.

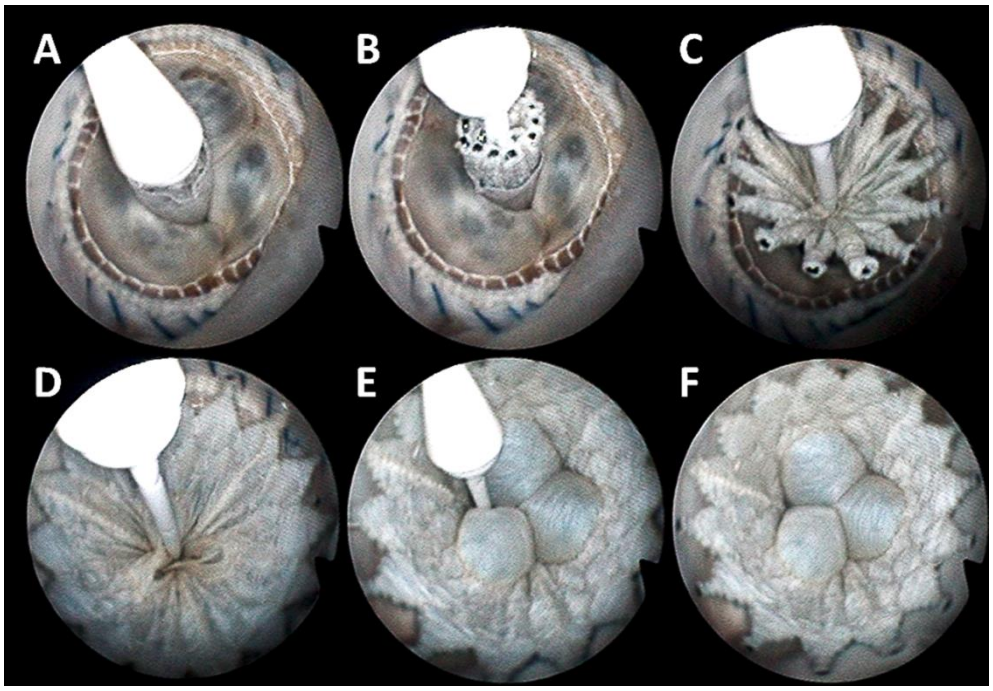

FIGURE 4.8: Snapshots of the valve-in-valve procedure (Left Ventricle View). (A) The delivery catheter is positioned across the Hancock II bioprosthesis. (B) The outer sheath is partially withdrawn, and (C) the CoreValve starts to flare outwards. (D and E) The valve is released, and (F) the delivery catheter is retracted. Movies are available as online supplements of the published paper [160].

4.3.3 Simulation of TAVI procedures in calcified valves under both fluoroscopic and endoscopic guidance

TAVI procedures were also performed using the passive beating heart platform, with the pathological model of aortic stenosis, in a catheterization lab (Figure 4.4, layout B). For these experiments, simultaneous fluoroscopy guidance and intracardiac endoscopic visualization were provided to the physicians.

The experimental procedure was the same as the one described in paragraph 4.3.2, with the addition of balloon valvuloplasty that was usually performed after the deployment to better expand the CoreValve and facilitate its proper opening in the calcified aortic valve. Figure 4.9 and 4.10 show some representative snapshots of the procedure obtained with fluoroscopy and intracardiac endoscopy, respectively.

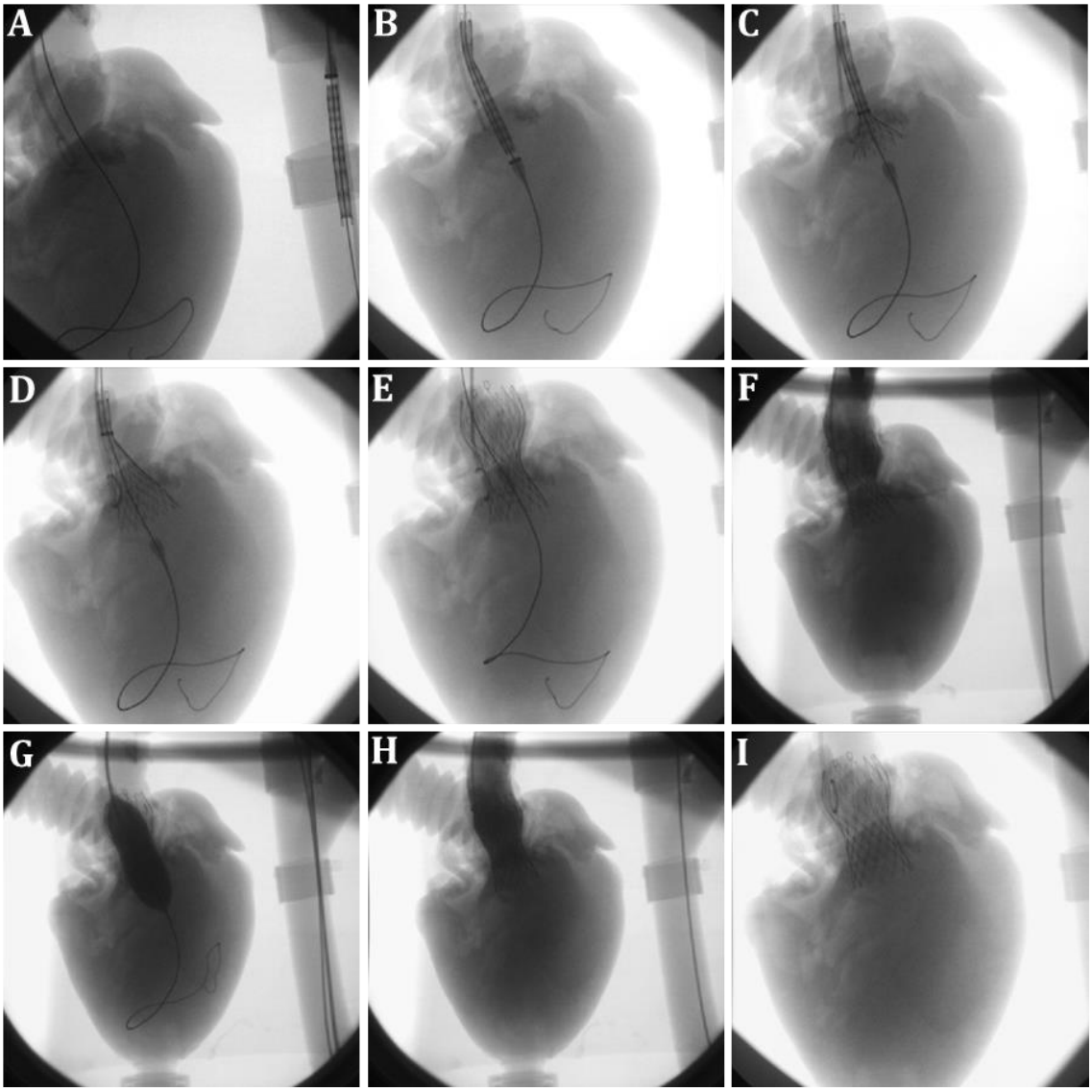

FIGURE 4.9: Fluoroscopic images obtained during the TAVI procedure on the pathological model. (A) The guide wire was inserted into the ventricle, with the pigtail positioned on the valve and the delivery catheter in the thoracic aorta. (B) The delivery catheter was positioned across the calcified aortic valve. (C-E) The outer sheath was partially withdrawn, the CoreValve started to flare outwards and was then released. (F) Angiography was performed, showing a significant leakage. (G) Hence, balloon valvuloplasty was performed trying to better expand the CoreValve and reduce the leakage. (H) Then, another angiography was performed showing a significantly reduced leakage. (I) The catheters were finally retracted and the TAVI procedure was concluded.

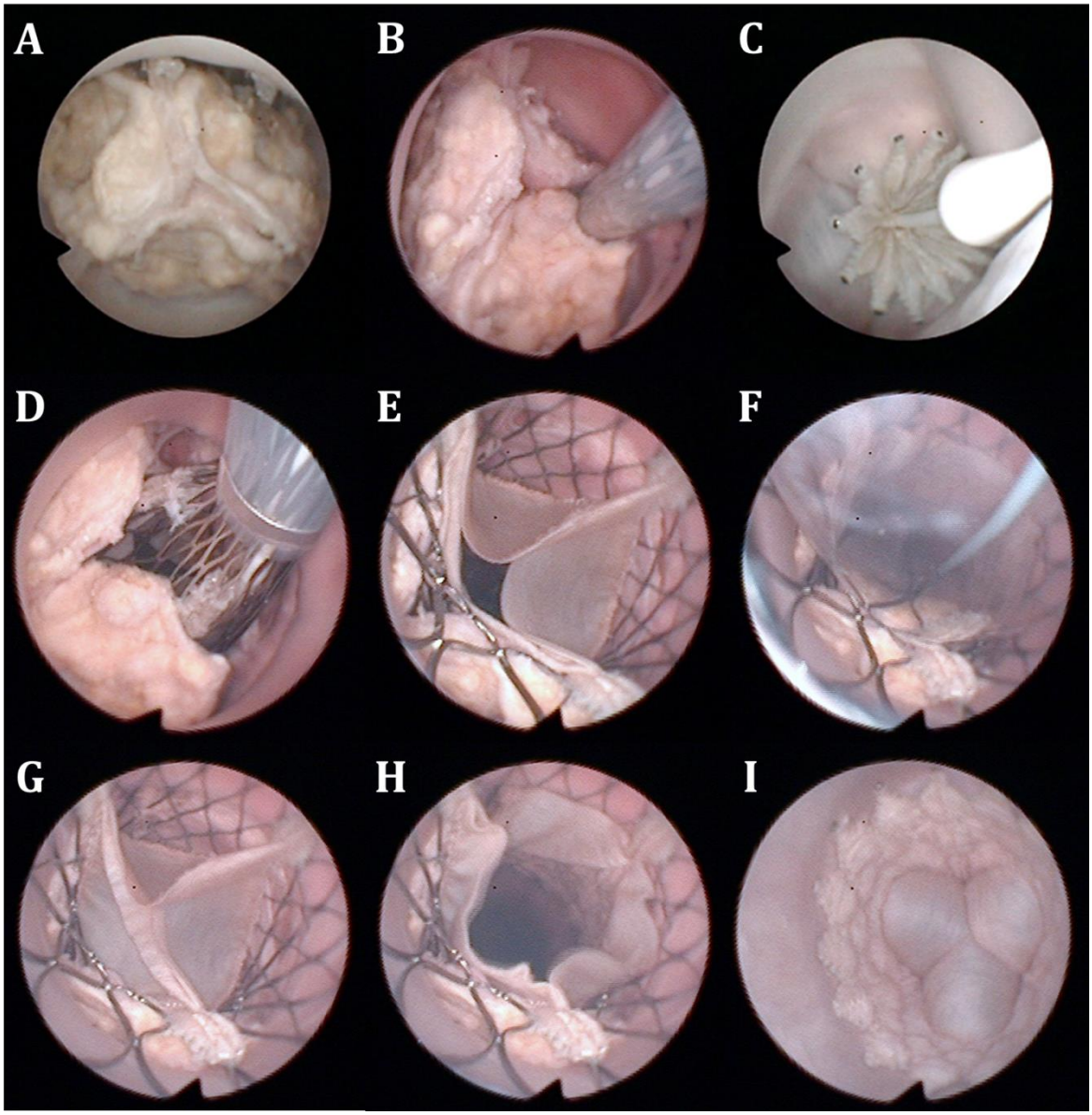

FIGURE 4.9: Representative endoscopic images obtained during the TAVI procedure on the pathological model. (A-B) The delivery catheter was positioned across the calcified aortic valve. (C-D) The valve was deployed withdrawing the outer sheath. (E) After the release, as confirmed by angiography (figure 4.8, F), the valve exhibited a significant regurgitation due to the presence of a central orifice. (F) Balloon valvuloplasty was performed to better expand the CoreValve. (G-H) Aortic view of the CoreValve after the expansion with the balloon, showing proper functioning. (I) Ventricular view of the valve, confirming proper diastolic closure.

4.4 Discussion

In this Chapter, the evolution for TAVI applications of the passive beating heart platform presented in Chapter 3 was described. Our goal was to develop a platform capable of simulating the typical environment physicians are working with when performing TAVI, in order to provide them with a multi-functional tool that could be used for training, research and educational purposes. The key requirements for our design were the possibility of performing multimodal imaging, the simulation of the anatomo-morphological environment and the achievement of physiologic hemodynamic conditions in a simple, reliable and cost-effective system. Thanks to the design solutions that were implemented, the passive beating heart platform was profitably used to perform TAVI under fluoroscopic guidance and simultaneous intracardiac visualization in a catheterization lab. An *in vitro* model of aortic stenosis was also developed, assessed, and used in the simulated TAVI procedures to mimic the real pathological scenario.

The experimental sessions that were carried out in the catheterization lab involved several experienced operators, proctors and representatives of Medtronic, who were interested in the system for both training and marketing purposes. Their feedbacks were very positive, with special regard to the realism of the simulated clinical scenario and to the possibility of performing the implantation under multimodal imaging guidance. The intracardiac movies that were recorded in the tests have a high educational relevance for both physicians and design engineers, as they allow for an immediate and accurate investigation of the transcatheter valve deployment steps and functioning. In particular, key factors such as height of implant, valve positioning, size mismatch and interactions with the surrounding structures (mitral-aortic junction, anterior mitral leaflet and coronary ostia) could be directly evaluated. Indeed, the immediacy and the insight that intrinsically characterize a movie are way higher than those provided by other imaging techniques, such as fluoroscopy or echo. Also, the possibility of simultaneously comparing these different imaging modalities allows for a better understanding of the implantation procedure and may increase the awareness of physicians and designers with respect to clinically relevant issues.

The important role that visualization studies can play for the development of transcatheter procedures has been already pointed out in literature by many researchers. The group of Mihaljevic recently proposed and tested in animal models an innovative

methodology to perform direct endoscopy-guided procedures [12,161], while other groups used *ex vivo* platforms to record intracardiac movies of both TAVI and valve repair procedures [16,19,131,132]. Our results were comparable to those obtained by these research groups, thus demonstrating the efficacy of the developed passive beating heart platform.

The main innovation our passive-heart system introduced with respect to the state of the art relies in the possibility of performing these investigations in a cost-effective manner, with experimental protocols that are extremely simple as compared to both *ex vivo* and animal models. Indeed, our platform does not require expensive equipment such as blood gas analyzers, oxygenators, blood filters, ECG etc. Also, the hearts we used were harvested from slaughtered pigs, thus without involving any ethical issue. Furthermore, the typical experimental cost (excluding labor) associated with a passive-heart platform is about 25€, which is negligible if compared to both *ex vivo* and animal models which are typically two orders of magnitude more expensive [70]. Moreover, the design solutions that were implemented made the system compact, versatile and reliable, thus allowing its use either in a laboratory environment or in a catheterization lab. With this respect, the new heart connectors did not require any surgical act or expensive disposable material, and allowed for a significant reduction of the preparation time, from 2 hours to about 45 min, when the stenosis was not reproduced *in vitro*. The new apical connector also showed an improved mechanical stability and a better sealing, thus allowing for the use of higher stroke volumes on the piston pump that resulted in higher achievable cardiac outputs (up to 5 lpm).

As regards the *in vitro* model of aortic stenosis that was developed, our main goal was to provide the physicians with a clear reference for TAVI under fluoroscopic guidance. At the same time, we aimed at mimicking the real morphology of a stenotic valve [162], stiffening the leaflets so to better reproduce the complex environment the transcatheter valve is subject to during both deployment and functioning. The experimental assessment demonstrated the efficacy of the proposed methodology. The gluing ensured a simple, stable and reliable fixation of the excised calcified leaflets to the native porcine cusps, both in normal working conditions and during the execution of TAVI procedures. The calcified leaflets were also clearly visible under fluoroscopy, thus providing the physician with an easily identifiable reference for the implantation and simulating in a very realistic way the scenario of a real TAVI performed on patients. Anyhow, the experimental procedure for the preparation of the stenotic model is time-consuming and requires the execution of several surgical acts, thus

representing a serious drawback in the view of developing a simple and user-friendly training platform.

The hemodynamic characterization of the stenotic model also highlighted the limited reproducibility of the adopted methodology. Indeed, out of five tested valves, severe aortic stenosis was achieved only in two cases, while mild stenosis was measured in the other samples. These relevant differences in the valve performance could be explained by several aspects. First, the characteristics of the excised calcified leaflets, in terms of both shape and morphology, differed from sample to sample. Moreover, a fine control of the actual position of the calcific leaflet during the gluing is hardly attainable. Finally, differently from a real stenotic valve in which the aortic annulus and the root are also calcified, our pathological model only stiffen the valve leaflets. This difference may result in a limited reduction of the valve orifice area, and therefore in mild alterations of the systolic pressure drops, as compared to the real stenotic valve. Indeed, the mobility of the aortic leaflets is strongly determined by the mechanical properties of the leaflets insertion region, which in our model was only partially affected by the gluing of the calcific leaflets. The best results in terms of induced degree of stenosis were obtained for the two samples in which three stitches were applied at the valve commissures to correct for the evidence of aortic valve insufficiency. This surgical act is well known in the clinical practice, and previous *in vitro* studies [107,163] showed how it induces an increased mean systolic pressure drop.

The model of aortic root and descending aorta that was adopted in our study was an extremely simplified representation of the real patient anatomy, and was only intended to mimic the typical layout of a transfemoral access. Nonetheless, our system is prone to the use of more realistic and patient-specific models of the vascular bed that would increase the training potential of the setup and allow further insights on the delivery procedure and on the catheters design and function. With respect to these aspects, an interesting future development of the proposed platform may be inspired by some recently published contributions, in which the design and characterization of rapid-prototyped patient specific models of both arteries and valves was carried out [164–167]. Another interesting development may consist in implementing new design solutions to enable the execution of transapical TAVI procedures. This would require either the relocation of the pump connection from the apex to another region of the left ventricle, or the design of an appropriate access port in the apical connector to allow the insertion of the delivery system.

In conclusion, our platform shows to be a promising tool for studying the TAVI deployment manoeuvres and their effects on the immediate outcome of the procedure. The simple design, the manageability and the cost-effectiveness in daily-use make it an ideal candidate as a widely-spread platform for training and research purposes in the field of minimally-invasive procedures.

Acknowledgements

A particular acknowledgement goes to Moira Pilloni for her contribution in the development of the *in vitro* pathological model of aortic stenosis.

5

A novel passive left heart platform for device testing and research

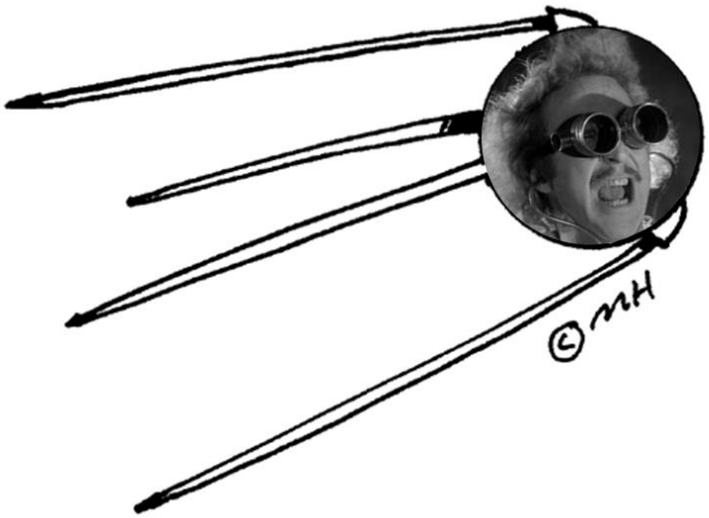

This Chapter is based on: Leopaldi A.M., Vismara R., van Tuijl S., Redaelli A., van de Vosse FN., Fiore G.B. and Rutten M., "*A novel passive left heart platform for device testing and research*". Artificial Organs, Submitted.

5.1 Improving the ventricular behaviour: external actuation of the heart

As already discussed in the previous Chapters, in order to represent valuable models, *in vitro* platforms must effectively replicate the *in vivo* environment in which the tested device will operate once implanted. In recent years, the spreading of reparative, minimally-invasive and transcatheter techniques [49,52,136,168], and the increased adoption of mechanical circulatory support [169,170], called for the development of more realistic *in vitro* apparatuses. Indeed, for these applications, being able to model the anatomical and functional interactions between the implanted device or repaired structure and the *in vivo* environment is crucial.

Chapter 2 presented a summary of the main approaches described in literature to address these issues, i.e. the use of *ex vivo* beating heart models [7,8,130], or the integration of passive excised biological samples into artificial *in vitro* setups [63,65,70]. The latter methodology is currently evolving from the sole use of excised valves, either aortic or mitral [65,66,96], towards the design of platforms able to house entire passive hearts [70,120,171].

Consistently with this panorama, the development of an *in vitro* passive-heart platform [171] and its use for the simulation of TAVI procedures [160] were described in Chapter 3 and 4, respectively. The design principle that we adopted, and that was firstly proposed by Richards [70], consisted in connecting the ventricular chamber through its apex to an external pulsatile pumping system, to attain a cyclical pressurization of its inner volume. This approach was shown to closely replicate physiological hemodynamic conditions, to allow the simulation of reparative and transcatheter procedures and to allow for echo and endoscopic imaging. Nevertheless, this methodology presents some drawbacks that limit its applicability. Firstly, it causes a paradoxical motion of the left ventricular walls during the cardiac cycle. Indeed, the ventricle dilates during systole due to the increased pressure, and deflate during diastole due to the retrograde motion of the piston pump. Furthermore, since the fluid flow is provided through the apex, an altered fluid dynamic field inside the left ventricle is ingenerated.

In order to overcome these limitations, the direct mechanical ventricular actuation may represent an interesting approach, aimed at better mimicking the physiologic dynamic behavior of the ventricles. The principle of directly actuating the ventricles has been proposed

in literature for a wide range of clinical applications, such as prolonged total circulatory support during ventricular fibrillation, resuscitation following cardiac arrest, circulatory support following ischemia and/or myocardial infarction, *in vivo* organ preservation [172–174]. The two main methodologies that were explored were the cardiomyoplasty technique, consisting in wrapping autologous electrostimulated muscles flaps around the ventricle, and the implantation of artificial devices applying compression forces on the failing heart. Cardiomyoplasty was proposed by Carpentier et al. [175,176], but the lack of a clear survival advantage in the long-term have limited its adoption for patients with end-stage heart failure [177,178].

Regarding the development of artificial devices, in 1965 Anstadt et al. firstly introduced an epicardial compression device for cardiopulmonary resuscitation [179]. The device consisted in an elliptically shaped cup that fit over both ventricles, was attached to the heart by means of vacuum, and featured an inflatable inner diaphragm compressing the heart. The hemodynamic effectiveness of direct mechanical ventricular actuation using this device was demonstrated by later investigations, which showed significant improvements both in terms of cardiac output and mean arterial pressure [180,181]. However, technical limitations of the Anstadt cup, e.g. the lack of synchronization with the heartbeat, significantly limited its clinical adoption.

The potential of the direct ventricular actuation methodologies was confirmed in more recent years by the interest of both industry and research groups. Abiomed (Danvers, MA) developed the Heart Booster, a device for long-term ventricular support [182], and its pediatric equivalent, the PediBooster [183]. Toki Corporation (Tokio, Japan) recently developed the BioMetal Helix, an electrically-activated helical coiled spring acting as an artificial muscle to compress the heart, reproducing the principle of cardiomyoplasty [184]. Cardio Technologies (Pine Brook, NJ) also designed a ventricular support device to stabilize the acutely failing heart [185], while Wang and colleagues proposed an electro hydraulic system to assist the myocardium [186].

Some research groups also applied the principle of direct ventricular actuation to the design of *in vitro* mock circulatory loops, developing systems with polymeric ventricles that were externally compressed to generate the desired cardiac outputs [27,187,188]. Nonetheless, to the best of our knowledge, the principle of direct ventricular actuation has

never been applied to the development of *in vitro* passive-heart platforms, i.e. actuating the ventricle of entire non-contractile hearts.

In this Chapter, we describe a novel *in vitro* platform able to house an entire porcine heart and to mimic the pulsatile pumping function of the left heart through the external dynamic pressurization of the ventricular walls. This represents the complementary approach with respect to that of internally pressurizing the ventricular chamber, and is intended to better simulate the dynamic behaviour of the ventricular walls. In order to demonstrate the potential of the developed system as a platform for device testing, an example application is reported, where the AV function under cf-LVAD support was analysed.

5.2 Materials and methods

5.2.1 Design of the mock loop

The functioning principle of the *in vitro* platform (Figure 5.1) is to drive the motion of the ventricular walls throughout the cardiac cycle, thus replicating its cyclic pumping function. To achieve this goal, the system should be able to selectively pressurize the left ventricle, while the atria should be excluded from external loads.

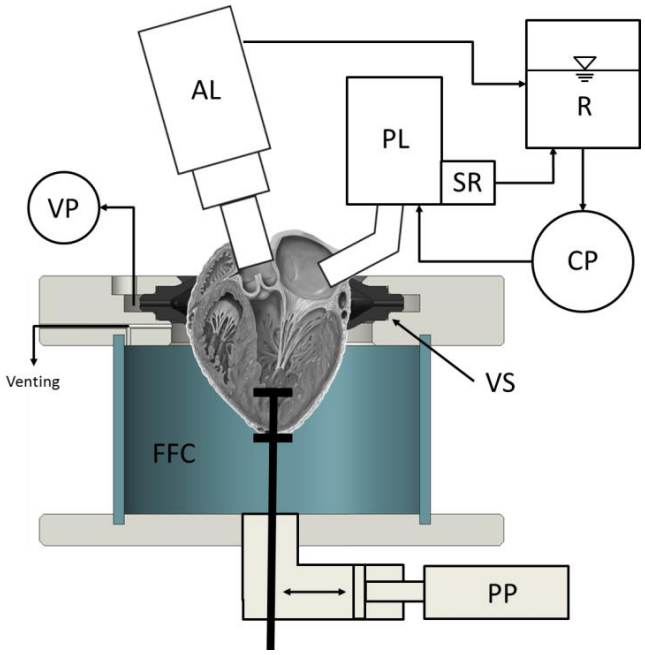

FIGURE 5.1. Schematic of the passive-heart platform: piston pump (PP), fluid-filled chamber (FFC), vacuum seal (VS), vacuum pump (VP), afterload module (AL), reservoir (R), centrifugal pump (CP), preload module (PL), starling resistor (SR).

The setup (Figure 5.2) comprises a fluid-filled chamber (FFC) in which the ventricles of a swine heart are housed. The FFC is composed of a cylinder ended by two plastic plates that are kept together by three threaded rods, and is connected to a computer-controlled piston pump (PP) (ETB32, Parker Hannifin, The Netherlands), that cyclically injects/withdraws fluid into/out of the FFC, hence directly actuating the ventricular walls.

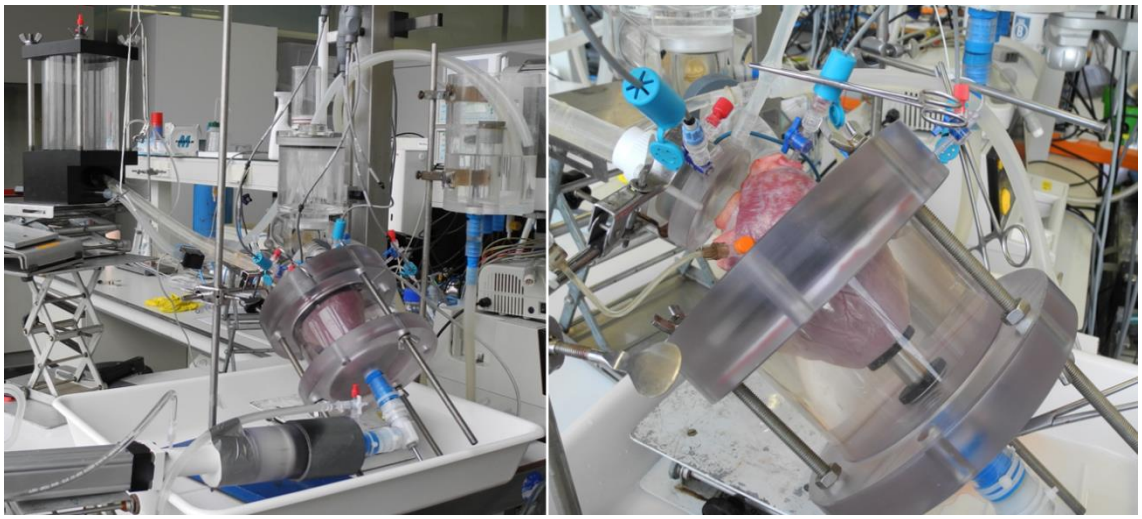

FIGURE 5.2. Pictures of the platform.

To achieve the selective pressurization of the ventricle, we developed an ad hoc rapid-prototyped vacuum seal (VS), printed with a Polyjet technology (Materialise NV, Leuven, Belgium). This design ensures the sealing of the FFC around the coronary sulcus and constrains the heart so as to avoid its axial displacement under pressure. In this way, proper cyclic actuation of the ventricle is possible. The VS design was based on anatomical measures carried out on seven porcine hearts, to characterize their typical anatomy and size. It has an ellipsoidal shape and features two flexible lips that allow it to easily adapt to the unavoidable variability in hearts' dimensions and shapes. The connection to the vacuum pump (VP) (Air Admiral; Cole-Parmer, Vernon Hills, IL, USA) is ensured through a circular channel in the FFC upper plate, which interconnects the radial holes of the VS that apply suction on the coronary sulcus epicardium. In order to further improve the stability of the heart, thus avoiding any residual bending and displacement under pressure, the heart apex is fixed to the bottom plate of the FFC by means of a rigid adjustable connector.

As for the hydraulic part of the mock circulatory loop, the aorta is connected to a windkessel afterload module (AL), designed to mimic the human systemic input impedance. In particular, the afterload circuit consists of a compliant polyurethane tube, designed to match the in-vivo aortic pressure wave speed, and an adjustable RCR model. The outflow of the AL drains into a reservoir (R), from which the fluid is pumped to the preload module (PL) by means of a centrifugal pump (CP) (Bio-Pump® Plus; Medtronic, Minneapolis, MN, USA). The

PL is connected to the left atrium through a compliant silicone tube, and is designed to control the atrial pressure using an adjustable Starling resistance (SR) overflow [8].

Accesses for endoscopic visualization and/or transcatheter procedures are provided in the AL through the aortic polyurethane tube, while the FFC enables the connection of LVADs, the execution of intracardiac endoscopy and the simulation of transcatheter apical procedures.

5.2.2 **Hemodynamic assessment**

Fresh entire swine hearts were obtained from the slaughterhouse and were examined to verify the absence of damages and/or pathologies. Preparation consisted in the ligation of the coronary arteries to avoid fluid loss towards the right atrium, and in the connection of the left heart vessels to ad-hoc designed plastic connectors. The heart apex was also fixed to the respective connector.

The FFC was then filled with saline (0.9% NaCl) to avoid oedema, and the heart was housed in the mock loop with the ventricles submerged in the FFC. Once a correct positioning of the heart was achieved, i.e. with the coronary sulcus aligned with the VS, the vacuum pump was switched on and set to 500 mmHg of vacuum pressure. After proper sealing of the heart was ensured, the FFC was completely de-aired and, if necessary, fluid was added or removed from the FFC in order to achieve a zero pressure acting on the ventricles in the end-diastolic configuration. The aorta and the left atrium were then connected to the AL and the PL respectively, and the circulatory loop was filled with saline solution, while the right heart was left empty. The PP was then gradually activated and the circulatory loop was set to replicate physiologic conditions. In particular, the RCR module was tuned to obtain physiological aortic pressure tracings (120/80 mmHg), and the stroke volume of the pump was adjusted in order to get the desired flow rate (about 4 l/min).

Pressures were monitored in the left atrium, in the left ventricle and downstream the AV with solid state sensors (P10EZ-1; Becton Dickinson Medical, Franklin Lakes, USA). The perivascular sensor for the measure of the pulsatile aortic flow (MA28PAX; Transonic Systems Inc., Ithaca, USA) was integrated in the aortic connector, while the mean cardiac output was measured at the outlet of the AL circuit (HFM-09-1; LifeTec Group, Eindhoven, The

Netherlands). Hemodynamic data were acquired at 1 kHz using a data-acquisition board (PCI 6221; National Instruments, Austin, TX, USA) and running dedicated software (LabVIEW 7.1, National Instruments).

5.2.3 Pilot study: AV opening in cf-LVAD support

To show the potential of the developed system as a flexible and effective platform to carry out research and visualization studies with cardiac devices, in this paper we present a pilot experiment in which a clinical issue was addressed, the interaction between cf-LVAD support and AV functioning. Indeed, clinical data showed that patients under prolonged cf-LVAD support exhibit improper AV function [189–193]. These alterations are related to the level of support and are due to the different hemodynamic environment that the aortic root functional unit is subject to, i.e. dampened aortic pulsatility, increased aortic pressure, decreased left ventricular pressure. This scenario leads to higher pressure load on the leaflets, changes in aortic flow dynamics [190], altered valve opening [191], dilatation of the annulus [194], and may eventually result in cusps fusion [189,193] and AV insufficiency [59,60,190].

In this preliminary experiment we aimed at replicating *in vitro* the acute post-operative scenario after the implantation of a cf-LVAD, in order to assess the potential of the passive-heart platform for device-testing applications. The hemodynamic and kinematic alterations experienced by the AV were simulated, for different pump speeds, by acquiring hydrodynamic quantities and high speed video recordings of the valve. A MicroMed deBakey LVAD (MicroMed Technology Inc., Houston, TX, USA) was connected to the apex of the heart through an access in the FFC bottom plate, and ejected directly into the aorta. In order to simulate a realistic clinical scenario, the mock circulatory loop was adjusted to simulate cardiogenic shock hemodynamic conditions, i.e. hypotensive conditions with a cardiac output of 3 l/min (Figure 5.4). Then, the LVAD was switched on and pump speed was progressively increased from 7.500 to 12.500 RPM in 500 RPM steps, without changing any of the settings of the mock circulatory loop. Using a 10 mm endoscope (Olympus Europe, Hamburg, Germany), coupled with a high-speed camera (MotionScope M5C; IDT Vision, Tallahassee, FL, USA) and a light source (Xenon Nova, 300W; Storz GmbH & Co. KG, Tuttlingen, Germany), AV motion was recorded at 200 fps for every experimental condition, together with hemodynamic data.

Based on these recordings, the mean AV pressure load and duty cycle, i.e. the fraction of time in which the AV is open during each cardiac cycle, were computed [30].

5.3 Validation of the system

5.3.1 Mock loop hemodynamic assessment

Figure 5.3 shows a representative example of the pressure and flow tracings measured in the mock loop, that were consistent with typical systemic *in vivo* waveforms. In particular, the aortic pressure was in the 125/75 mmHg range, ventricular pressure was in the 125/5 mmHg range, while the mean atrial pressure was about 18 mmHg. Regarding the pumping action of the platform, left ventricular stroke volumes of about 65 ml were generated, leading to cardiac outputs up to 4.5 L/min, with aortic peak flows of 25-30 L/min. The hemodynamic conditions of the mock loop were easily adjustable by tuning the AL and the PL and by changing the PP settings, and the beat rate could be increased up to 120 bpm.

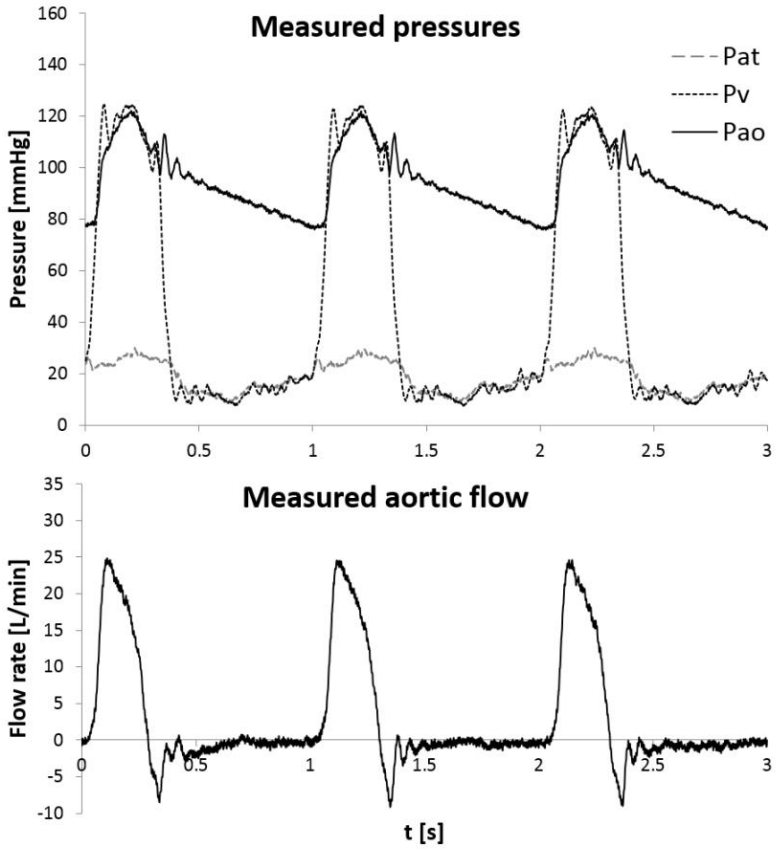

FIGURE 5.3. Representative pressures (top) and flow (bottom) tracings measured in the mock loop. Pat: atrial pressure. Pv: ventricular pressure. Pao: aortic pressure.

5.3.2 **LVAD study**

The acute post-operative scenario following the implantation of a cf-LVAD was simulated with the passive-heart platform. Figure 5.4 shows the pressure tracings measured in the simulated shock condition and at maximum support. Mean aortic pressure increased from 62 mmHg to 93 mmHg at full pump speed, with a significantly reduced pulse pressure (from about 50 mmHg to 15 mmHg). High levels of support also induced negative pressures in both the left atrium and ventricle.

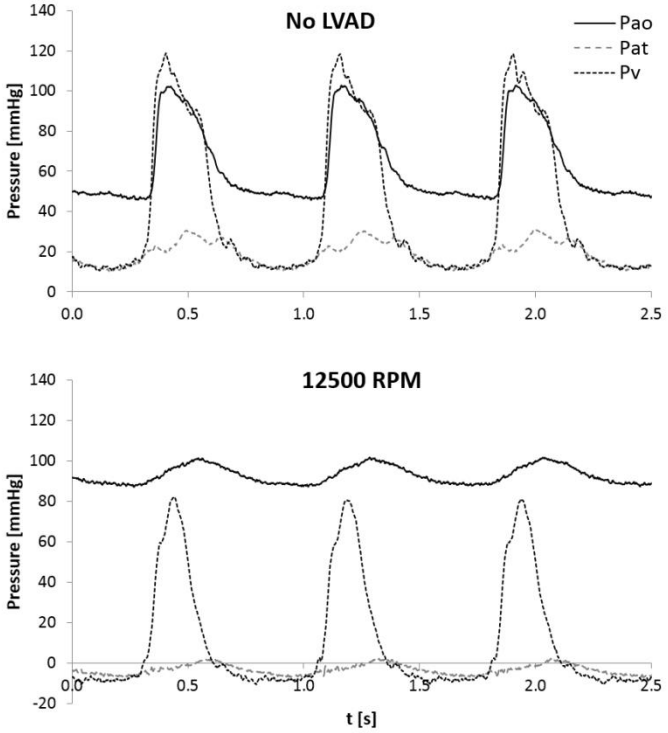

FIGURE 5.4. Measured pressures tracings in the cf-LVAD experiment under simulated shock conditions (top) and full support (bottom). Pat: atrial pressure. Pv: ventricular pressure. Pao: aortic pressure.

Figure 5.5 shows the computed AV pressure load and duty cycle for the different levels of support. As expected, the pressure load acting on the AV increased with increasing pump speed, while the AV duty cycle decreased from physiological levels at no support to zero for pump speeds higher than 12.000 rpm. The high-speed video recordings confirmed these findings and allowed the visualization of AV behaviour for the different levels of support. Figure 5.6 shows the instances of the AV at its maximum opening for all the tested pump speeds. Consistent with the hemodynamic data, which show a null duty cycle at full support,

the AV remained permanently closed only for pump speeds higher than 12.000 rpm. At 11.500 rpm, with a duty cycle of about 5%, AV opening did occur, but without a complete leaflet separation in the commissural region. At 11.000 rpm and lower, with duty cycles higher than 10%, the valve commissures separated completely at peak systole.

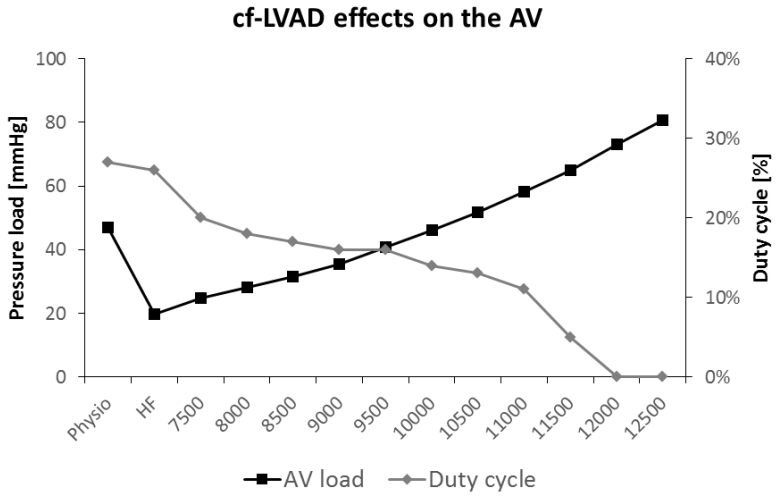

FIGURE 5.5. Mean aortic valve pressure load (mmHg) and duty cycle (%) for all the tested condition: physiologic systemic conditions (Physio), heart failure (HF), and different pump speeds.

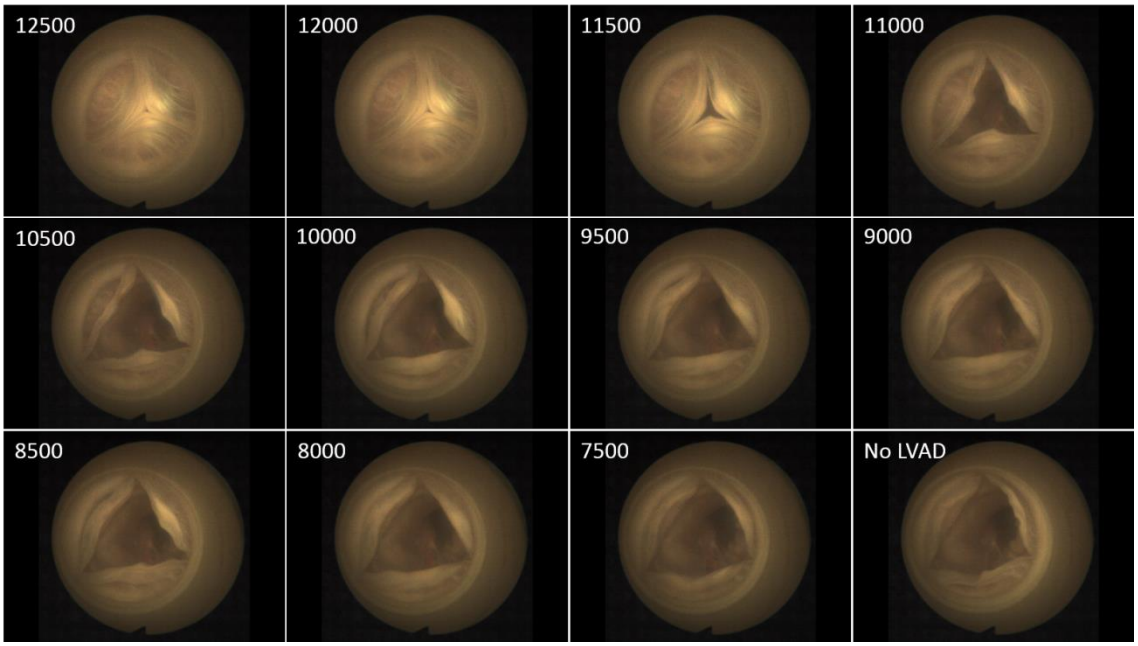

FIGURE 5.6. Snapshots of the aortic valve at maximum opening recorded with the high speed camera for all the tested conditions.

5.4 Discussion

In this paper, we described a novel *in vitro* platform, able to house an entire swine heart and to simulate its pumping function by driving the motion of the ventricular walls during the cardiac cycle through their dynamic external pressurization. The rationale of the work was to develop a system capable of merging the advantages of the classical hydraulic mock loops, with the preservation of the heart anatomy and with a better mimicking of the *in vivo* pumping action of the heart with respect to the state-of-the-art passive-heart simulators. The mock loop was able to replicate physiological hemodynamic conditions, both in terms of pressure and flow tracings, and showed to be an effective platform for both device-testing and visualization studies.

In the experimental assessment, the morphology of all the experimental tracings resembled the typical *in vivo* waveforms. The aortic pressure showed a sharp systolic pressure rise, a dicrotic notch and a smooth diastolic fall. Similarly, the ventricular and atrial pressure waveforms were as expected, without remarkable oddities. In addition, the measured flow rates were comparable with other *in vitro* state-of-the-art setups [8,171]. Concerning valve function (Figure 5.7), endoscopic visualization of the AV showed proper leaflet coaptation and an opening phase qualitatively consistent with other investigations [7,62,63]. Visual inspection of the mitral valve confirmed its continence in all the experimental conditions. However, with increasing stroke volumes, the anterior mitral leaflet progressively exhibited a remarkable prolapse in most of the tested hearts, which occurred without any apparent fluid regurgitation. This behaviour was possibly due to a less-than-physiological tension of the chordae tendineae, caused by the absence of the papillary muscle function, given by the non-contractility of the myocardium. This effect showed to become more relevant when the ventricular wall motion was more pronounced, i.e. for higher stroke volumes.

From a technical viewpoint, the main challenge of the proposed approach was the achievement of an optimal sealing of the pressurized fluid chamber around the coronary sulcus. With respect to this, the design of the flexible rapid-prototyped vacuum seal allowed for an easy, efficient and reliable sealing of the pressurized chamber around the ventricles, enabling physiological ventricular stroke volumes. Together with the adjustable circulatory

loop, this ultimately led to the achievement of appropriate hemodynamic conditions in the setup, with respect to both physiological and pathological scenarios.

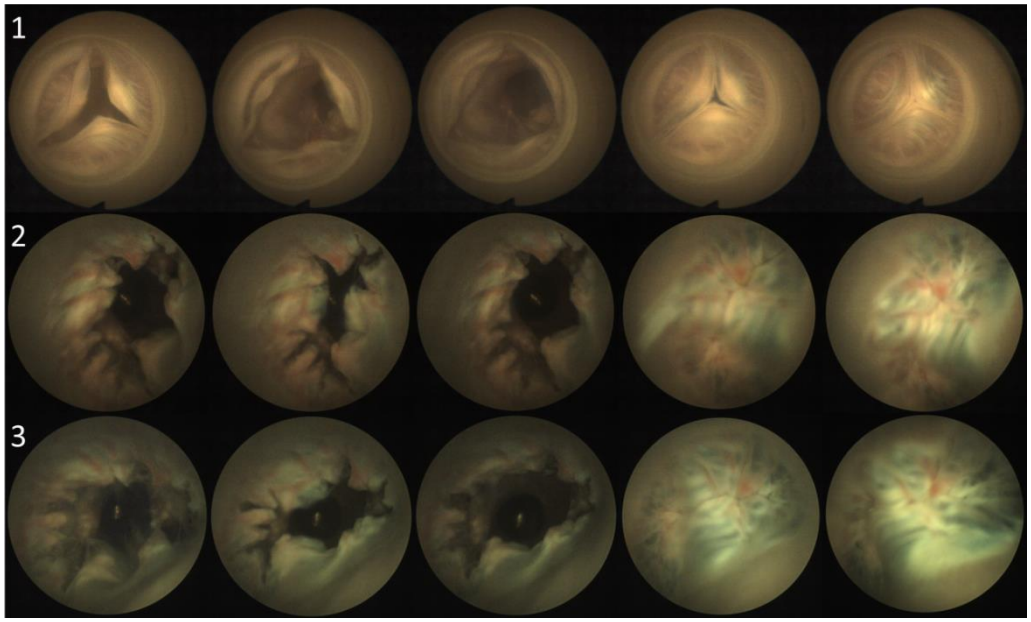

FIGURE 5.7. Representative snapshots of both the aortic (1) and mitral (2-3) valve, recorded with the high speed camera. Line 2 shows the mitral valve with a stroke volume of about 50 ml, showing proper coaptation and a physiological behaviour. The bottom line shows the mitral valve for stroke volumes of 65 ml, with the last snapshot (bottom right) highlighting the prolapse of the anterior leaflet due to the absence of papillary muscle function.

Regarding the behavior of the passive left ventricle, the proposed platform represents a more realistic model of the *in vivo* ventricular dynamics if compared to the state-of-the-art passive-heart mock loops, based upon the internal pressurization of the ventricular chamber, avoiding any paradox behavior of the ventricular walls [70,171]. However, the complex *in vivo* ventricular physiology that involves a specific distributed, three-dimensional dynamic myocardial contraction with ventricular twisting cannot be mimicked with the proposed approach, which only involves applying a uniform and simultaneous pressure on the whole ventricle epicardium. Similarly, atrial contraction is absent, as the left atrium is not subject to any external load and is only provided with a controlled filling pressure through the preload circuit.

The LVAD pilot experiment was meant to demonstrate the potential of the developed mock loop for research, device testing and visualization studies. The passive-heart platform

was able to effectively simulate the post-operative scenario, allowing hemodynamic measurements with simultaneous visualization of the AV under well controllable experimental conditions. In particular, the hemodynamic and kinematic effects of different levels of mechanical support on the AV function were assessed, obtaining results that are coherent with both clinical observations [191] and published *in vitro* studies [30]. Moreover, the possibility of performing high speed video acquisitions allows deeper insights on the kinematic and morphological alterations that cf-LVAD induce on the AV function. In this experiment, we analyzed AV opening and showed, for duty cycles smaller than 10%, how the AV opens without complete separation of the AV leaflets. This phenomenon only seems to occur in a very narrow pump speed range, just below the speed at which valve opening is completely inhibited (12000 rpm in our test). This finding may suggest that, for some patients, a fine tuning of the cf-LVAD speed may prevent altered AV opening, still without significantly impairing the support that is given to the patient.

With respect to the clinical gold standard for the evaluation of heart valve diseases, echo imaging, the described setup showed some limitations. Indeed, the access to the heart was inhibited by the presence of the rigid chamber around the ventricles; however, the acquisition of the most common views is technically feasible using a transesophageal probe placed on the left atrium surface. The design of an ad-hoc port for standard echo probes in the fluid-filled chamber may significantly facilitate the performance of echo imaging on the heart. Future developments of the proposed platform may also address its evolution into a 4-chamber model of the circulation, facing the challenge of properly managing the different compliances of the ventricles. Moreover, a better simulation of the *in vivo* ventricular dynamics may be achieved with an appropriate and controlled motion of the heart apex, which might be mechanically actuated modifying the existing apical holder. As for the LVAD study, the main limitation lies in the fact that the fluid used, i.e. saline, did not mimic the blood rheology, thus potentially introducing a bias in our findings. Anyway, the mock loop is capable of working with any fluid, including blood. Also, the outflow graft was used to connect the outflow of the LVAD to the aorta was longer than the set of tubes and cannulae used in patients.

In conclusion, the proposed *in vitro* mock circulatory loop represents a valid and cost-effective platform for a wide range of purposes, including devices-testing applications, simulation of valve repair or transcatheter procedures, visualization studies and training.

6

Towards the development of four-chamber passive and beating heart platforms

6.1 Rationale

The relevance of the interplays between left and right circulation is well known in literature and involves complex hemodynamic, functional and morphological aspects. Being able to model these aspects is crucial for the study of many clinically relevant issues, such as biventricular heart failure [195,196], right ventricular failure secondary to left ventricular dysfunction [197] or cf-LVAD implantation [198–200], tricuspid regurgitation after left-sided valvular surgery [201–203], inter-ventricular conduction delays [204–206], inter-ventricular shunts [207,208].

As discussed in Chapter 2, these issues have been addressed by several researchers, who developed hybrid closed-loop *in vitro* mock ups of the whole circulation [41,42,44,89,209]. These platforms are able to provide a very controllable environment, in which variations in the heart contractile behavior can be mimicked and the hemodynamic interplays between left and right circulation can be assessed. Nonetheless, given the purely hydraulic nature of these platforms, their use was substantially limited to the hemodynamic assessment of mechanical circulatory support devices [26,28,87,90,210]. Indeed, in order to simulate the minimally-invasive closure of septal defects, or investigate the effects of left-sided surgeries on the right-heart valves, or even to study resynchronization therapies, being able to model the heart anatomy, morphology and physiology is fundamental.

Regarding these issues, as shown in the previous Chapters, *ex vivo* models undoubtedly represent the best solution in order to achieve a very close simulation of the *in vivo* scenario. Nonetheless, to the best of our knowledge, none of the state-of-the-art *ex vivo* models is capable of working in a 4-chamber closed-loop configuration. De Hart and colleagues presented some preliminary results of an *ex vivo* two-chamber working pig heart-lung model [211], and claimed their PhysioHeart platform to be able to work in a 4-chamber open-loop working heart mode. Chinchoy and Hill also published two papers describing four-chamber open-loop beating heart experiments using large heart models [7,9]. However, the hemodynamics that were achieved in these latter investigations were far from physiologic, as extremely simplified models were used for both the preloads and the afterloads.

An alternative option, that allows for the preservation of the cardiac anatomy and morphology, is represented by the *in vitro* passive-heart approach. Indeed, this methodology could potentially overcome the anatomical limitations of the state-of-the-art hydraulic mock

loops, still maintaining the possibility of a model-controlled actuation in a 4-chamber closed-loop working mode. As described in the previous Chapters, two passive left-heart platforms were developed and used to perform TAVI and LVAD investigations. In both cases, the systems were designed and assessed in a 2-chamber open-loop working mode, i.e. neglecting the right-sided circulation and uncoupling the preload and afterload circuits.

In this Chapter we present the redesign of an existing 4-chamber purely hydraulic model-controlled mock circulatory loop, that was developed at the Cardiovascular Biomechanics Laboratory of the TU/e [26]. Our challenging goal is developing a platform capable of working in a 4-chamber closed-loop mode with entire heart structures, being either passive hearts actuated by model-controlled pumps, or isolated beating hearts. Since the project is ongoing, this Chapter is only intended to provide the reader with an overlook of the current directions that the presented research is undertaking, together with preliminary results of a geometrical/anatomical study for a standardized hydraulic interface for the heart samples.

6.2 The TU/e model-controlled mock loop

The existing system (Figure 6.1), whose redesign will be described in the following paragraphs, is an hydraulic model-controlled mock circulation loop, featuring a systemic, pulmonary, and coronary vascular bed [26].

The mock circulation is actuated by two synchronized servomotor-operated piston pumps, acting as left and right ventricle, which are controlled using the heart model proposed by Bovendeerd et al. [212]. Each ventricle is constituted by a plastic chamber that includes two polyurethane valves (LifeTec Group, Eindhoven, The Netherlands). The aorta is modeled by a polyurethane tube (diameter of 25 mm, length of 45 cm and thickness of 0.1 mm) that features a branch mimicking the brachiocephalic arteries and a physiological coronary flow model. The latter is constituted by a collapsible tube, which is externally subjected to the ventricular pressure and, therefore, mimics the variable resistance of the myocardium [213]. The systemic and pulmonary impedances are modeled by adjustable four-element Windkessel models, positioned distal from the aorta and pulmonary valve, respectively. Atria are modeled with two compliance chambers that function as preloads for ventricular filling.

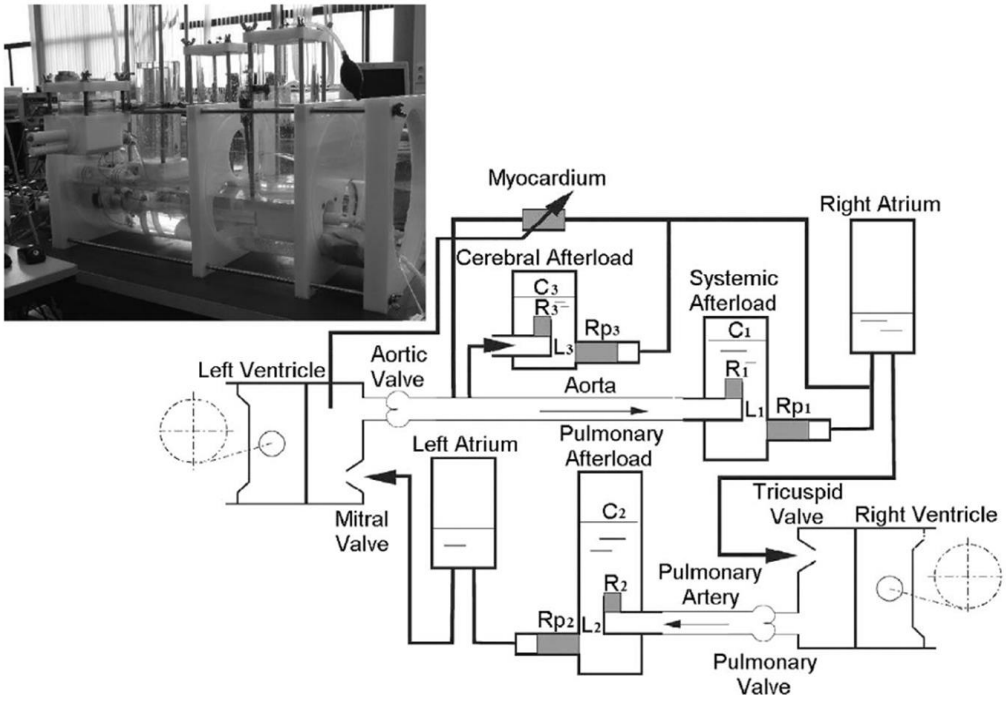

FIGURE 6.1. The model-controlled mock circulation (upper left) and a schematic representation of it (lower right). Figure from Schampaert et al. [26].

6.3 Redesign of the mock loop

6.3.1 General considerations

As stated in the introduction, our purpose is to modify the existing hybrid 4-chamber closed-loop setup in order to allow the execution of experiments with either passive or beating hearts. In practice, this means redesigning the setup to substitute the set of components that model the heart function (pumps, valves, ventricles and atria), with the real heart structure that will be used instead.

To do so, the first mandatory step is the design of a standard interface that allows the easy connection of the main heart vessels to the mock circulation loop. Indeed, while for a purely hydraulic system the position and layout of the components is not restricted *a priori*, the use of an entire heart poses some challenges. In particular, the design of the connection should avoid any distortion or malpositioning of the heart vessels, and guarantee satisfying hemodynamic properties. The first requirement is intended to avoid oddities in both the vessels and the valves behavior, as distorted configurations of the vessels may induce valve malfunction. To avoid these issues, a reasonable approach would consist in trying to maintain as much as possible the physiological orientation and relative position of the heart vessels. Regarding the achievement of satisfying hemodynamics in the mock loop, key aspects in the design of the heart-loop connection would be providing short and flexible connections, and minimizing the hydraulic discontinuities that the fluid may encounter. The design of the interface between the heart and the afterload circuit was based on an anatomical study aimed at determining the orientation and relative position of the heart vessels, and will be described in detail in paragraph 6.3.3.

The redesign of the loop also took into account the requirements that arise from the different working modalities the platform should be designed for, i.e. passive and beating heart. In particular, the latter case represents the most demanding situation, as the management of an isolated beating heart requires a more complex experimental procedure and entails additional requirements, such as blood oxygenation, optimal venting and possibility of switching between different working modes. For this reason, the *ex vivo* configuration was considered as the reference one for the design of the mock circulatory loop.

With respect to it, the passive-heart configuration will represent a simplified design scenario, where no Langendorff perfusion, or blood oxygenation, is needed. The two working modes are described in paragraph 6.3.4.

The actual redesign of the setup, that is briefly described in paragraph 6.3.5, made use of the results of the anatomical campaign and tried to maintain the system as similar as possible to the existing one. This approach was intended to minimally alter the good hydraulic properties of the existing system and to ensure a good compatibility, interchangeability and modularity between the two rigs. A summary of the design requirements is reported in the following paragraph.

6.3.2 **Design requirements**

In the light of the above mentioned considerations, the system will be designed in order to meet the following requirements:

- Being able to host entire porcine hearts and enable the connection of their main afferent and efferent vessels, i.e. pulmonary veins, aorta, superior caval vein and pulmonary artery, with the mock circulatory loop.
- Avoid any oddities or malfunctioning of both the heart vessels and the valves due to the connection to the mock loop.
- Provide the heart with a full circulation loop that represents the systemic and pulmonary trees.
- Recreate, *in vitro*, hemodynamic conditions that closely resemble the typical physiological waveforms and can be adjusted to simulate pathological scenarios.
- Enable the use of passive hearts, actuated by piston pumps that dynamically pressurize the ventricles with either one of the two approaches that were presented in the previous Chapters.
- Allow the performance of *ex vivo* experiments with isolated beating hearts. In particular, with this respect, the platform should:
    - Be able to use blood as working fluid, and guarantee its appropriate oxygenation and heating.

  - Provide the possibility of easily switching between Langendorff perfusion and working-heart mode.
  - Enable an easy and effective venting of the heart and the loop, to avoid the presence of any air bubble and, therefore, reduce the risk of inducing ischemia.
- Allow the study of cardiovascular devices, e.g. left ventricular assist devices, transcatheter valves, intra-aortic balloon pumps.

6.3.3 Anatomical study

An anatomical investigation was performed on 7 swine hearts, in order to characterize the spatial orientation and relative position of the heart vessels and to accordingly design a standard connection between the heart and the mock loop.

Before deepening into the details of the campaign, two anatomical differences existing between the human and the swine heart should be pointed out. Firstly, while in the human right atrium the caval veins are almost aligned, in the porcine heart they enter the chamber at right angles [214]. Given this peculiar orientation, the inferior caval vein is typically ligated in the preparation of the hearts for *ex vivo* and *in vitro* experiments, and only the superior caval vein is used to fill the right atrium. Therefore, the orientation of the inferior caval vein was not assessed in the anatomical study.

The second difference regards the left atrium; indeed, the porcine one receives only 2 pulmonary veins, while in the human left atrium there are generally four orifices [214]. For the sake of ease, in the typical preparation of swine hearts the pulmonary veins are removed, allowing the insertion of a large cannula into the left atrium [8]. Consistently with this protocol, the pulmonary veins were also removed in the tested hearts, and the orientation of the resulting orifice in the left atrium was rather assessed.

Given its orientation, which is approximately coaxial with the heart's longitudinal axis, the aorta was taken as a reference to characterize the relative orientation and position of the other three anatomical elements (superior caval vein, pulmonary artery and left atrial orifice). The superior caval vein was assumed to be parallel to the aorta [214]. Figure 6.2 shows some representative pictures that were acquired during the anatomical study and a schematic

representation of the measurements that were performed on the images. Briefly, fresh hearts were harvested from a local abattoir and the main vessels were isolated. A go-no-go gauge was placed inside the aorta, and was fixed in vertical position with a laboratory clamp. Then, a second go-no-go gauge was sequentially inserted in each of the other vessels. For every vessel, pictures of the heart were acquired from the equivalent of the caudo-cranial view (Figure 6.2, A), antero-posterior view (Figure 6.2, B) and from the latero-lateral view (Figure 6.2, C).

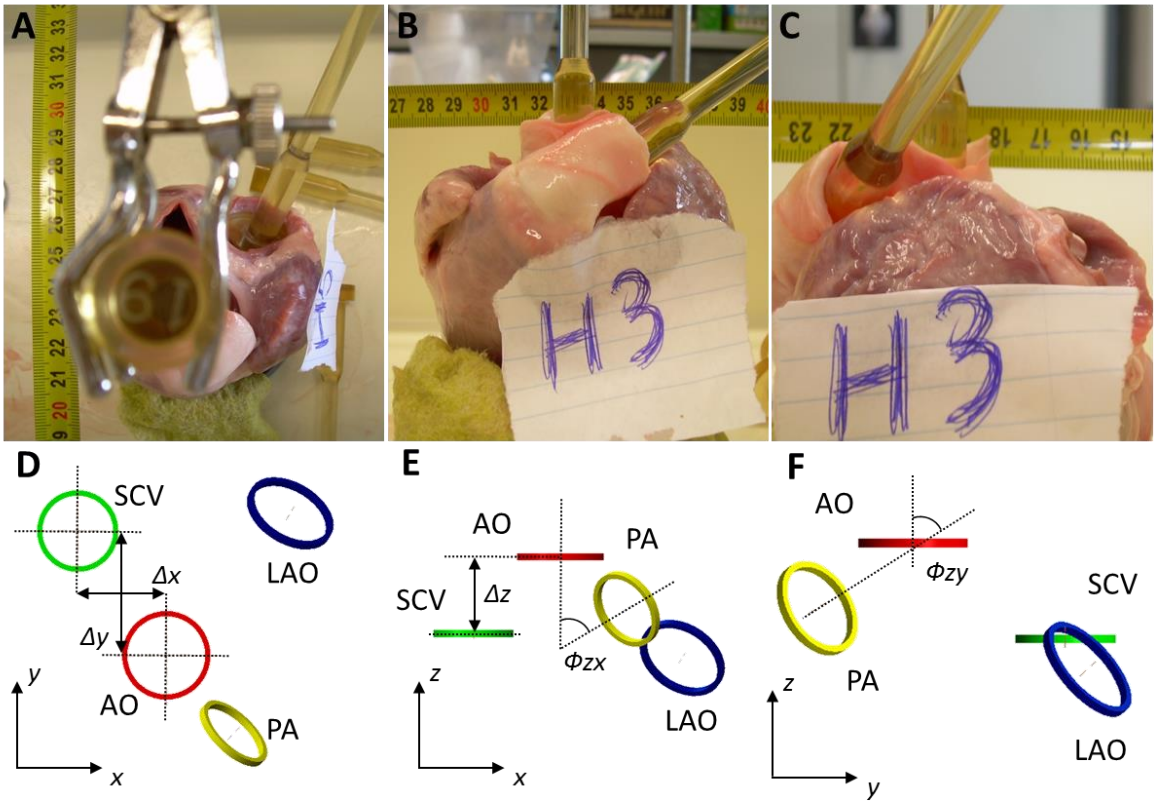

FIGURE 6.2. Anatomical study to assess the orientation and position of the heart anatomical elements, i.e. superior caval vein (SCV), pulmonary artery (PA), left atrial orifice (LAO) with respect to the aorta (AO). Top: representative pictures of the heart with the go-no-go gauge inserted in the aorta and in other vessels from the caudo-cranial (A), antero-posterior (B) and latero-lateral (C) view. Bottom: schematic exemplification showing how, from the images, the measures were made in the caudo-cranial (D), antero-posterior (E) and latero-lateral (F) view.

For every sample, the images were analyzed with ImageJ (National Institute of Health, Bethesda, Maryland, USA) to estimate the relative position (Δx, Δy, Δz) and orientation (Φzx, Φzy) of the heart anatomical elements with respect to the aorta. For every image, five

measurements were performed and averaged. Table 6.1 shows the results of the study, averaged over the tested hearts.

TABLE 6.1. Results (mean ± SD) of the anatomical study performed. Aorta (AO), pulmonary artery (PA), left atrial orifice (LAO), superior caval vein (SCV).

	Diameter [mm]	**Δx [mm]**	**Δy [mm]**	**Δz [mm]**	**Φzx [°]**	**Φzy [°]**
AO	23.0 ± 1.4	-	-	-	-	-
PA	21.2 ± 0.4	22 ± 5.3	19 ± 1.3	15 ± 7.1	41 ± 7.7	56 ± 5.7
LAO	26.2 ± 1.3	40 ± 7.6	35 ± 13.8	29 ± 7.6	43 ± 5.5	34 ± 11.3
SCV	22.2 ± 1.1	29 ± 2.6	22 ± 5.1	22 ± 6.1	0	0

The data reported in Table 6.1 were used as input for the CAD design (Figure 6.3), in order to have a precise idea of the heart vessels orientation and redesign the setup accordingly.

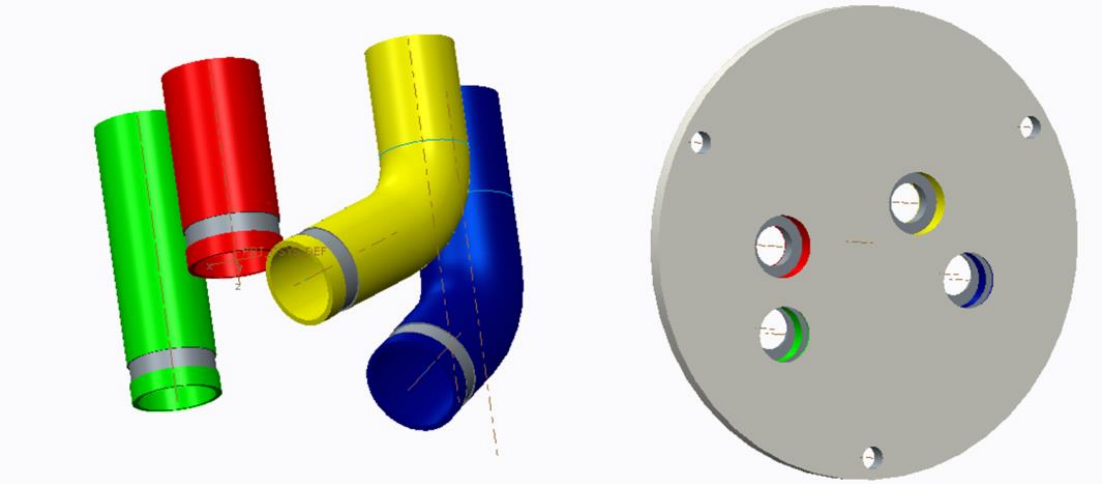

FIGURE 6.3. Left: CAD model showing the designed heart outflow conduits. The orientation was designed in order to match that of the heart anatomical elements. Right: the standardized interface to the circulatory loop that was designed accordingly. The aorta is shown in red, the superior caval vein in green, the pulmonary artery in yellow and the left atrial orifice is shown in blue.

6.3.4 **Working modes**

Figure 6.4 shows the schematic of the mock circulatory loop for the Langendorff perfusion (top) and the 4-chamber closed-loop working mode (bottom).

Langendorff perfusion is typically used in *ex vivo* experiments to resuscitate the heart after the ischemic time [7,8,130], as well as to stabilize its function in case of any abnormality that the heart may exhibit during the working mode configuration, e.g. fibrillation, decrease in contractility, localized ischemia etc. In this configuration, the myocardium is perfused with either nutrient rich solutions or warm oxygenated blood by means of a centrifugal pump. Flow is provided in a reverse way in the aorta, thus causing the closure of the aortic valve and the perfusion of the coronary bed through the coronary ostia. The blood is then collected in the right atrium and is pumped by the right ventricle, through the pulmonary valve, to a reservoir. All the other vessels, i.e. pulmonary veins, superior caval vein and the aorta, are clamped.

In the four-chamber working mode (Figure 6.4, bottom), blood is flowing through the right and the left heart as in the physiological circulation. Blood heating and oxygenation is achieved with an external loop connected to the pulmonary afterload. As Figure 6.4 should exemplify, the system is designed to allow for an easy switching between the Langendorff perfusion and the working mode simply by clamping/unclamping some circuital branches and closing the pulmonary afterload compliance chamber.

In both configurations, to ensure proper thermo stasis, the whole afterload circuit is submerged into a bath, which is connected to an external heat exchanger. Furthermore, the blood volume in the circuit can be adjusted by means of roller pumps, which are connected to both afterloads. The roller pumps can also be used to recirculate the blood in the loop before the beginning of the experiment, so to avoid stagnation and precipitation of the particulated fraction.

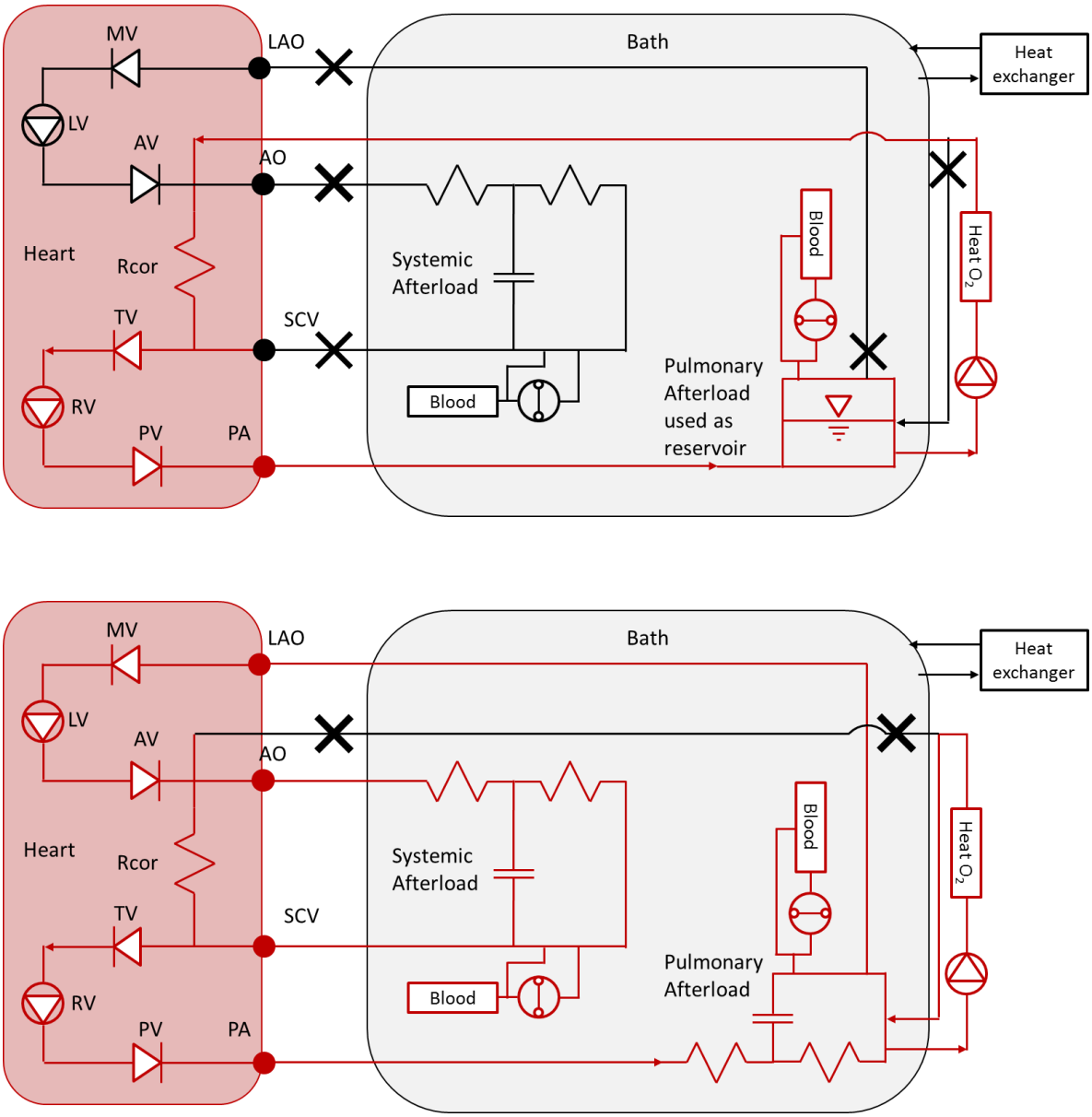

FIGURE 6.4. Schematic of the mock circulatory loop in the Langendorff perfusion mode (top) and in the 4-chamber closed-loop working mode (bottom). The heart is represented by the red box: mitral valve (MV), left ventricle (LV), aortic valve (AV), coronary resistance (Rcor), tricuspid valve (TV), right ventricle (RV), pulmonary valve (PV). The heart anatomical elements (LAO, AO, SCV, PA) are connected to the mock circulatory loop, which is submerged in a heated bath (light blue box). The red lines indicate the circuit in which the blood is flowing, while the black lines indicate the lines that are closed in this working mode.

6.3.5 Design of the setup

As already discussed, the design of the system was driven by the outcomes of the anatomical study (Table 6.1, Figure 6.3) and by the requirements listed in paragraph 6.3.2, trying not to alter the design solutions of the existing mock loop.

Without lingering on details, the mock loop (Figure 6.5) was restructured so to allow the positioning of the heart in an open-thorax configuration. In this configuration, the aorta and the superior caval vein are heading out of the heart in parallel on the left, while the pulmonary artery and veins are pointing to the right. The afterload circulatory loop was adapted accordingly, and both Windkessel modules were redesigned in compliance with the new heart-loop interface. Anyhow, the redesign did not alter the hydraulic properties of the afterloads' components, i.e. the dimensioning of the resistances, compliances and inertances. According to the circuital schemes that are reported in Figure 6.4, accesses for the heating and oxygenation loop, as well as for blood recirculation and filling, were provided in the bottom of the Windkessel. Furthermore, the afterload modules were placed in a higher position with respect to the heart, leading to a mild inclination (about 5-10°) of the conduits that should facilitate the venting. Figure 6.6 shows a picture of the assembled setup.

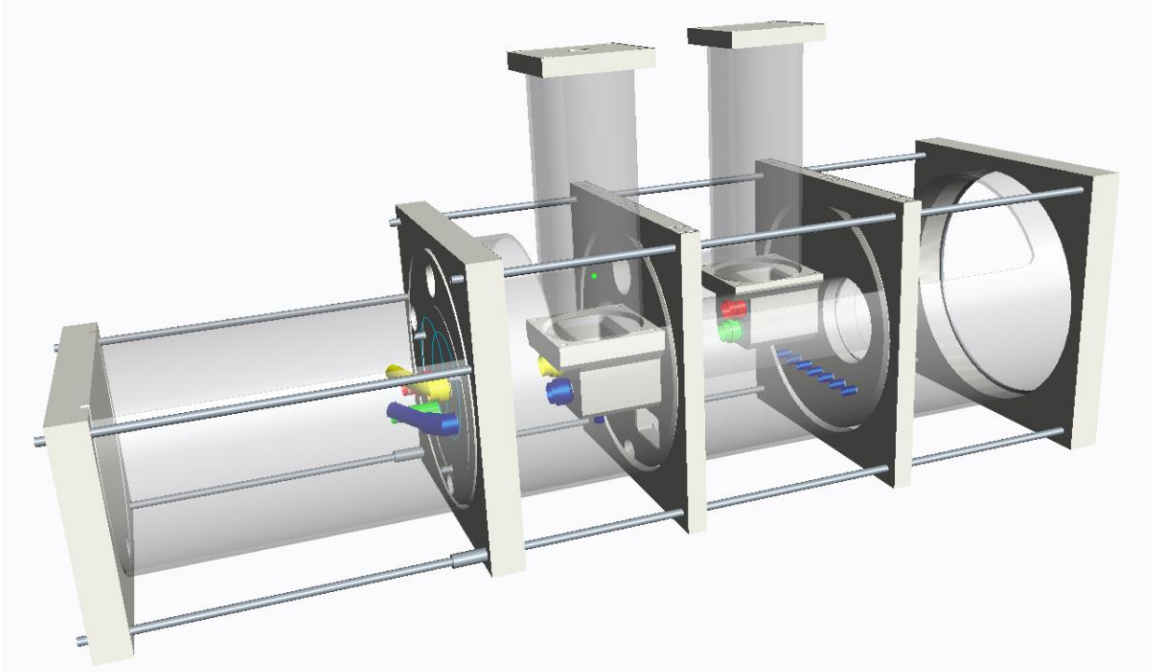

FIGURE 6.5. CAD model of the mock loop.

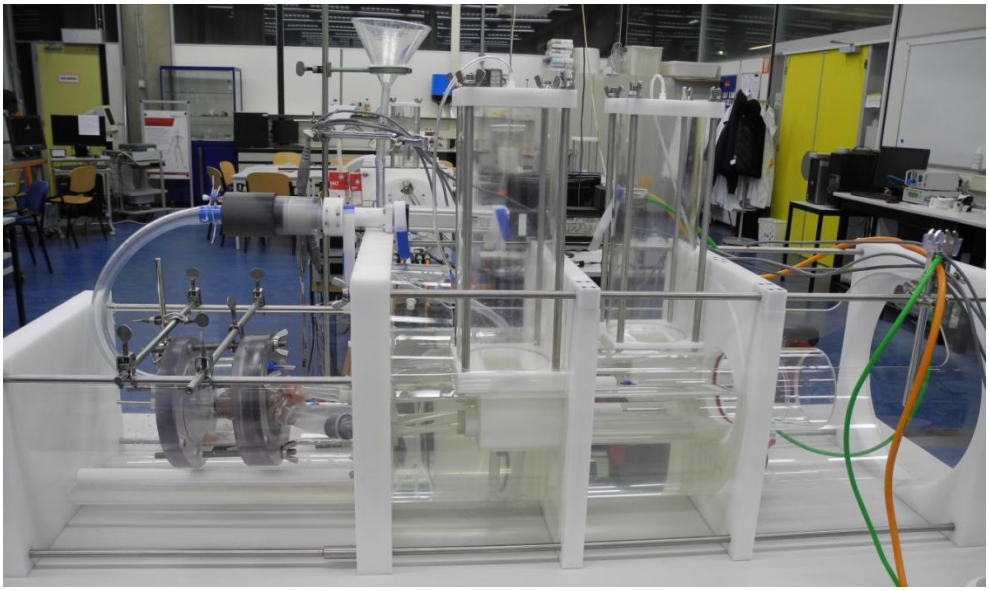

FIGURE 6.6. Picture of the setup.

6.4 Current directions

Preliminary assessments are currently being performed using passive hearts (Figure 6.7), to verify the proficiency of the developed system. The first experimental evidences demonstrated the efficacy of the developed heart-loop connection, which do not induce any oddity in the vessels and allow the preservation of their physiological orientation.

Pilot experiments are also being performed to investigate the feasibility of the passive-heart approach in which external cyclic pressurization is applied to the ventricular walls in a 4-chamber working mode. With this respect, as discussed in Chapter 5, the main issue that is being addressed is represented by the different compliance of the right and left ventricles, which leads to substantial abnormalities in the actuation. Indeed, if not treated, the right ventricle impulsively collapses during systole, due to the pressure generated in the fluid-filled chamber and to its lower stiffness as compared to the left ventricle. This incorrect behaviour also leads to an altered distribution of the stroke volumes, as the left ventricular ejection starts after the collapse of the right ventricle. Therefore, the left heart generates lower cardiac

outputs as compared to the right one, with a relative ratio depending on the pump stroke volume.

In order to solve this issues we are currently investigating the possibility of reducing the physiological compliance gap by stiffening the right ventricle with classical chemical fixation methodologies. In particular, we are considering the use of Glyoxal, a dialheid that in the last 20 years has become one of the most used alternative to formaldehyde as a histological fixative [215–217]. Indeed, Glyoxal's main advantages as compared to other compounds, e.g. formaline, are the low inhalation risk and the faster reaction rate (around 1-3 h). Preliminary tests, in which the right heart was treated with Glyoxal, showed encouraging results with selective stiffening of the right ventricle that was achieved after 3 hours. Dynamic experiments with direct ventricular actuation highlighted a fairly uniform compressibility of the right and left heart, although the hemodynamic results do not fall within the physiological range yet.

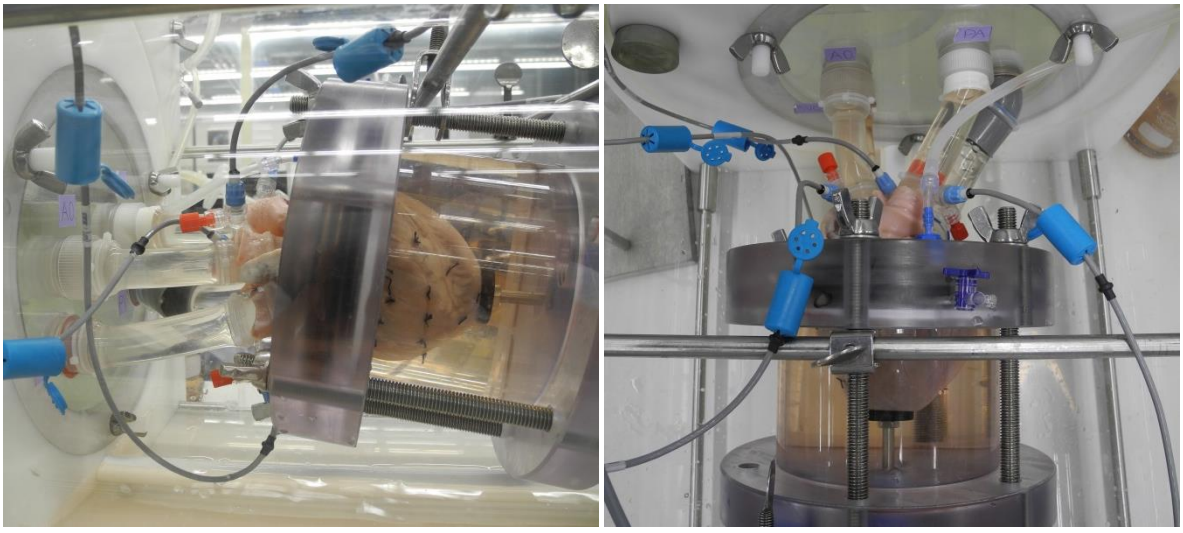

FIGURE 6.7. Pictures of the developed 4-chamber mock loop during one of the experimental assessments with passive hearts.

Acknowledgements

A particular acknowledgement goes to Luca Vicentini for the experiments he is performing on the 4-chamber passive-heart mock loop.

7

Conclusive remarks

7.1 Main findings

Within the evolving context of surgical techniques and cardiovascular devices, calling for innovative and realistic assessment methodologies, the present work underlined the importance of *in vitro* platforms in which the modelling of the *in vivo* environment includes the heart anatomy and morphology. In particular, we investigated a promising approach that was substantially unexplored in literature, i.e. the development of mock circulatory loops for entire passive hearts. This thesis elucidated the potentiality and the relevance of such systems, that can be applied as multi-functional platforms for research, device-testing, visualization studies, and training purposes. Our findings demonstrated how passive-heart mock loops can provide valuable and cost-effective solutions for various needs and may fill the gap between classical *in vitro* simulators and *ex vivo* and animal models. Indeed, the developed platforms were capable of *i)* closely reproducing the physiologic hemodynamics, *ii)* allowing intracardiac endoscopy and multimodal imaging, *iii)* performing surgical and/or transcatheter procedures, *iv)* assessing cardiovascular devices and *v)* being used as training platforms.

The first system was inspired by the work of Richards et al. [70]. In an episodic work that, to the best of our knowledge, didn't give birth to any systematic application, Richards proposed a functioning principle consisting in the cyclic internal pressurization of the left ventricle by means of a piston pump connected to the heart apex. The design of our mock loop was aided by an *ad-hoc* defined lumped parameter model, that was used as a predictive tool and led to the achievement of hemodynamic conditions that closely mimicked the physiological ones. The system also showed excellent imaging capabilities, and good valve function. As a main drawback, the actuation methodology caused a paradoxical motion of the ventricular walls during the cardiac cycle, which, however, didn't impair the mitral valve competence, and an altered fluid dynamic field inside the left ventricle.

The passive-heart platform concept was shown to be perfectly suitable for performing realistic *in vitro* studies of TAVI applications. Our aim was to simulate *in vitro* the typical scenario in which TAVI procedures are performed *in vivo*, so to provide physicians with a multi-functional tool that could be used for both training and research purposes. To achieve this goal, the passive-heart system was optimized with improved design solutions, that led to the development of a simple, reliable and cost-effective system capable of closely simulating

the hemodynamic and anatomo-morphological *in vivo* environment. The system was successfully used to perform TAVI under fluoroscopic guidance and simultaneous intracardiac visualization in a catheterization lab. An *in vitro* model of aortic stenosis was also developed, assessed, and used in the simulated TAVI procedures to better mimic the pathological scenario.

We then tackled the development of another passive-heart mock loop, that adopted a complementary working principle as compared to the first passive-heart setup in order to better simulate the physiological behaviour of the ventricles avoiding oddities in the ventricle wall motion. Indeed, this platform mimicked the pulsatile pumping function of the left heart through the cyclic external pressurization of the ventricular walls. The system was capable of reproducing physiologic hemodynamic conditions, and allowed for endoscopic imaging of the cardiac structures. Anyhow, differently from the former passive-heart approach, this actuation methodology induced mitral valve prolapse at high stroke volumes, due to the absence of papillary muscle contraction. The system was also used to perform a pilot study, in which the acute post-operative scenario after the implantation of a cf-LVAD was simulated, and the AV function for different levels of support was analysed. Our results were in line with clinical observations and previous studies, and the acquisition of high-speed video recordings of the aortic valve allowed deeper insights into the kinematic and morphological alterations that cf-LVAD may induce on the AV function.

Finally, we described the first steps that have been made towards the development of a 4-chamber closed-loop mock loop for entire hearts, being either passive hearts actuated by model-controlled pumps, or isolated beating hearts. An existing hybrid 4-chamber system, developed at the TU/e, was redesigned to substitute the set of hydraulic components modelling the heart function with the real heart structure that will be used instead. Thus, an anatomical study was conducted to develop an interface allowing the connection of the main heart vessels to the mock circulatory loop preserving their physiologic configuration. The mock loop was then redesigned accordingly, also considering the requirements related to the performance of *ex vivo* experiments.

Beyond the specific contribution of each Chapter, this thesis as a whole elucidates the importance of adopting a methodological approach for the design of cardiovascular *in vitro* platforms housing biological samples. More specifically, the development of all the different setups was based on quantitative and objective procedures aimed at optimizing the functional

interaction between the artificial and the biological components. Two examples of this methodology are the model-assisted design of the internally pressurized passive-heart platform and the anatomo-morphological study performed to standardize the heart-loop interface. In our view, the implementation of such a systematic approach for the design of *in vitro* platforms represents a critical step towards the attainment of functional and reliable models.

7.2 Future directions

Given the substantial novelty of the work presented in this thesis, the opportunities for developments are numerous and the future improvements should aim at reducing the gap existing between the proposed passive-heart systems, which were only developed to the stage of prototype systems, and the other state-of-the-art platforms, which nowadays are enjoying maturity. In particular, the simulation of the heart behaviour should be improved to provide a more solid alternative to *ex vivo* models, while implementing a model-controlled actuation in a four-chamber working mode would bridge the gap with hybrid *in vitro* mock loops.

Regarding the actuation methodologies, two different and complementary solutions for the generation of the cardiac output were assessed. The internal pressurization of the ventricle induced a paradoxical ventricular behaviour, while the external driving of the ventricular walls provided for a better simulation of the heart function but caused mitral valve prolapse for high stroke volumes. An interesting evolution may consist in combining these two approaches, to achieve high cardiac outputs maintaining proper mitral valve function and a ventricular behaviour resembling the physiological one. In particular, the external actuation of the ventricular walls could be adopted to mimic the ventricular wall motion without requiring high stroke volumes, thanks to the direct contribution of the apical pump to the generation of the cardiac output. Furthermore, speculations could be made on the possibility of simulating the *in vivo* ventricular twisting and apex-base motion through a proper mechanical actuation.

Concerning the simulation of the dynamic contractile behaviour of the heart, which is typically implemented in hybrid mock loops with a model-controlled actuation of the pumps,

the use of entire hearts poses some challenges. Indeed, differently from a purely hydraulic and rigid system in which the ventricular volumes are only determined by the position of the piston pumps, the heart is a compliant structure characterized by a non-linear pressure-volume relation. Therefore, implementing a model-controlled actuation for passive-heart mock loops would require the adaptation of the existing models to account for the passive behaviour of the heart. Moreover, to overcome the issues deriving from the unavoidable biological variability, the design of a learning algorithm may be of significant importance.

As already mentioned in Chapter 6, future improvements should also address the development of four-chamber closed-loop systems, to allow the study of many clinical issues and devices that involve relevant interactions between the left and the right circulation. With this respect, preliminary experiments focusing on the management of the different compliances of right and left heart are currently carried out, to verify the feasibility of the approach in which the ventricles are externally actuated. Nevertheless, the direct internal pressurization of the ventricle may represents a more easily achievable solution for such working mode, that will also be pursued in the near future.

In conclusion, this thesis elucidated the role played by passive-heart mock circulatory loop in the broad panorama of the experimental platforms for cardiovascular research. Given the results of our research, we believe that in the near future passive-heart platforms may become the choice of election among the *in vitro* platforms for many applications, potentially reducing the need for *ex vivo* and animal models. Furthermore, they might represent an interesting option for physicians training and protocol optimization, owing to the tremendous awareness that the operator experiences when simulating surgical/interventional manoeuvres with these laboratory apparatuses.

References

[1] World Health Organization. Global Atlas on cardiovascular disease prevention and control. Geneva, Switz WHO 2012.

[2] Smith SC, Collins A, Ferrari R, Holmes DR, Logstrup S, McGhie DV, et al. Our time: a call to save preventable death from cardiovascular disease (heart disease and stroke). J Am Coll Cardiol 2012;60:2343–8.

[3] Laslett LJ, Alagona P, Clark BA, Drozda JP, Saldivar F, Wilson SR, et al. The worldwide environment of cardiovascular disease: prevalence, diagnosis, therapy, and policy issues: a report from the American College of Cardiology. J Am Coll Cardiol 2012;60:S1–49.

[4] Roger VL, Go AS, Lloyd-Jones DM, Benjamin EJ, Berry JD, Borden WB, et al. Heart disease and stroke statistics--2012 update: a report from the American Heart Association. Circulation 2012;125:e2–e220.

[5] Yancy CW, Jessup M, Bozkurt B, Butler J, Casey DE, Drazner MH, et al. 2013 ACCF/AHA Guideline for the Management of Heart Failure: A Report of the American College of Cardiology Foundation/American Heart Association Task Force on Practice Guidelines. Circulation 2013;128:e240–319.

[6] Langendorff O. Untersuchungen am überlebenden Säugethierherzen. Pflüger, Arch Für Die Gesammte Physiol Des Menschen Und Der Thiere 1895;61:291–332.

[7] Edward Chinchoy, Charles L. Soule, Andrew J. Houlton, William J. Gallagher, Mark A. Hjelle, Timothy G. Laske, Jose´e Morissette and PAI. Isolated Four-Chamber Working Swine Heart Model. Ann Thorac Surg 2000;70:1607–14.

[8] De Hart J, de Weger A, van Tuijl S, Stijnen JM, van den Broek CN, Rutten MC, et al. An ex vivo platform to simulate cardiac physiology: a new dimension for therapy development and assessment. Int J Artif Organs 2011;34:495–505.

[9] Hill AJ, Laske TG, Coles Jr JA, Sigg DC, Skadsberg ND, Vincent SA, et al. In Vitro Studies of Human Hearts. Ann Thorac Surg 2005;79:168–77.

[10] Granegger M, Mahr S, Horvat J, Aigner P, Roehrich M, Stoiber M, et al. Investigation of hemodynamics in the assisted isolated porcine heart. Int J Artif Organs 2013;36:1–9.

[11] Laske TG, Skadsberg ND, Iaizzo PA. A novel ex vivo heart model for the assessment of cardiac pacing systems. J Biomech Eng 2005;127:894–8.

[12] Shiose A, Takaseya T, Fumoto H, Horai T, Kim HI, Fukamachi K, et al. Cardioscopy-guided surgery: intracardiac mitral and tricuspid valve repair under direct visualization in the beating heart. J Thorac Cardiovasc Surg 2011;142:199–202.

[13] Tuzun E, Pennings K, van Tuijl S, de Hart J, Stijnen M, van de Vosse F, et al. Assessment of aortic valve pressure overload and leaflet functions in an ex vivo beating heart loaded with a continuous flow cardiac assist device. Eur J Cardiothorac Surg 2013.

[14] Iaizzo PA, Hill AJ, Laske TG. Cardiac device testing enhanced by simultaneous imaging modalities: the Visible Heart, fluoroscopy and echocardiography. Expert Rev Med Devices 2008;5:51–8.

[15] Aviles M, Mangual J, Ebner A, Ritter J. Isolated swine heart ventricle perfusion model for implant assisted-magnetic drug targeting. Int J Pharm 2008;361:202–8.

[16] Hasegawa H, Araki Y, Usui A, Yokote J, Saito S, Oshima H, et al. Mitral valve motion after performing an edge-to-edge repair in an isolated swine heart. J Thorac Cardiovasc Surg 2008;136:590–6.

[17] Saito S, Araki Y, Usui A, Akita T, Oshima H, Yokote J, et al. Mitral valve motion assessed by high-speed video camera in isolated swine heart. Eur J Cardio-Thoracic Surg 2006;30:584–91.

[18] Schuster A, Grünwald I, Chiribiri A, Southworth R, Ishida M, Hay G, et al. An isolated perfused pig heart model for the development, validation and translation of novel cardiovascular magnetic resonance techniques. J Cardiovasc Magn Reson 2010;12:53.

[19] De Weger A, van Tuijl S, Stijnen M, Steendijk P, de Hart J. Direct Endoscopic Visual Assessment of a Transcatheter Aortic Valve Implantation and Performance in the PhysioHeart, an Isolated Working Heart Platform. Circulation 2010;121:e261–e262.

[20] Bateman MG, Iaizzo PA. Comparative imaging of cardiac structures and function for the optimization of transcatheter approaches for valvular and structural heart disease. Int J Cardiovasc Imaging 2011;27:1223–34.

[21] Schampaert S, van 't Veer M, Rutten MCM, van Tuijl S, de Hart J, van de Vosse FN, et al. Autoregulation of coronary blood flow in the isolated beating pig heart. Artif Organs 2013;37:724–30.

[22] Sigg D, Iaizzo P. In vivo versus in vitro comparison of swine cardiac performance: Induction of cardiodepression with halothane. Eur J Pharmacol 2006;543:97–107.

[23] Görge G, Erbel R, Dobbertin A, Hänggi M, Hake U, Meyer J. Isolated in-vitro perfusion of pig hearts obtained from the abattoir: an alternative to animal experiments? Eur Heart J 1994;15:851–7.

[24] Modersohn D, Eddicks S, Grosse-Siestrup C, Ast I, Holinski S, Konertz W. Isolated hemoperfused heart model of slaughterhouse pigs. Int J Artif Organs 2001;24:215–21.

[25] Frank O. Die Grundform des arteriellen Pulses. Z Biol 1899;37:483–526.

[26] Schampaert S, van't Veer M, van de Vosse FN, Pijls NHJ, de Mol BA, Rutten MCM. In Vitro Comparison of Support Capabilities of Intra-Aortic Balloon Pump and Impella 2.5 Left Percutaneous. Artif Organs 2011;35:893–901.

[27] Sharp MK, Richards CM, Gillars KJ, Giridharan G, Pantalos GM. The influence of mock circulation input impedance on valve acceleration during in vitro cardiac device testing. ASAIO J 2008;54:341–6.

[28] Timms D, Fraser J, Hayne M, Dunning J, McNeil K, Pearcy M. The BiVACOR rotary biventricular assist device: concept and in vitro investigation. Artif Organs 2008;32:816–9.

[29] Gohean J, Figliola R, Camp T, McQuinn T. Comparative in vitro study of bileaflet and tilting disk valve behavior in the pulmonary position. J Biomech Eng 2006;128:631–5.

[30] Tuzun E, Rutten M, Dat M, van de Vosse F, Kadipasaoglu C, de Mol B. Continuous-Flow Cardiac Assistance: Effects on Aortic Valve Function in a Mock Loop. J Surg Res 2010;171:443–7.

[31] Verdonck PR. Mock Loop Testing of On-X Prosthetic Mitral Valve with Doppler Echocardiography. Artif Organs 2002;26:872–8.

[32] Vismara R, Laganà K, Migliavacca F, Schievano S, Coats L, Taylor A, et al. Experimental Setup to Evaluate the Performance of Percutaneous Pulmonary Valved Stent in Different Outflow Tract Morphologies. Artif Organs 2009;33:46–53.

[33] Westerhof N, Bosman F, De Vries CJ, Noordergraaf A. Analog studies of the human systemic arterial tree. J Biomech 1969;2:121–43.

[34] Toy SM, Melbin J, Noordergraaf A. Reduced models of arterial systems. IEEE Trans Biomed Eng 1985;32:174–6.

[35] Suga H, Sagawa K. Instantaneous pressure-volume relationships and their ratio in the excised, supported canine left ventricle. Circ Res 1974;35:117–26.

[36] deBoer RW, Karemaker JM, Strackee J. Hemodynamic fluctuations and baroreflex sensitivity in humans: a beat-to-beat model. Am J Physiol 1987;253:H680–9.

[37] Cox LGE, Loerakker S, Rutten MCM, de Mol BAJM, van de Vosse FN. A Mathematical Model to Evaluate Control Strategies for Mechanical Circulatory Support. Artif Organs 2009;33:593–603.

[38] Sharp MK, Dharmalingham RK. Development of a hydraulic model of the human systemic circulation. ASAIO J 1999;45:535–40.

[39] Swanson WM, Clark RE. A simple cardiovascular system simulator: design and performance. J Bioeng 1977;1:135–45.

[40] Kozarski M, Ferrari G, Clemente F, Górczyńska K, De Lazzari C, Darowski M, et al. A hybrid mock circulatory system: development and testing of an electro-hydraulic impedance simulator. Int J Artif Organs 2003;26:53–63.

[41] Baloa LA, Boston JR, Antaki JF. Elastance-Based Control of a Mock Circulatory System. Ann Biomed Eng 2001;29:244–51.

[42] Pantalos GM, Koenig SC, Gillars KJ, Giridharan GA, Ewert DL. Characterization of an Adult Mock Circulation for Testing Cardiac Support Devices. ASAIO J 2004;50:37–46.

[43] Timms D. A Complete Mock Circulation Loop for the Evaluation of Left, Right, and Biventricular Assist Devices. Artif Organs 2005;29:564–72.

[44] Colacino FM, Arabia M, Danieli GA, Moscato F, Nicosia S, Piedimonte F, et al. Hybrid test bench for evaluation of any device related to mechanical cardiac assistance. Int J Artif Organs 2005;28:817–26.

[45] Westerhof N, Elzinga G, Sipkema P. An artificial arterial system for pumping hearts. J Appl Physiol 1971;31:776–81.

[46] Fraser Jr. CD, Cosgrove 3rd DM. Surgical techniques for aortic valvuloplasty. Texas Hear Inst J 1994;21:305–9.

[47] Lansac E, Di Centa I, Sleilaty G, Crozat EA, Bouchot O, Hacini R, et al. An aortic ring: from physiologic reconstruction of the root to a standardized approach for aortic valve repair. J Thorac Cardiovasc Surg 2010;140:S28–35; discussion S45–51.

[48] David TE, Maganti M, Armstrong S. Aortic root aneurysm: principles of repair and long-term follow-up. J Thorac Cardiovasc Surg 2010;140:S14–19.

[49] Schmitto JD, Mokashi SA, Cohn LH. Minimally-invasive valve surgery. J Am Coll Cardiol 2010;56:455–62.

[50] Makkar RR, Fontana GP, Jilaihawi H, Kapadia S, Pichard AD, Douglas PS, et al. Transcatheter Aortic-Valve Replacement for Inoperable Severe Aortic Stenosis. N Engl J Med 2012.

[51] Yuksel UC, Kapadia SR, Tuzcu EM. Percutaneous mitral repair: patient selection, results, and future directions. Curr Cardiol Rep 2011;13:100–6.

[52] Karimov J. Overview of current sutureless and transcatheter mitral valve replacement technology. Expert Rev Med … 2013;10:73–83.

[53] Mihaljevic T, Cohn LH, Unic D, Aranki SF, Couper GS, Byrne JG. One thousand minimally invasive valve operations: early and late results. Ann Surg 2004;240:529–34.

[54] Murphy GJ, Reeves BC, Rogers CA, Rizvi SI, Culliford L, Angelini GD. Increased mortality, postoperative morbidity, and cost after red blood cell transfusion in patients having cardiac surgery. Circulation 2007;116:2544–52.

[55] Généreux P, Head SJ, Hahn R, Daneault B, Kodali S, Williams MR, et al. Paravalvular leak after transcatheter aortic valve replacement: the new Achilles' heel? A comprehensive review of the literature. J Am Coll Cardiol 2013;61:1125–36.

[56] Vallabhajosyula P, Bavaria JE. Transcatheter aortic valve implantation: complications and management. J Hear Valve Dis 2011;20:499–509.

[57] Vergnat M, Levack MM, Jackson BM, Bavaria JE, Herrmann HC, Cheung AT, et al. The effect of surgical and transcatheter aortic valve replacement on mitral annular anatomy. Ann Thorac Surg 2013;95:614–9.

[58] De Chiara B, Moreo A, De Marco F, Musca F, Oreglia J, Lobiati E, et al. Influence of corevalve revalving system implantation on mitral valve function. Catheter Cardiovasc Interv 2011;78:638–44.

[59] Aggarwal A, Raghuvir R, Eryazici P, Macaluso G, Sharma P, Blair C, et al. The development of aortic insufficiency in continuous-flow left ventricular assist device-supported patients. Ann Thorac Surg 2013;95:493–8.

[60] Soleimani B, Haouzi A, Manoskey A, Stephenson ER, El-Banayosy A, Pae WE. Development of aortic insufficiency in patients supported with continuous flow left ventricular assist devices. ASAIO J 2012;58:326–9.

[61] Erasmi A, Sievers H, Scharfschwerdt M, Eckel T, Misfeld M. In vitro hydrodynamics, cusp-bending deformation, and root distensibility for different types of aortic valve–sparing operations: Remodeling, sinus prosthesis, and reimplantation. J Thorac Cardiovasc Surg 2005;130:1044–9.

[62] Notzold A, Scharfschwerdt M, Thiede L, Huppe M, Sievers H. In-vitro study on the relationship between progressive sinotubular junction dilatation and aortic regurgitation for several stentless aortic valve substitutes. Eur J Cardio-Thoracic Surg 2005;27:90–3.

[63] Vismara R, Fiore GB, Mangini A, Contino M, Lemma M, Redaelli A, et al. A novel approach to the in vitro hydrodynamic study of the aortic valve: mock loop development and test. ASAIO J 2010;56:279–84.

[64] Choon Hwai Yap , Hee-Sun Kim , Kartik Balachandran , Michael Weiler , Rami Haj-Ali APY. Dynamic deformation characteristics of porcine aortic valve leaflet under normal and hypertensive conditions. Am J … 2010:395–405.

[65] Arita M, Tono S, Kasegawa H, Umezu M. Multiple purpose simulator using a natural porcine mitral valve. Asian Cardiovasc Thorac Ann 2004;12:350–6.

[66] Vismara R, Pavesi A, Votta E, Taramasso M, Maisano F, Fiore GB. A pulsatile simulator for the in vitro analysis of the mitral valve with tri-axial papillary muscle displacement. Int J Artif Organs 2011;34:383–91.

[67] Ritchie J, Jimenez J, He Z, Sacks MS, Yoganathan AP. The material properties of the native porcine mitral valve chordae tendineae: an in vitro investigation. J Biomech 2006;39:1129–35.

[68] Dolensky JR, Casa LDC, Siefert AW, Yoganathan AP. In vitro assessment of available coaptation area as a novel metric for the quantification of tricuspid valve coaptation. J Biomech 2013;46:832–6.

[69] Spinner EM, Shannon P, Buice D, Jimenez JH, Veledar E, Del Nido PJ, et al. In vitro characterization of the mechanisms responsible for functional tricuspid regurgitation. Circulation 2011;124:920–9.

[70] Richards AL, Cook RC, Bolotin G, Buckner GD. A Dynamic Heart System to Facilitate the Development of Mitral Valve Repair Techniques. Ann Biomed Eng 2009;37:651–60.

[71] Harken DE, Soroff HS, Taylor WJ, Lefemine AA, Gupta SK, Lunzer S. Partial and complete prostheses in aortic insufficiency. J Thorac Cardiovasc Surg 1960;40:744–62.

[72] Braunwald NS, Cooper T, Morrow AG. Complete replacement of the mitral valve. Successful clinical application of a flexible polyurethane prosthesis. J Thorac Cardiovasc Surg 1960;40:1–11.

[73] Westerhof N, Noordergraaf A. Arterial viscoelasticity: a generalized model. Effect on input impedance and wave travel in the systematic tree. J Biomech 1970;3:357–79.

[74] Jager GN, Westerhof N, Noordergraaf A. Oscillatory flow impedance in electrical analog of arterial system: representation of sleeve effect and non-newtonian properties of blood. Circ Res 1965;16:121–33.

[75] Pollack GH, Reddy R V, Noordergraaf A. Input impedance, wave travel, and reflections in the human pulmonary arterial tree: studies using an electrical analog. IEEE Trans Biomed Eng 1968;15:151–64.

[76] Noordergraaf A, Verdouw D, Boom HB. The use of an analog computer in a circulation model. Prog Cardiovasc Dis 1963;5:419–39.

[77] Westerhof N, Noordergraaf A. Errors in the measurement of hydraulic input impedance. J Biomech 1970;3:351–6.

[78] Murgo JP, Westerhof N. Input impedance of the pulmonary arterial system in normal man. Effects of respiration and comparison to systemic impedance. Circ Res 1984;54:666–73.

[79] Bjork VO, Intonti F, Meissl a. A Mechanical Pulse Duplicator for Testing Prosthetic Mitral and Aortic Valves. Thorax 1962;17:280–3.

[80] Duran CG, Gunning a. J, McMillan T. A Simple Versatile Pulse Duplicator. Thorax 1964;19:503–6.

[81] Cornhill JF. An aortic--left ventricular pulse duplicator used in testing prosthetic aortic heart valves. J Thorac Cardiovasc Surg 1977;73:550–8.

[82] Störmer B, Mendling W, Köhler J, Kivelitz H, Kremer K, Staib W. Comparative study of in vitro flow characteristics between a human aortic valve and a designed aortic valve and six corresponding types of prosthetic heart valves. Eur Surg Res 1976;8:117–31.

[83] Arts T, Bovendeerd PH, Prinzen FW, Reneman RS. Relation between left ventricular cavity pressure and volume and systolic fiber stress and strain in the wall. Biophys J 1991;59:93–102.

[84] Hyndman BW, Kitney RI, Sayers BM. Spontaneous rhythms in physiological control systems. Nature 1971;233:339–41.

[85] Saul JP, Berger RD, Albrecht P, Stein SP, Chen MH, Cohen RJ. Transfer function analysis of the circulation: unique insights into cardiovascular regulation. Am J Physiol 1991;261:H1231–45.

[86] Van Roon AM, Mulder LJM, Althaus M, Mulder G. Introducing a baroreflex model for studying cardiovascular effects of mental workload. Psychophysiology 2004;41:961–81.

[87] Ferrari G, De Lazzari C, Mimmo R, Tosti G, Ambrosi D, Gorczynska K. A computer controlled mock circulatory system for mono- and biventricular assist device testing. Int J Artif Organs 1998;21:26–36.

[88] Ferrari G, Nicoletti A, De Lazzari C, Clemente F, Tosti G, Guaragno M, et al. A physical model of the human systemic arterial tree. Int J Artif Organs 2000;23:647–57.

[89] Ferrari G, De Lazzari C, Kozarski M, Clemente F, Górczyńska K, Mimmo R, et al. A hybrid mock circulatory system: testing a prototype under physiologic and pathological conditions. ASAIO J 2002;48:487–94.

[90] Fresiello L, Khir AW, Di Molfetta A, Kozarski M, Ferrari G. Effects of intra-aortic balloon pump timing on baroreflex activities in a closed-loop cardiovascular hybrid model. Artif Organs 2013;37:237–47.

[91] Gregory SD, Stevens MC, Wu E, Fraser JF, Timms D. In vitro evaluation of aortic insufficiency with a rotary left ventricular assist device. Artif Organs 2013;37:802–9.

[92] Colacino FM, Moscato F, Piedimonte F, Danieli G, Nicosia S, Arabia M. A modified elastance model to control mock ventricles in real-time: numerical and experimental validation. ASAIO J 2008;54:563–73.

[93] Vaes M, Rutten M, Van de Molengraft R V de VF. Left ventricular assist device evaluation with a model-controlled mock circulation. Proc. ASME 2007 Summer Bioeng. Conf. 2007, 2007.

[94] Saikrishnan N, Yap C-H, Milligan NC, Vasilyev N V, Yoganathan AP. In vitro characterization of bicuspid aortic valve hemodynamics using particle image velocimetry. Ann Biomed Eng 2012;40:1760–75.

[95] Siefert AW, Rabbah JPM, Koomalsingh KJ, Touchton SA, Saikrishnan N, McGarvey JR, et al. In Vitro Mitral Valve Simulator Mimics Systolic Valvular Function of Chronic Ischemic Mitral Regurgitation Ovine Model. Ann Thorac Surg 2013;95:825–30.

[96] Rabbah J-P, Saikrishnan N, Yoganathan AP. A Novel Left Heart Simulator for the Multi-modality Characterization of Native Mitral Valve Geometry and Fluid Mechanics. Ann Biomed Eng 2012.

[97] Rabbah J-P, Chism B, Siefert A, Saikrishnan N, Veledar E, Thourani VH, et al. Effects of Targeted Papillary Muscle Relocation on Mitral Leaflet Tenting and Coaptation. Ann Thorac Surg 2013;95:621–8.

[98] Rabbah J-PM, Siefert AW, Spinner EM, Saikrishnan N, Yoganathan AP. Peak Mechanical Loads Induced in the In Vitro Edge-to-Edge Repair of Posterior Leaflet Flail. Ann Thorac Surg 2012;94:1446–53.

[99] Padala M, Hutchison R a, Croft LR, Jimenez JH, Gorman RC, Gorman JH, et al. Saddle shape of the mitral annulus reduces systolic strains on the P2 segment of the posterior mitral leaflet. Ann Thorac Surg 2009;88:1499–504.

[100] Jimenez JH, Soerensen DD, He Z, Ritchie J, Yoganathan AP. Mitral Valve Function and Chordal Force Distribution Using a Flexible Annulus Model: An In Vitro Study. Ann Biomed Eng 2005;33:557–66.

[101] Jimenez JH, Soerensen DD, He Z, Ritchie J, Yoganathan AP. Effects of papillary muscle position on chordal force distribution: an in-vitro study. J Heart Valve Dis 2005;14:295–302.

[102] Jimenez JH, Soerensen DD, He Z, Ritchie J, Yoganathan AP. Mitral valve function and chordal force distribution using a flexible annulus model: an in vitro study. Ann Biomed Eng 2005;33:557–66.

[103] He Z, Sacks MS, Baijens L, Wanant S, Shah P, Yoganathan AP. Effects of papillary muscle position on in-vitro dynamic strain on the porcine mitral valve. J Heart Valve Dis 2003;12:488–94.

[104] He Z, Ritchie J, Grashow JS, Sacks MS, Yoganathan AP. In vitro dynamic strain behavior of the mitral valve posterior leaflet. J Biomech Eng 2005;127:504–11.

[105] Erek E, Padala M, Pekkan K, Jimenez J, Yalçinba YK, Salihoğlu E, et al. Mitral web--a new concept for mitral valve repair: improved engineering design and in-vitro studies. J Heart Valve Dis 2009;18:300–6.

[106] Vismara R, Antona C, Mangini A, Cervo M, Contino M, Bosisio E, et al. In Vitro Study of Aortic Valves Treated with Neo-Chordae Grafts: Hydrodynamics and Tensile Force Measurements. Ann Biomed Eng 2011;39:1024–31.

[107] De Kerchove L, Vismara R, Mangini A, Fiore GB, Price J, Noirhomme P, et al. In vitro comparison of three techniques for ventriculo-aortic junction annuloplasty. Eur J Cardiothorac Surg 2012.

[108] Babin-Ebell J, Sievers HH, Misfeld M, Runge M, Vogt PR, Scharfschwerdt M. In-vitro hemodynamics of stented bioprosthetic heart valves in the tilted implantation position. J Heart Valve Dis 2008;17:566–70.

[109] Babin-Ebell J, Freiherr Grote H, Sievers H-H, Scharfschwerdt M. Impact of graft size and commissural resuspension height on aortic valve competence in valve-sparing aortic replacement under physiological pressures. Thorac Cardiovasc Surg 2009;57:399–402.

[110] Richardt D, Karluss A, Schmidtke C, Sievers HH, Scharfschwerdt M. A new sinus prosthesis for aortic valve-sparing surgery maintaining the shape of the root at systemic pressure. Ann Thorac Surg 2010;89:943–6.

[111] Scharfschwerdt M, Misfeld M, Sievers H-H. The influence of a nonlinear resistance element upon in vitro aortic pressure tracings and aortic valve motions. ASAIO J 2004;50:498–502.

[112] Scharfschwerdt M, Pawlik M, Sievers H-H, Charitos EI. In vitro investigation of aortic valve annuloplasty using prosthetic ring devices. Eur J Cardiothorac Surg 2011;40:1127–30.

[113] Scharfschwerdt M, Sievers H-H, Greggersen J, Hanke T, Misfeld M. Prosthetic replacement of the ascending aorta increases wall tension in the residual aorta. Ann Thorac Surg 2007;83:954–7.

[114] Soda A, Tanaka R, Saida Y, Takashima K, Hirayama T, Umezu M, et al. Hydrodynamic characteristics of porcine aortic valves cross-linked with glutaraldehyde and polyepoxy compounds. ASAIO J 2009;55:13–8.

[115] Kasegawa H, Iwasaki K, Kusunose S, Tatusta R, Doi T, Yasuda H, et al. Assessment of a novel stentless mitral valve using a pulsatile mitral valve simulator. J Heart Valve Dis 2012;21:71–5.

[116] Hopkins RA. Aortic valve leaflet sparing and salvage surgery: evolution of techniques for aortic root reconstruction. Eur J Cardiothorac Surg 2003;24:886–97.

[117] Cheng A, Dagum P, Miller DC. Aortic root dynamics and surgery: from craft to science. Philos Trans R Soc B Biol Sci 2007;362:1407–19.

[118] Padala M, Powell SN, Croft LR, Thourani VH, Yoganathan AP, Adams DH. Mitral valve hemodynamics after repair of acute posterior leaflet prolapse: quadrangular resection versus triangular resection versus neochordoplasty. J Thorac Cardiovasc Surg 2009;138:309–15.

[119] Tsang W, Bateman MG, Weinert L, Pellegrini G, Mor-Avi V, Sugeng L, et al. Accuracy of aortic annular measurements obtained from three-dimensional echocardiography, CT and MRI: human in vitro and in vivo studies. Heart 2012;98:1146–52.

[120] Zheng M, Li X, Zhang P, Shentu W, Ashraf M, Imanbayev G, et al. Assessment of interventricular dyssynchrony by real time three-dimensional echocardiography: an in vitro study in a porcine model. Echocardiography 2010;27:709–15.

[121] Skrzypiec-Spring M, Grotthus B, Szelag A, Schulz R. Isolated heart perfusion according to Langendorff - Still viable in the new millennium. J Pharmacol Toxicol Methods 2007;55:113–26.

[122] Gomes OM. Myocardium functional recovery protection by omeprazole after ischemia-reperfusion in isolated rat hearts. Rev Bras Cir Cardiovasc 2010;25:388–92.

[123] Baker KE, Curtis MJ. Left regional cardiac perfusion in vitro with platelet-activating factor, norepinephrine and K+ reveals that ischaemic arrhythmias are caused by independent effects of endogenous “mediators” facilitated by interactions, and moderated by paradoxical antago. Br J Pharmacol 2004;142:352–66.

[124] How O, Aasum E. Influence of substrate supply on cardiac efficiency, as measured by pressure-volume analysis in ex vivo mouse hearts. Am J Physiol Hear Circ Physiol 2005:2979–85.

[125] Ytrehus K. The ischemic heart--experimental models. Pharmacol Res 2000;42:193–203.

[126] Zimmer HG. Modifications of the isolated frog heart preparation in Carl Ludwig's Leipzig Physiological Institute: relevance for cardiovascular research. Can J Cardiol 2000;16:61–9.

[127] Van Rijk-Zwikker GL, Mast F, Schipperheyn JJ, Huysmans HA, Bruschke A V. Comparison of rigid and flexible rings for annuloplasty of the porcine mitral valve. Circulation 1990;82:IV58–64.

[128] Van Rijk-Zwikker GL, Schipperheyn JJ, Huysmans HA, Bruschke A V. Influence of mitral valve prosthesis or rigid mitral ring on left ventricular pump function. A study on exposed and isolated blood-perfused porcine hearts. Circulation 1989;80:I1–7.

[129] Rosenstrauch D, Akay HM, Bolukoglu H, Behrens L, Bryant L, Herrera P, et al. Ex vivo resuscitation of adult pig hearts. Tex Heart Inst J 2003;30:121–7.

[130] Araki Y, Usui A, Kawaguchi O, Saito S, Song M-H, Akita T, et al. Pressure–volume relationship in isolated working heart with crystalloid perfusate in swine and imaging the valve motion. Eur J Cardio-Thoracic Surg 2005;28:435–42.

[131] Quill JL, Hill AJ, Menk AR, McHenry BT, Iaizzo PA. Multimodal Imaging of a Transcatheter Aortic Valve Implantation Within an Isolated Heart. JACC Cardiovasc Imaging 2011;4:1138–9.

[132] Quill JL, Laske TG, Hill AJ, Bonhoeffer P, Iaizzo PA. Direct Visualization of a Transcatheter Pulmonary Valve Implantation Within the Visible Heart: A Glimpse Into the Future. Circulation 2007;116:e548–e548.

[133] Iaizzo PA. The functional anatomy of human cardiac valves and unique visualization of transcatheter-delivered valves being deployed. Conf Proc IEEE Eng Med Biol Soc 2009;2009:1098–9.

[134] Silbiger JJ, Bazaz R. Contemporary insights into the functional anatomy of the mitral valve. Am Heart J 2009;158:887–95.

[135] Lansac E, Di Centa I, Raoux F, Bulman-Fleming N, Ranga A, Abed A, et al. An expansible aortic ring for a physiological approach to conservative aortic valve surgery. J Thorac Cardiovasc Surg 2009;138:718–24.

[136] Aicher D, Fries R, Rodionycheva S, Schmidt K, Langer F, Schafers HJ. Aortic valve repair leads to a low incidence of valve-related complications. Eur J Cardio-Thoracic Surg 2010;37:127–32.

[137] Seeburger J, Borger MA, Falk V, Kuntze T, Czesla M, Walther T, et al. Minimal invasive mitral valve repair for mitral regurgitation: results of 1339 consecutive patients. Eur J Cardio-Thoracic Surg 2008;34:760–5.

[138] Yoffe B, Vaysbeyn I, Urin Y, Waysbeyn I, Zubkova O, Chernyavskiy V, et al. Experimental study of a novel suture-less aortic anastomotic device. Eur J Vasc Endovasc Surg 2007;34:79–86.

[139] Standardization IO for. ISO5840: Cardiovascular implants — Cardiac valve prostheses. 2005.

[140] Lanzarone E, Vismara R, Fiore GB. A new pulsatile volumetric device with biomorphic valves for the in vitro study of the cardiovascular system. Artif Organs 2009;33:1048–62.

[141] Reul H, Talukder N, Muller EW. Fluid mechanics of the natural mitral valve. J Biomech 1981;14:361–72.

[142] Pennati G, Fiore GB, Lagana K, Fumero R. Mathematical modeling of fluid dynamics in pulsatile cardiopulmonary bypass. Artif Organs 2004;28:196–209.

[143] Idelchik IE. Handbook of Hydraulic Resistance. Jaico Publishing House; 2005.

[144] Vismara R, Soncini M, Talò G, Dainese L, Guarino A, Redaelli A, et al. A Bioreactor with Compliance Monitoring for Heart Valve Grafts. Ann Biomed Eng 2009;38:100–8.

[145] Diamond G. Diastolic Pressure-Volume Relationship in the Canine Left Ventricle. Circ Res 1971;29:267–75.

[146] Mirsky I. Assessment of Passive Elastic Stiffness for Isolated Heart Muscle and the Intact Heart. Circ Res 1973;33:233–43.

[147] Pinto JG, Fung YC. Mechanical properties of the heart muscle in the passive state. J Biomech 1973;6:597–616.

[148] Hess OM. Diastolic simple elastic and viscoelastic properties of the left ventricle in man. Circulation 1979;59:1178–87.

[149] Schmitt B, Steendijk P, Lunze K, Ovroutski S, Falkenberg J, Rahmanzadeh P, et al. Integrated Assessment of Diastolic and Systolic Ventricular Function Using Diagnostic Cardiac Magnetic Resonance CatheterizationValidation in Pigs and Application in a Clinical Pilot Study. J Am Coll Cardiol Cardiovasc Imaging 2009;2:1271–81.

[150] Lentner C. Geigy Scientific Tables. Basel: CIBA-GEIGY Limited; 1981.

[151] Rodés-Cabau J. Transcatheter aortic valve implantation: current and future approaches. Nat Rev Cardiol 2011;9:15–29.

[152] Alli OO, Booker JD, Lennon RJ, Greason KL, Rihal CS, Holmes Jr. DR. Transcatheter aortic valve implantation: assessing the learning curve. JACC Cardiovasc Interv 2012;5:72–9.

[153] Hayashida K, Lefevre T, Chevalier B, Hovasse T, Romano M, Garot P, et al. True Percutaneous Approach for Transfemoral Aortic Valve Implantation Using the Prostar XL Device: Impact of Learning Curve on Vascular Complications. JACC Cardiovasc Interv 2012;5:207–14.

[154] Kempfert J, Rastan A, Holzhey D, Linke A, Schuler G, van Linden A, et al. Transapical aortic valve implantation: analysis of risk factors and learning experience in 299 patients. Circulation 2011;124:S124–9.

[155] Gurvitch R, Cheung A, Ye J, Wood DA, Willson AB, Toggweiler S, et al. Transcatheter Valve-in-Valve Implantation for Failed Surgical Bioprosthetic Valves. J Am Coll Cardiol 2011;58:2196–209.

[156] Azadani AN, Jaussaud N, Matthews PB, Ge L, Chuter TA, Tseng EE. Transcatheter aortic valves inadequately relieve stenosis in small degenerated bioprostheses. Interact Cardiovasc Thorac Surg 2010;11:70–7.

[157] Azadani AN, Jaussaud N, Matthews PB, Ge L, Guy TS, Chuter TA, et al. Valve-in-valve implantation using a novel supravalvular transcatheter aortic valve: proof of concept. Ann Thorac Surg 2009;88:1864–9.

[158] Bonow RO, Carabello B a, Kanu C, de Leon AC, Faxon DP, Freed MD, et al. ACC/AHA 2006 guidelines for the management of patients with valvular heart disease: a report of the American College of Cardiology/American Heart Association Task Force on Practice Guidelines (writing committee to revise the 1998 Guidelines for the Manage. 2006.

[159] Lancellotti P, Tribouilloy C, Hagendorff A, Moura L, Popescu B a, Agricola E, et al. European Association of Echocardiography recommendations for the assessment of valvular regurgitation. Part 1: aortic and pulmonary regurgitation (native valve disease). Eur J Echocardiogr 2010;11:223–44.

[160] Leopaldi AM, Vismara R, Gelpi G, Romagnoni C, Fiore GB, Redaelli A, et al. Intracardiac Visualization of Transcatheter Aortic Valve and Valve-in-Valve Implantation in an In Vitro Passive Beating Heart. JACC Cardiovasc Interv 2013;6:92–3.

[161] Horai T, Fukamachi K, Fumoto H, Takaseya T, Shiose A, Arakawa Y, et al. Direct endoscopy-guided mitral valve repair in the beating heart: an acute animal study. Innovations (Phila) 2011;6:122–5.

[162] Bahler RC, Desser DR, Finkelhor RS, Brener SJ, Youssefi M. Factors leading to progression of valvular aortic stenosis. Am J Cardiol 1999;84:1044–8.

[163] Vismara R, Leopaldi AM, Mangini A, Romagnoni C, Contino M, Antona C, et al. In vitro study of the Aortic Interleaflet Triangle Reshaping. J Biomech 2013.

[164] Biglino G, Verschueren P, Zegels R, Taylor AM, Schievano S. Rapid prototyping compliant arterial phantoms for in-vitro studies and device testing. J Cardiovasc Magn Reson 2013;15:2.

[165] Kalejs M, von Segesser LK. Rapid prototyping of compliant human aortic roots for assessment of valved stents. Interact Cardiovasc Thorac Surg 2009;8:182–6.

[166] Pott D, Malasa M, Urban U, Kütting M, Safi Y, Roggenkamp J, et al. A novel approach to an anatomical adapted stent design for the percutaneous therapy of tricuspid valve diseases: preliminary experiences from an engineering point of view. ASAIO J n.d.;58:568–73.

[167] Schievano S, Migliavacca F, Coats L, Khambadkone S, Carminati M, Wilson N, et al. Percutaneous pulmonary valve implantation based on rapid prototyping of right ventricular outflow tract and pulmonary trunk from MR data. Radiology 2007;242:490–7.

[168] Tang GHL, Lansman SL, Cohen M, Spielvogel D, Cuomo L, Ahmad H, et al. Transcatheter aortic valve replacement: current developments, ongoing issues, future outlook. Cardiol Rev 2013;21:55–76.

[169] Abraham WT, Smith SA. Devices in the management of advanced, chronic heart failure. Nat Rev Cardiol 2013;10:98–110.

[170] Moazami N, Hoercher KJ, Fukamachi K, Kobayashi M, Smedira NG, Massiello A, et al. Mechanical circulatory support for heart failure: past, present and a look at the future. Expert Rev Med Devices 2013;10:55–71.

[171] Leopaldi AM, Vismara R, Lemma M, Valerio L, Cervo M, Mangini A, et al. In vitro hemodynamics and valve imaging in passive beating hearts. J Biomech 2012;45:1133–9.

[172] Chachques JC, Argyriadis PG, Fontaine G, Hebert J-L, Frank RA, D'Attellis N, et al. Right ventricular cardiomyoplasty: 10-year follow-up. Ann Thorac Surg 2003;75:1464–8.

[173] Oz MC, Artrip JH, Burkhoff D. Direct cardiac compression devices. J Heart Lung Transplant 2002;21:1049–55.

[174] Anstadt MP, Anstadt GL, Lowe JE. Direct mechanical ventricular actuation: a review. Resuscitation 1991;21:7–23.

[175] Carpentier A, Chachques JC. Myocardial substitution with a stimulated skeletal muscle: first successful clinical case. Lancet 1985;1:1267.

[176] Chachques JC, Grandjean PA, Carpentier A. Patient management and clinical follow-up after cardiomyoplasty. J Card Surg 1991;6:89–99.

[177] Moreira LF, Stolf NA. Dynamic cardiomyoplasty as a therapeutic alternative: current status. Heart Fail Rev 2001;6:201–12.

[178] Acker MA. Dynamic cardiomyoplasty: at the crossroads. Ann Thorac Surg 1999;68:750–5.

[179] Anstadt G, Blakemore W, Baue A. A new instrument for prolonged mechanical cardiac massage. Circulation 1965;31-32:43–4.

[180] McCabe JB, Ventriglia WJ, Anstadt GL, Nolan DJ. Direct mechanical ventricular assistance during ventricular fibrillation. Ann Emerg Med 1983;12:739–44.

[181] Bartlett RL, Stewart NJ, Raymond J, Anstadt GL, Martin SD. Comparative study of three methods of resuscitation: closed-chest, open-chest manual, and direct mechanical ventricular assistance. Ann Emerg Med 1984;13:773–7.

[182] Kung RT, Rosenberg M. Heart booster: a pericardial support device. Ann Thorac Surg 1999;68:764–7.

[183] Kavarana MN, Loree HM, Stewart RB, Milbocker MT, Hannan RL, Pantalos GM, et al. Pediatric Mechanical Support with an External Cardiac Compression Device. J Cardiovasc Dis Diagnosis 2013;1.

[184] Suzuki Y, Daitoku K, Minakawa M, Fukui K, Fukuda I. Dynamic cardiomyoplasty using artificial muscle. J Artif Organs 2008;11:160–2.

[185] Williams MR, Artrip JH. Direct cardiac compression for cardiogenic shock with the CardioSupport system. Ann Thorac Surg 2001;71:S188–9.

[186] Wang Q, Yambe T, Shiraishi Y, Duan X. An artificial myocardium assist system: electrohydraulic ventricular actuation improves myocardial tissue perfusion in goats. Artif … 2004;28:853–7.

[187] Depaulis R, Schmitz C, Scaffa R, Nardi P, Chiariello L, Reul H. In vitro evaluation of aortic valve prosthesis in a novel valved conduit with pseudosinuses of Valsalva. J Thorac Cardiovasc Surg 2005;130:1016–21.

[188] Gregory S, Timms D, Pearcy MJ, Tansley G. A naturally shaped silicone ventricle evaluated in a mock circulation loop: a preliminary study. J Med Eng Technol 2009;33:185–91.

[189] Connelly JH, Abrams J, Klima T, Vaughn WK, Frazier OH. Acquired commissural fusion of aortic valves in patients with left ventricular assist devices. J Heart Lung Transplant 2003;22:1291–5.

[190] Cowger J, Pagani FD, Haft JW, Romano MA, Aaronson KD, Kolias TJ. The development of aortic insufficiency in left ventricular assist device-supported patients. Circ Heart Fail 2010;3:668–74.

[191] Hatano M, Kinugawa K, Shiga T, Kato N, Endo M, Hisagi M, et al. Less Frequent Opening of the Aortic Valve and a Continuous Flow Pump Are Risk Factors for Postoperative Onset of Aortic Insufficiency in Patients With a Left Ventricular Assist Device. Circ J 2011;75:1147–55.

[192] Pak S-W, Uriel N, Takayama H, Cappleman S, Song R, Colombo PC, et al. Prevalence of de novo aortic insufficiency during long-term support with left ventricular assist devices. J Heart Lung Transplant 2010;29:1172–6.

[193] Mudd JO, Cuda JD, Halushka M, Soderlund KA, Conte J V, Russell SD. Fusion of aortic valve commissures in patients supported by a continuous axial flow left ventricular assist device. J Heart Lung Transplant 2008;27:1269–74.

[194] Bryant AS, Holman WL, Nanda NC, Vengala S, Blood MS, Pamboukian S V, et al. Native aortic valve insufficiency in patients with left ventricular assist devices. Ann Thorac Surg 2006;81:e6–8.

[195] Magliato KE, Kleisli T, Soukiasian HJ, Tabrizi R, Coleman B, Hickey A, et al. Biventricular support in patients with profound cardiogenic shock: a single center experience. ASAIO J n.d.;49:475–9.

[196] Kindo M, Radovancevic B, Gregoric ID, Conger JL, Kadipasaoglu K, Tamez DA, et al. Biventricular support with the Jarvik 2000 ventricular assist device in a calf model of pulmonary hypertension. ASAIO J n.d.;50:444–50.

[197] Schwarz K, Singh S, Dawson D, Frenneaux MP. Right Ventricular Function in Left Ventricular Disease: Pathophysiology and Implications. Hear Lung Circ 2013;22:507–11.

[198] Dandel M, Potapov E, Krabatsch T, Stepanenko A, Löw A, Vierecke J, et al. Load dependency of right ventricular performance is a major factor to be considered in decision making before ventricular assist device implantation. Circulation 2013;128:S14–23.

[199] Vivo RP, Cordero-Reyes AM, Qamar U, Garikipati S, Trevino AR, Aldeiri M, et al. Increased right-to-left ventricle diameter ratio is a strong predictor of right ventricular failure after left ventricular assist device. J Heart Lung Transplant 2013;32:792–9.

[200] Cordtz J, Nilsson JC, Hansen PB, Sander K, Olesen PS, Boesgaard S, et al. Right ventricular failure after implantation of a continuous-flow left ventricular assist device: early haemodynamic predictors. Eur J Cardiothorac Surg 2013:ezt519–.

[201] Izumi C, Miyake M, Takahashi S, Matsutani H, Hashiwada S, Kuwano K, et al. Progression of Isolated Tricuspid Regurgitation Late After Left-Sided Valve Surgery. Circ J 2011.

[202] Fazio S, Carlomagno G. The Importance of Tricuspid Regurgitation and Right Ventricular Overload in ICD/CRT Recipients: Beside the Left, beyond the Left. Pacing Clin Electrophysiol 2011;34:1181–4.

[203] Kim JB, Yoo DG, Kim GS, Song H, Jung SH, Choo SJ, et al. Mild-to-moderate functional tricuspid regurgitation in patients undergoing valve replacement for rheumatic mitral disease: the influence of tricuspid valve repair on clinical and echocardiographic outcomes. Heart 2011.

[204] Lumens J, Ploux S, Strik M, Gorcsan J, Cochet H, Derval N, et al. Comparative electromechanical and hemodynamic effects of left ventricular and biventricular pacing in dyssynchronous heart failure: electrical resynchronization versus left-right ventricular interaction. J Am Coll Cardiol 2013.

[205] Edvardsen T, Rodevand O, Endresen K, Ihlen H. Interaction between left ventricular wall motion and intraventricular flow propagation in acute and chronic ischemia. Am J Physiol Heart Circ Physiol 2005;289:H732–7.

[206] Kalogeropoulos AP, Georgiopoulou V V, Howell S, Pernetz M-A, Fisher MR, Lerakis S, et al. Evaluation of right intraventricular dyssynchrony by two-dimensional strain echocardiography in patients with pulmonary arterial hypertension. J Am Soc Echocardiogr 2008;21:1028–34.

[207] Massabuau P, Dumonteil N, Berthoumieu P, Marcheix B, Duterque D, Fournial G, et al. Left-to-Right Interventricular Shunt as a Late Complication of Transapical Aortic Valve Implantation. JACC Cardiovasc Interv 2011;4:710–2.

[208] Testuz A, Roffi M, Bonvini RF. Left-to-right shunt reduction with intra-aortic balloon pump in postmyocardial infarction ventricular septal defect. Catheter Cardiovasc Interv 2013;81:727–31.

[209] Timms DL, Gregory SD, Greatrex NA, Pearcy MJ, Fraser JF, Steinseifer U. A compact mock circulation loop for the in vitro testing of cardiovascular devices. Artif Organs 2011;35:384–91.

[210] Timms D, Hayne M, Tan A, Pearcy M. Evaluation of left ventricular assist device performance and hydraulic force in a complete mock circulation loop. Artif Organs 2005;29:573–80.

[211] De Weger A, de Hart J, Stijnen M, van Tuijl S, Dion RA. Ex vivo 2 chamber working pig heart-lung model. Interact Cardiovasc Thorac Surg 2007;6:223–80.

[212] Bovendeerd PHM, Borsje P, Arts T, Vosse FN. Dependence of Intramyocardial Pressure and Coronary Flow on Ventricular Loading and Contractility: A Model Study. Ann Biomed Eng 2006;34:1833–45.

[213] Geven MCF, Bohté VN, Aarnoudse WH, Berg PMJ van den, Rutten MCM, Pijls NHJ, et al. A physiologically representative in vitro model of the coronary circulation. Physiol Meas 2004;25:891–904.

[214] Crick SJ, Sheppard MN, Ho SY, Gebstein L, Anderson RH. Anatomy of the pig heart: comparisons with normal human cardiac structure. J Anat 1998;193 (Pt 1:105–19.

[215] Dapson RW. Glyoxal fixation: how it works and why it only occasionally needs antigen retrieval. Biotech Histochem 2007;82:161–6.

[216] Umlas J, Tulecke M. The effects of glyoxal fixation on the histological evaluation of breast specimens. Hum Pathol 2004;35:1058–62.

[217] Wang YN, Lee K, Pai S, Ledoux WR. Histomorphometric comparison after fixation with formaldehyde or glyoxal. Biotech Histochem 2011;86:359–65.

List of publications

Papers on international peer-reviewed journals

1) Leopaldi A.M., Vismara R., Lemma M., Valerio L., Mangini A., Contino M., Redaelli A., Antona C. and Fiore G.B., *"In vitro hemodynamics and valve imaging in passive beating hearts"*. Journal of Biomechanics, 2012, 45(7):1133-39.
2) Leopaldi A.M., Vismara R., Gelpi G., Romagnoni C., Fiore G.B., Redaelli A., Lemma M. and Antona C., *"Intracardiac visualization of transcatheter aortic valve and valve-in-valve implantation in an in vitro passive beating heart"*. JACC Cardiovascular Intervention, 2013, 6(1):92-3.
3) Vismara R., Leopaldi A.M., Mangini A., Romagnoni C., Contino M., Antona C. and Fiore G.B., *"In vitro study of the Aortic Interleaflet Triangle Reshaping"*. Journal of Biomechanics – http://dx.doi.org/10.1016/j.jbiomech.2013.11.036.
4) Leopaldi A.M., Vismara R., van Tujl S., Redaelli A., van de Vosse F.N., Fiore G.B., Rutten M.C.M., *"Development of a passively-contracting left heart platform for device testing and research: analysis of aortic valve opening dynamics in cf-LVAD support"*. Artificial Organs – Submitted.
5) Vismara R., Leopaldi A.M., Romagnoni C., Lancini B., Contino M., Fiore G.B., and Antona C., *"A novel standardized technique for aortic cusps extension"*. International Journal of Artificial Organs – Submitted.
6) Romagnoni C., Mangini A., Vismara R., Leopaldi A.M., Contino M., Lemma M.G., Fiore G.B., Antona C., *"The interleaflets triangles reshaping: in vitro analysis of morphological, kinematic and hydrodynamic effects on the aortic root"*. Journal of Heart Valve Disease – Submitted.

Conference proceedings

1) A.M. Leopaldi, L. Valerio, M. Lemma, R. Vismara, M. Cervo, A. Mangini, M. Contino, G. B. Fiore, C. Antona and A. Redaelli, *"A New Pulsatile Mock Loop For In vitro Simulation Of Heart Valve Procedures In Porcine Heart"*. Abstract, 4th Joint ESAO-IFAO Congress 2011, Porto, 9-12 Ottobre 2011.

2) Leopaldi A.M., Vismara R., Lemma M., Gelpi G., Mangini A., Antona C., Redaelli A. and Fiore G.B., *"A novel in vitro platform for the simulation of surgical procedures for heart valve repair in porcine hearts"*. Oral presentation - 18th Congress of the European Society of Biomechanics, 1-4 July 2012, Lisbon, Portugal.
3) Mangini A., Contino M., Romagnoni C., Lemma M., Gelpi G., Vismara R., Leopaldi A.M. and Antona C., *"Aortic Valve Repair: influence of the Ventriculo-Aortic Junction and the Sino-Tubular Junction on the leaflets coaptation"*. 4th Annual Joint Scientific Session of the Heart Valve Society of America and Society of Heart Valve Diseases, New York City, N.Y., April 12-14, 2012. Cardiology. 121(2):87-148, 2012.
4) A. Mangini, C. Romagnoni, M. Contino, R. Vismara, A.M. Leopaldi, G. Gelpi, M.G. Lemma, C. Antona, *"Aortic valve repair: influence of the ventriculo-aortic junction and the sino-tubular junction on the leaflets coaptation"*. 26th European Association of Cardio-Thoracic Surgery Annual Meeting, 27-31 October 2012, Barcelona, Spain.
5) Leopaldi A.M., van Tuijl S., Vismara R., Fiore G.B., van de Vosse F. and Rutten M.C.M., *"Development of a passive-contracting heart platform for device testing & research"*. Poster presentation - ASAIO 59th Annual Conference, Chicago, 12-15 Giugno 2013.
6) Rutten M.C.M, van de Vosse F. and Leopaldi A.M., *"Aortic valve opening dynamics in cf-LVAD support"*. Poster presentation - ASAIO 59th Annual Conference, Chicago, 12-15 Giugno 2013.
7) Gelpi G., Romagnoni C., Vismara R., Leopaldi A.M., Mangini A., Contino M. and Antona C., *"Intracardiac endoscopic and angiographic view of step-by-step transcatheter aortic valve implantation in a beating porcine heart: transcatheter valve platform"*. 27th Annual Meeting of the European Association for Cardio-Thoracic Surgery, 5-9 October 2013, Vienna, Austria. Interact CardioVasc Thorac Surg. 17(suppl 2): S148, 2013.
8) Gelpi G., Romagnoni C., Vismara R., Leopaldi A.M., Mangini A., Contino M. and Antona C., *"Transcatheter aortic valve and valve-in-valve implantation in a beating stenotic bicuspid and tricuspid porcine aortic valve: intracardiac endoscopic view"*. 27th Annual Meeting of the European Association for Cardio-Thoracic Surgery, 5-9 October 2013, Vienna, Austria. Interact CardioVasc Thorac Surg. 17(suppl 2): S105, 2013.